4-24-2015

The Role of DYX1C1 in Motile Cilia and Axonemal Dynein Assembly

Aarti Tarkar
University of Connecticut - Storrs, aarti.tarkar@uconn.edu

The Role of DYX1C1 in Motile Cilia and Axonemal Dynein Assembly

Aarti Tarkar, Ph.D.

University of Connecticut, 2015

Motile cilia and flagella are essential to many biological functions that require cellular or fluid movement. The motility of cilia and flagella in turn is dependent upon the action of large protein complexes that serve as molecular motors. Such axonemal motors are composed of multiple dyneins assembled in the cytoplasm of cells with motile cilia. The mechanisms underlying this assembly are not fully understood. Fortuitously, we found that genetic deletion of exons 2–4 of Dyx1c1 in mice caused a phenotype resembling Primary Ciliary Dyskinesia (PCD), a disorder characterized by chronic airway disease, laterality defects and male infertility. Ultrastructural and immunofluorescence analyses of Dyx1c1-mutant motile cilia in mice showed disruptions of outer and inner dynein arms (ODAs and IDAs, respectively). Dyx1c1 localizes to the cytoplasm of respiratory epithelial cells. Its interactome is enriched for molecular chaperones, and it interacts with the cytoplasmic axonemal motor assembly factor DNAAF2 (KTU) as well as transition zone protein Septin2. Additionally, a missense mutation in DYX1C1 found to lead to PCD in humans exhibits a weaker interaction of DYX1C1 with Sept2 and KTU and has reduced activity in promoting association of dyneins. These findings suggest that Dyx1c1 (DNAAF4) plays a role in dynein arm assembly or trafficking and when mutated leads to primary ciliary dyskinesia with laterality defects. Dyx1c1 interacts with intermediate and light chain subunits

of the dynein arm complex in the cytoplasm of tracheal epithelial cells. Light and intermediate chains fail to form complexes in the cytoplasm of tracheal epithelial cells of Dyx1c1 mutants. Dyx1c1 increases by four fold the association of light chain subunits Dnal1 and Dnal4 in heterologously expressing HEK 293-T cells. Finally, a missense mutation in Dyx1c1 (p.L19Q) which cause PCD in humans is impaired in its ability to assembly Dnal1 and Dnal4. In conclusion, we identify a step in axonemal dynein pre-assembly in which Dyx1c1 facilitates formation of light and intermediate chain dynein complexes.

The Role of DYX1C1 In Motile Cilia and Axonemal Dynein Assembly

Aarti Tarkar

B.E., Mumbai University, 2008

M.S., University of Connecticut, 2013

A Dissertation

Submitted in Partial Fulfillment of the

Requirements for the Degree of Doctor of Philosophy

at the

University of Connecticut

2015

APPROVAL PAGE

Doctor of Philosophy Dissertation

The Role of DYX1C1 in Motile Cilia and Axonemal Dynein Assembly

Presented by

Aarti Tarkar, B.E., M.S.

Major Advisor: _____

Joseph J. LoTurco, Ph.D.

Associate Advisor: _____

Randall Walikonis, Ph.D.

Associate Advisor: _____

Marie Cantino, Ph.D.

Associate Advisor: _____

Joanne Conover, Ph.D.

Associate Advisor: _____

Rahul Kanadia, Ph.D.

University of Connecticut

2015

This work is dedicated to

My Parents

ACKNOWLEDGEMENTS

First, I would like to thank Dr. Joseph Loturco, who I met a few months after arriving in graduate school and knew almost immediately that I had found what I was looking for. Joe has the excitement that you can find in the eyes of every five-year old child, and it is powerfully contagious. He has challenged me to think carefully, complete any task, and to become an independent scientist. In the future I can only hope to be a fraction of the mentor he has been to me. He has given me the freedom to try some pretty fun experiments. Thank you Joe, I am truly grateful.

Second, I would like to thank my parents for everything that they have done for me. They have encouraged me to think for myself and make my own decisions. This venture would not have been possible without your unconditional love and support. I am truly blessed to have them in my life.

Big thanks to the members of my thesis committee Dr. Randall Walikonis, Dr. Marie Cantino, Dr. Joanne Conover and Dr. Rahul Kanadia for their guidance in my project as well as their help and support. Thank you Rahul for teaching the embryonic mouse dissections. Special thanks to Marie and Steve for their tremendous help in the design and analysis of electron microscopy experiments, their expertise is truly valued. I would also like to thank every faculty in the PNB Department for all discussions and their inputs during my graduate career.

Amalia, Roman, Justin and Joel you all have been great to me as lab mates and friends. Thank you for making the lab a fun place to work in. Those coffee breaks and lunches with science discussions interspersed with gossips will be greatly missed. I am going to miss each and every one of you so much. I wish all of you continued success, and happiness in all that you undertake. I am lucky to count numerous members of the LoTurco Lab as friends and mentors. Brady Maher, Radmila Filipovic and Anne Booker were the best post-docs and mentors to the

graduate students in our lab. Faez, Chris and Yu were the seniors who taught me a lot of the basic experiments. Alicia and Matt were great lab mates and even wonderful friends. Thank you to Fuyi, Saranya, Prakhar, Xiuyin, Komal and my undergrads Becca, Maritza and Greg for being amazing lab mates and a great support system.

I cannot thank UCONN and especially the PNB department enough for providing the perfect challenging and supportive environment for my graduate training. I want to thank all of our instructors for relentlessly challenging us to question everything and for giving us the tools answer these questions.

Varsha is the best roommate that I could have hoped for. She was fun to hang out with and one of the most understanding people I have met. Thank you for dealing with my tantrums. Big thanks to Tai, Dada and Aarya for all the fun times. Thanks for the memories and friendship, I look forward to the future.

There are countless others that I could name, but I hope that they aren't unhappy that I didn't mention them by name. If you think this refers to you, then I hope you know that I appreciate you, and know that you have played a significant role in shaping my life.

TABLE OF CONTENTS

1. INTRODUCTION

1.1 CILIA

1.1.1 History of the Cilium

Cilia are the oldest known organelles, the discovery of which dates back to over three centuries. In September 1965, Anton Van Leeuwenhoeck, the father of microscopy, used a simple mounted lens and first described the cilia as “thin feet or little legs that moved very nimbly”. The term ‘cilia’ meaning eyelash, was however coined in 1786 by O.F. Muller[1]. The ciliary motility was the first function that was ever described. The most common organisms to study this motility were ciliated protozoa, the clam gill, spermatozoa and the ciliated epithelia of vertebrates. On June 28, 1978, Leeuwenhoeck wrote: “One can’t be satisfied with just looking at so wonderful a structure, chiefly because one can’t get clear on how such an unbelievable motion is brought about..”[2]; thus posing the question: how do cilia work? Since then studies have focused on the biology of the ciliary assembly and motility giving us insights about the function, categories as well as ultrastructure of this organelle.

1.1.2 Cilia structure

Cilia and flagella are structures that project outward from the cell surface and have important sensory and motile functions. They are composed of a microtubule-based axoneme that is generated from a modified centriole called a basal body. The axoneme is surrounded by a specialized plasma membrane that

is continuous with the plasma membrane of the cell body. At the distal end of the basal body is the transition zone, where the triplet microtubule basal body extends into the doublet microtubule axoneme. Transition fibers link the transition zone of the centriole to a specialized region of the plasma membrane called the "ciliary necklace"[3]. It has been proposed that this region acts similar to the nuclear pore complexes of the nuclear envelope to selectively allow transport in and out of the ciliary compartment (Fig 1-1).

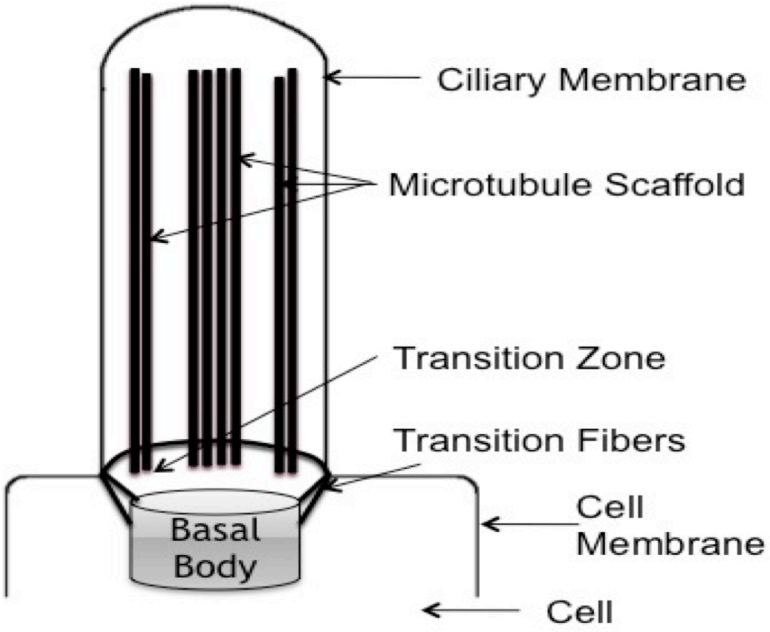

Figure 1-1 Schematic of the ultrastructure of cilia. Cilia consist of a microtubular scaffold that is connected to the cell via basal bodies. The region between the basal bodies and the base of the microtubules is called the transition zone that functions as trafficking region for the entry and exit of proteins. The apparatus is ensheathed in an extension of the plasma membrane, known as the ciliary membrane.

All cilia are composed of a central microtubular scaffold, an intraflagellar transport (IFT) system, and transmembrane proteins. The basal body, a root-like

structure comprised of microtubule triplets, acts as a template for the ciliary ultrastructure. It is known that the basal bodies originate from the mitotic centriole. In cells with a primary cilium, the mother centriole migrates to the surface and, upon docking to the cell membrane, becomes known as the basal body[4,5]. In multiciliated cells however, the centriole is thought to first differentiate and multiply before their migration to the apical cell surface[3,6-8]. The mechanism of this duplication of the centriole has recently spurred a lot of interest in ciliary research.

1.1.3 Classification of cilia

The microtubules are arranged as nine outer doublets consisting of a complete A-tubule and a fused incomplete B-tubule. These 9 doublets are connected to each other via nexin links. In primary cilia, the central microtubules are arranged as doublets in a 9+0 arrangement, whereas in motile cilia they are usually arranged in a 9+2 arrangement[9]. However, there are some motile cilia where the microtubules are in a 9+0 arrangement. Cilia are commonly grouped into two broad classifications: motile and non-motile cilia[10,11] (Fig 1-2).

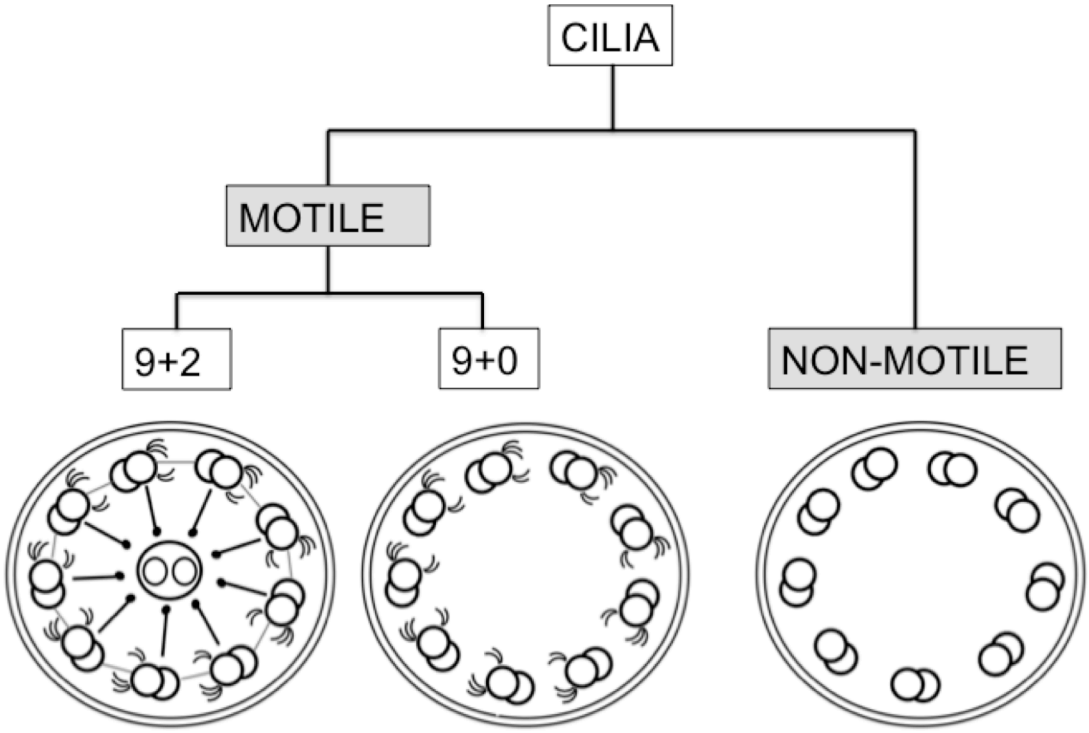

Figure 1-2 Classification of cilia: Cross-section of non-motile (9 + 0 arrangement) and motile cilia (9 + 2 and 9 + 0 arrangement) is shown.

1.1.3.1 Motile Cilia

Motile cilia generally have a “9+2” structure, which refers to the nine doublet microtubules and a central pair that make the axoneme. The nine outer doublets are composed of A and B subfibers that are connected by nexin linkages. In addition to the two central singlets, motile cilia also contain outer dynein arms (ODA), inner dynein arms (IDA) and radial spokes along their length. The above three structures are critical for the motility of the cilia. The movement occurs due to the sliding of the microtubule doublets past each other in the presence of ATP. The ODAs are known to be responsible for the ciliary beat generation while the IDA and radial spokes regulate the beat waveform or pattern. Motility is conferred

by the sliding of doublet microtubules relative to each other and this requires the central pair microtubules, outer and inner dynein arms that project from the A tubule and reversibly bind the neighboring B-tubule, and by radial spokes that connect the A tubule of the outer doublet to the central pair[12-14].

In mammals, motile cilia are found on cells of the airway epithelium, brain ventricles, oviduct, sperm and embryonic node. Each of these, with the exception of sperm and the ciliated cells of the embryonic node, possesses hundreds of motile cilia, and their coordinated beating is vital for movement of fluid and particles over the surface of the epithelium. In the node, motile cilia are unique in that they lack a central pair ("9+0" motile cilia) but are able to rotate due to the activity of ciliary dynein, and this movement generates nodal flow that it critical for the establishment of left-right asymmetry[15]. The rotational motion allows the cilia to move morphogens in developing tissue. Nodal cilia defects are associated with left-right asymmetry and developmental defects[16,17].

1.1.3.2 Non-motile cilia

The "9+0" primary cilium is distinct from the motile cilium in that it lacks a central pair and the dynein arms required for ciliary motility, and only one is found per cell. Primary cilia have been found on almost every cell in the human body with the exception of the myeloid and lymphoid lineages. Once thought to be vestigial, primary cilia are now known to be important for detecting chemical and mechanical stimuli. Examples of specialized types of cilia are the olfactory

receptor cilium, mechanosensing cilia in the kidney tubule epithelium and in bone, and the connecting cilium of photoreceptor sensory neurons. In addition, important developmental signaling pathways such as Sonic hedgehog, platelet-derived growth factor receptor (PDGFR) alpha, polycystin and Wnt are transduced through primary cilia. Kinocilia are microtubule-based ciliary structures that contain a motile cilia-like ultrastructure but are not motile. These cilia of the inner ear are thought to play a role in the planar cell polarity of the stereocilia[18].

1.1.4 Cilia formation and basal body generation

Vertebrate ciliogenesis was first described by electron microscopy (EM) examination of ciliated tissues such as the multiciliated epithelia of rat airway epithelium[8]. The early studies described ciliogenesis as proceeding in a series of steps: 1) cytoplasmic generation of basal bodies, where they acquire appendages required for basal body function, 2) basal body migration to the surface of the cell, where vesicles fuse with the plasma membrane, allowing the basal body to dock 3) and ciliary membrane growth and axoneme extension from the basal body. How ciliary length is then maintained is not well characterized in vertebrates, but in Chlamydomonas, this is achieved by balanced rates of assembly and disassembly[6,19,20].

Different pathways exist for the generation of basal bodies. In cells that make a single cilium, the basal body derives from the mother centriole, which is

duplicated according to the canonical centrosome cycle of dividing cells. In cells that make multiple cilia, basal bodies are generated according to two mechanisms: the canonical templated pathway and the acentrosomal non-templated pathway. In the non-templated pathway, basal bodies arise de novo, multiple basal bodies grow from an electron-dense mass termed the deuterosome, which are present in multiples in the cytoplasm. In the template pathway, a single centriole grows off the side of a pre-existing mother centriole in the cytoplasm[21,22]. Another difference is that centriole duplication and maturation occurs during G0 in multiciliated cells, which are terminally differentiated, whereas in most cells in the body centrioles are duplicated once per cell cycle and only in S-phase, and mature later in the cell cycle. Several studies have identified that cilia are only observed in quiescent cells, or in cells that are in the G0-G1 phase of the cell cycle. Furthermore, when the cell divides, the cilia must be resorbed to free up the centriole for the mitotic spindle[23-26]. Post-division, the centriole once again becomes a basal body, leading to ciliogenesis. The ability of the cells to not undergo cell division in the presence of the cilium raises the possibility of cilium as a cell division checkpoint organelle[18].

1.1.5 Intraflagellar Transport

Protein synthesis does not occur inside the cilium, so components for cilia growth and function are trafficked there. This is achieved by intraflagellar transport (IFT), which was first identified in the unicellular flagellated algae Chlamydomonas reinhardtii. IFT particles consist of “core” structural protein complexes, molecular

motors and adaptor proteins, and there are two types of IFT: anterograde and retrograde. In vertebrates, the anterograde IFT complex consists of IFT particles B and the microtubule plus-end directed kinesin-II complex consisting of KIF3A, KIF3B and KAP. Retrograde IFT complexes consist of IFT particles A and cytoplasmic dynein 2. IFT complex B and A are composed of at least 10 and 6 proteins, respectively, and are thought to facilitate cargo transport through interaction with protein binding domains [27]. Accumulations of IFT particles have been detected at transition fibers, leading to the hypothesis that docking at the transition zone might also be an important regulatory step for transport in and out of the cilium [28-31].

1.2 MOTILITY OF CILIA

Within the ciliary axoneme, multi-protein complexes exist by interconnecting the different components like the radial spokes, nexin links, central sheath and dynein arms. The dynein arms are attached to the peripheral microtubules with certain periodicity and are known to generate motility by ATP-dependent mechanism. The dynein arms are large, multi-subunit complexes assembled with polypeptides of different sizes: heavy chain (HC of 400-500 KDa), intermediate chain (IC of 45-110 KDa) and light chains (LC of 8-55 KDa). The ATPase activity, that provides the energy to produce the sliding movement between the microtubules resulting in ciliary beating, resides in the HC molecules. The motility of the dynein arms requires the orchestrated functioning of many dynein

components[32,33].

Studies have identified aberrant motility in Chlamydomonas strains. By mutational analysis, a number of axonemal dyneins have been identified and these studies indicate that 30-40 axonemal dyneins (14 HC, 7 IC and 15 LC) combine to form the dynein arms. There are two general types of dyneins built into motile axonemes: the outer-arm dyneins found towards the outside of the axoneme, and inner-arm dyneins, which are positioned closest to the central-apparatus radial spokes[12,14,32,34,35]. The docking complex that attaches the outer arm (ODA-DC) is composed of three polypeptides, whereas the one for the inner arm has not yet been solved.

1.2.1 Outer Dynein Arms

Functional analysis has revealed that the outer arms provide about 80% of the power generated during ciliary beating. Cilia that lack ODAs beat significantly more slowly than wild type and thus defects in the outer arms are a major cause of primary ciliary dyskinesia (PCD) in humans. In all organisms examined to date, outer arms contain multiple either two (e.g. mammals and sea urchins) or three (e.g. Chlamydomonas and Tetrahymena) HCs associated with two WD-repeat ICs, a core set of LCs, and coiled-coil proteins involved in assembly within the axoneme. Most of the homologous genes encoding axonemal polypeptides in mammals have been identified. Furthermore, outer arms contain additional components that act in various signaling pathways to control motor function. Literature suggests that outer-arm dyneins contain a system that senses

mechanical strain and allows the motors to compensate for increased load[33,36].

ODA in eukaryotic cilia/flagella is a multimeric complex that is composed of heavy chains (HCs) that contain ATPase/motor domains, intermediate chains (ICs), and several light chains (LCs). The structure, subunit composition, and regulation of ODA are best studied using the green alga Chlamydomonas reinhardtii because numerous mutants with defects in the ODA subunit genes have been isolated. In Chlamydomonas, three HCs are bound like a bouquet, and two ICs and several LCs form a complex at the base of the bouquet (IC-LC complex) (Fig. 1-3a). The exceptions are LC1, LC3, LC4, and LC5, which are bound to either the motor domains or N- terminal regions of the HCs. The composition of the ODA is shown in Fig. 1-3b.

a

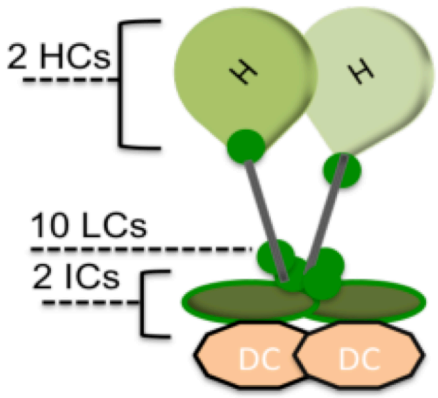

b

Heavy Chain	Intermediate Chain	Light Chain
DNAH9 DNAH17 DNAH11 DNAH8 DNAH5	DNAI2 DNAI1 TXNDC3	DNAL1 DNAL4 TCTE3 DYNLRB1/2 DYNLL1/2 DYNLT1/3

Figure 1-3: Composition of the outer dynein arm. (a) In mammals, the outer dynein arm comprises of two heavy chains, two intermediate chains and about ten light chains. (b) The individual outer dynein arm subunit composition. (Adapted from Fliegauf et al. 2008)

ODAs are arranged linearly on specific sites of the A-tubule of doublet microtubules with a regular spacing of 24 nm, through interaction with the outer-dynein-arm docking complex (ODA-DC). The ODA-DC was first identified as a projection on the ODA-lacking mutants in Chlamydomonas. Biochemical and genetic analyses revealed that ODA-DC is composed of three subunits (termed DC1, DC2, and DC3). The subunit composition of ODA-DC in other organisms is different from that in Chlamydomonas. In humans, DC1 does not appear to be conserved but two genes seem to be DC2 orthologs[36-40].

1.2.2 Inner Dynein Arms

In contrast to the outer dynein arm, which is homogeneous in composition and organization; genetic, biochemical, and structural analysis in Chlamydomonas have revealed seven major species of inner-arm dyneins: a, b, c, d, e, f (I1 dynein), and g, and at least three minor species of inner-arm dyneins: DHC3, DHC4, and DHC11.

Based on genomic and structural analyses, the organization and complexity of the inner dynein arms and 96 nm axonemal repeat was shown to be a highly conserved feature of all motile axonemes[36,41-44]. The complete composition as well as the predicted schematic of the IDA is presented in Fig. 1-4. Biochemical studies have revealed that certain dyneins within the flagellum act as monomeric motors and have a distinct complement of associated proteins including actin and either an essential LC (termed p28 in Chlamydomonas) or the calcium-binding calmodulin homolog centrin. Dimeric inner dynein arm contains two distinct HC motors and plays a key role in the regulation of axonemal motility. Mutants that lack this dynein exhibit slow swimming due to alterations in flagellar waveform that result in a less efficient beat. There is one copy of the IDA located within each 96 nm axonemal repeat and both HCs are necessary for its assembly[32,35,45,46].

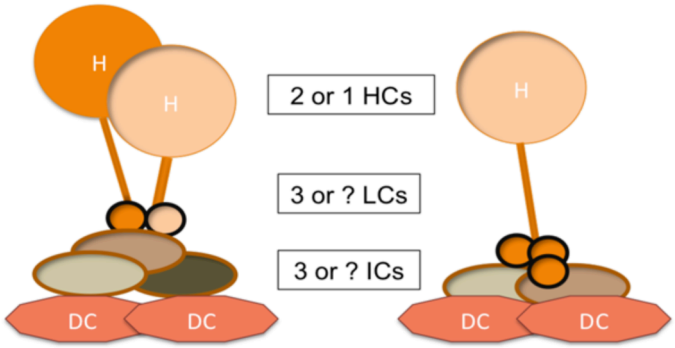

Heavy Chain	Intermediate Chain	Light Chain
DNAH1, DNAH2, DNAH3, DNAH7, DNAH6, DNAH10, DNAH12, DNAH14	IC138 IC140 WD63 WD78 CASC1 DNALI1	TCX2 DYNLRB1/2 DYNLL1/2 DYNLT1/3

Figure 1-4: Schematic of the inner dynein arm and their subunit composition. Inner dynein arm could consist of either one or two heavy chains, three or more intermediate chains and three or more light chains. The detailed structure of the inner dynein arms is not yet identified completely. The known subunit composition of the inner dynein arms is shown in the bottom panel. (Adapted from Fliegauf et al. 2008)

1.2.3 Ciliary beat generation

The ODAs are responsible for the beat frequency and power required for generation of normal axonemal motility, whereas the inner-arm dyneins regulate the size and shape of the axonemal bend, parameters that are referred to as “waveform”. The beat pattern of motile cilia consists of an effective stroke and a

recovery stroke. The effective stroke is established when the cilia bend and move in a vertical manner, and this movement is mediated by the ODA[12,34,47]. During the recovery stroke, the cilia are found to travel in the horizontal direction respective to the fluid flow. Thus, the motion of motile cilia results in a net transport of particles in a single direction, a property that is essential especially for the effective clearance of particulates from the airway.

As discussed briefly above, literature has revealed that the basis for ciliary motility lies in controlled dynein-driven microtubule sliding-a "sliding microtubule" model for ciliary bending (Fig. 1-5) [48-50]. In addition, it was determined that the dynein motors generate force in one direction (minus-end direction) relative to microtubule polarity[48,51]. Thus, since all dyneins are minus-end motors, this observation directly led to a "switching" model for alternating effective (principal/forward) and recovery (reverse) bending: dyneins on one side of a structural and functional axis of the axoneme are active for bending in one direction. When the direction of bending changes or "switches", there is a switch in activity where the previously inactive dyneins, on one side of the axis, are activated, and the formerly active dyneins on the opposite side, are turned off.

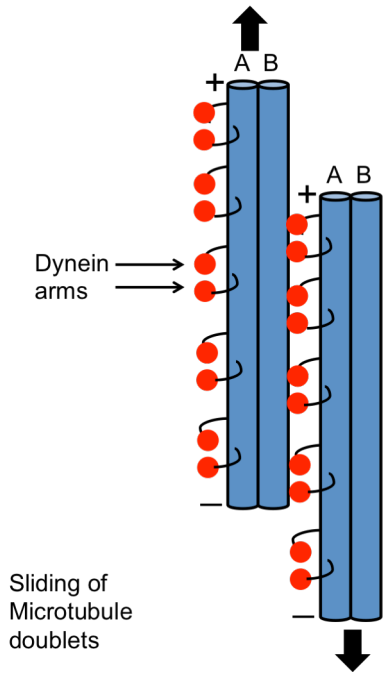

Figure 1-5: Sliding model of microtubule doublets. Bending of a cilium involves ATP-dependent walking of motor domains of A-tubule dynein arms along adjacent B tubules, toward the minus end. This causes the sliding of microtubule doublets. Minus ends are anchored in the basal body, and flexible links between doublets (radial spokes and nexin links) limit sliding. The result is bending of the cilium. (Adapted from https://www.rpi.edu/dept/bcbp/molbiochem/MBWeb/mb2/part1/kinesin.htm)

The precise mechanism for sensing the end point of each bend direction is not understood but clearly for oscillatory bending, dynein motors must be regulated. Detailed experimental evidence indicates the basic oscillatory movement, and "switches" in bend direction, are inherent properties of the dynein motors involving microtubule curvature and a mechanical feedback control (Fig. 1-6) [50,52-54]. The switching sensor is not known, but one model includes the outer

dynein arm playing a role as a sensor of microtubule curvature[53,55].

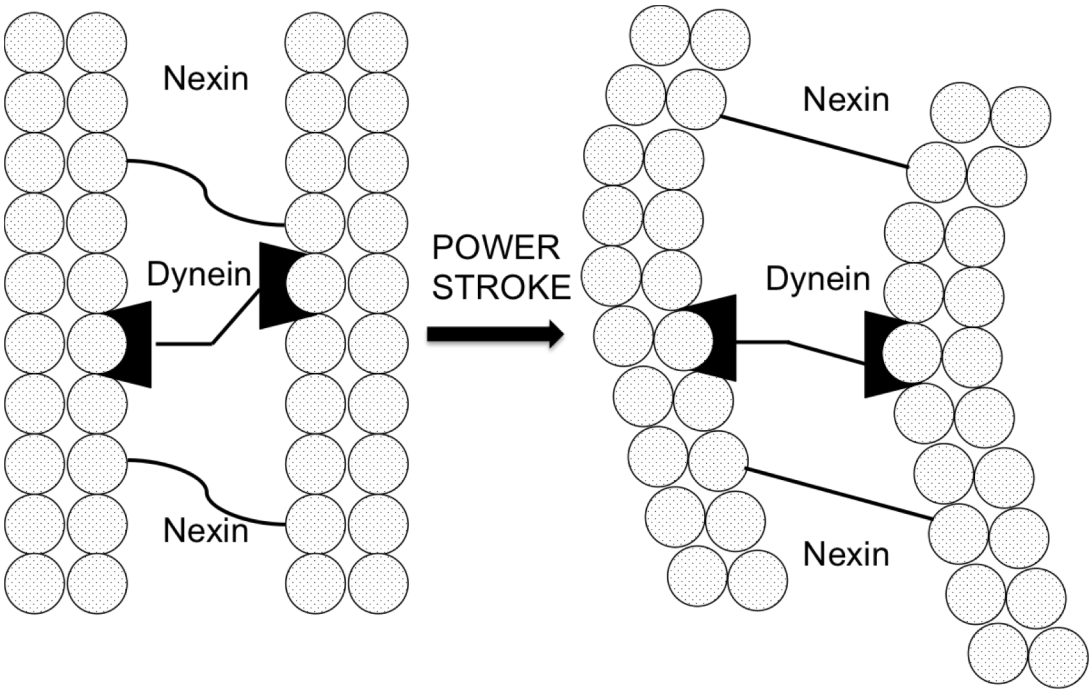

Figure 1-6: Schematic of power stroke. The power stroke of the motor protein, dynein, attached to one microtubule, against subfiber B of a neighboring microtubule causes the fibers to slide past each other. The flexible linker protein, nexin, converts the sliding motion to a bending motion. (Adapted from http://www.arn.org/docs/behe/mb_mm92496.htm)

1.2.4 Molecular Pathways of Axonemal Dynein Assembly and Transport

Although axonemal dyneins function in cilia/flagella, these complex multi-component enzymes are assembled in the cytoplasm and then transported into the cilium. Initial evidence for this came from the analysis of the assembly state of outer-arm dynein components in the cytoplasm of Chlamydomonas mutants

defective for various dynein proteins and assembly factors. The assembly of the outer-arm HCs and ICs with another HC was defective in the cytoplasm of strains lacking either the intermediate chains or the HCs[56]. In contrast, the core motor was completely assembled in the absence of the docking complex or ODA5 proteins[57]. Oda7 is a Leucine rich repeat (LRR) protein that resides in the cell body and associates with both outer and inner arms. This protein possibly functions as a linker that joins these two dyneins arms together and is dissociated from the dynein complexes prior to their transport into the ciliary axoneme[58,59].

Additional cytoplasmic assembly factors for axonemal dyneins have recently been described; both are members of the PIH group, which interact with heat-shock family proteins. One protein encoded by the kintoun (ktu) gene was identified in medaka following a mutant screen and also in humans with PCD. In addition, the Chlamydomonas ortholog of Ktu, PF13 defects in which result in the failure of both outer and inner dynein arm assembly. The Ktu/PF13 protein was found to bind both dyneins and Hsp70, leading to the hypothesis that it acts as a co-chaperone to aid dynein assembly in cytoplasm[60,61]. A second PIH protein (MOT48) that is encoded at the IDA10 locus was identified as being required for the assembly of a subset of monomeric inner dynein arms. Bioinformatics analysis has identified additional PIH domain proteins in Chlamydomonas and indicates that these PIH proteins are present only in organisms that bear motile cilia. Furthermore, one of the uncharacterized Chlamydomonas PIH proteins appears to be homologous to the TWISTER protein in zebrafish defects in which

leads to polycystic kidneys and morphogenetic abnormalities[61]. An additional protein ODA16 in Chlamydomonas was revealed that is required for transport of outer-arm dyneins into the flagellum. This protein interacts directly with IFT46, which is part of the IFT complex B and is thought to act essentially as a cargo adaptor for outer-arm transport[62].

1.3 CILIOPATHIES

Inherited human mutations that result in the broad disruption of cilia cause severe developmental and adult phenotypes. Cilia are found on nearly every cell of the human body and are diverse in form and function. Cilia function to clear mucus, move fluid, to sense fluid flow and other mechanical forces, to intercept extracellular signaling molecules and to concentrate and activate intracellular signaling molecules. Cilia participate in developmental processes from breaking the left-right symmetry of the embryo to tooth formation, and in adult processes ranging from kidney tubule homeostasis to vision, olfaction, and hearing. Mutations could affect a gene that disrupts an isolated cilia function and thus cause a mild disease like retinal degeneration, or they could affect a gene essential for all cilia functions and thus cause severe disease in all tissues where cilia are found and result in embryonic lethality. Collectively, diseases or developmental defects caused by an underlying defect in the assembly or function of 9+2 or 9+0 cilia, or both, are termed ciliopathies[11,63].

1.3.1 Primary cilia-related ciliopathies

Of the 80 genes now linked to ciliary diseases, nearly three-quarters of them are linked to cilia functions other than motility. Connecting cilia of retinal photoreceptors are essential for vision. Rhodopsin, as well other proteins, are produced in the inner segment of the photoreceptor and moved into the outer segment via intraflagellar transport along the microtubules of the connecting cilium. In the absence of this transport, photoreceptors die via apoptosis and the retina degrades, resulting in progressive loss of vision. Retinitis Pigmentosa and Leber Congenital Amaurosis are two types of retinal degeneration that have been linked to mutations in gene products associated with the cilium. RPGR (retinitis pigmentosa GTPase regulator) localizes to the connecting cilium of retina and mutations in the gene encoding it account for 20% of all retinitis pigmentosa cases. Interestingly, however, RPGR localizes to the transition zone of motile cilia in the trachea, and mutations in *RPGR* have been identified in PCD[64].

Autosomal dominant polycystic kidney disease (ADPKD), autosomal recessive polycystic kidney disease (ARPKD), and nephronophthisis (NPHP) are progressive cystic diseases of the kidney[64-66]. The genes mutated in ADPKD, ARPKD, and NPHP localize to the primary cilia lining the tubules of the kidney, where many cysts originate. This supports the hypothesis that cilia are involved in these diseases. Positional cloning revealed that the gene *Ift88* was mutated in the Oak Ridge Polycystic Kidney disease mouse (*Tg737orpk*), a mouse model of ARPKD[67,68]. Two gene products polycystin-1, and polycystin-2, encoded by *Pkd1*

and *Pkd2* respectively, are hypothesized to form a mechanosensory complex that can sense the bending of primary cilia in response to the flow of fluid in kidney tubules. The sensation of flow in the kidney tubule is required both for the proper formation of tubules during development, and for the maintenance of these tubules in adulthood. Mutation of *Pkd1* or *Pkd2* likely abolishes flow sensation and causes a compensatory proliferation or rearrangement of tubular cells. Mutation of *Pkd1* or *Pkd2* causes renal cystic disease due to the abolished flow sensation causing a rearrangement of tubular cells. Interestingly, a few genes, when mutated, can cause simultaneous cystic kidney disease and retinal degeneration, a condition known as Senior Løken syndrome[18,24,66,69,70].

Bardet-Biedl syndrome (BBS), Joubert syndrome (JS) and Meckel syndrome (MKS) are all multisystem, complex, recessively inherited human diseases, which display distinct but partially overlapping phenotypes. Common to these disorders are ocular/retinal abnormalities, polydactyly, renal cystic disease, CNS malformations or impairments, and situs inversus. Unique among these disorders is cognitive impairments and obesity in BBS, cerebellar vermis hypoplasia in JS and encephalocele and perinatal lethality in MKS. Genetically, there are numerous commonalities between JS and MKS, yet very little overlap between BBS and any other ciliopathy[18,67,71-74].

1.3.2 Motile cilia-associated ciliopathies

Motile cilia play an important role during the development of, and in the

adulthood of, humans. The motile cilia of the node play a role in patterning the left-right axis of vertebrates, and thus mutations that affect cilia in this structure can result in *situs inversus*. Motile cilia with a 9+2 arrangement of microtubules are found in the ependymal cells of the brain, epithelial cells of the trachea and bronchioles, in sperm tails and throughout the female reproductive tract. As discussed above, primary cilia dyskinesia (PCD), also known as Kartagener's syndrome[75], affects the motility of all cilia while leaving other functions intact. Afzelius predicted that the gene mutated in his Kartagener patients might encode the protein comprising the axonemal dynein arms that allow for the motility of cilia. Nearly every gene variant linked to Kartagener's syndrome since then has been found to encode an axonemal dynein. However, recent studies have led to the identification of other genes apart from axonemal dyneins that are known to cause PCD[76].

The diseases associated with defects in motile cilia tend to be more straightforward due to the fact that motile cilia are primarily known for their role in fluid movement. Ciliary beat frequency (CBF) is probably the best-studied aspect of motile cilia biology, as defects in beating have numerous effects on human health. It has been known that CBF can change in response to exogenous signals. The many biological and chemical compounds that can affect CBF include prostaglandin, extracellular ATP, cytokines, cigarette smoke, ethanol and Vicks VapoRub[77-81]. Many neurotransmitters have been reported to modulate CBF, although the pathways are complex since effects seem to differ between

species. Recently it was found that motile cilia on mammalian airway epithelial cells are also sites for G-protein coupled receptor proteins, and that motile cilia alter their beating in response to exposure to bitter taste compounds[82]. Although the functions ascribed to motile cilia and primary cilia have historically been separate, this finding suggests that there may be more overlap than previously thought.

1.3.3 Candidate PCD genes

Dynein arm defects account for 90% of PCD cases with defined ultrastructural abnormalities. The newly discovered disease-causing gene mutations cause functional defects but are not associated with a consistent ultrastructural defect. Thus the presence of normal axonemal ultrastructure does not exclude PCD[83]. In addition to the identification of cilia-related proteins, advances in techniques of genetic screening and sequencing are leading the way for the use of genetic testing as a diagnostic tool[84]. PCD, an autosomal recessive disorder, is highly heterogenic owing to the large number of proteins involved in cilia assembly, structure, and function. A growing number of genes that are involved in axonemal motors, ciliary structure and regulation, or ciliary assembly and preassembly have been implicated in PCD (Table 1-1).

Gene	Axonemal component	Ciliary ultrastructural defects	OMIM
DNAH5	ODA-HC	ODA defects	603335
DNAH11	ODA-HC	Normal	603339
DNAI1	ODA-IC	ODA defects	604366
DNAI2	ODA-IC	ODA defects	605483
DNAL1	ODA-LC	ODA defects	610062
TXNDC3	ODA-LC/IC	Partial ODA defects	607421
RSPH4A	RSH	CP defects	612647
RSPH9	RSH	CP defects or normal	612648
CCDC39	DRC	Microtubule disorganization	613798
CCDC40	DRC	Microtubule disorganization	613799
CCDC164	DRC	DRC link defects	615288
CCDC103	ODA docking	ODA defects	614677
CCDC114	ODA docking	ODA defects	615038
HYDIN	Central pair	CP defects	610812
DNAAF1	Cytoplasmic	ODA+IDA defects	613190
DNAAF2	Cytoplasmic	ODA+IDA defects	612517
DNAAF3	Cytoplasmic	ODA+IDA defects	614566
HEATR2	Cytoplasmic	ODA+IDA defects	614864
LRRC6	Cytoplasmic	ODA+IDA defects	614930

Table 1-1: Genes mutated in Primary Ciliary Dyskinesia (PCD). *ODA: Outer Dynein Arm, IDA: Inner Dynein Arm, HC: Heavy chain, IC: Intermediate chain, LC: Light chain, CP: Central Pair, DRC: Dynein Regulatory Complex, and RSH: Radial Spokes.*

The identification of PCD-associated genes has relied on a combination of experimental models, proteomic analysis, and sequencing of candidate genes. The best-studied model of motile cilia is the alga, *C. reinhartii*[11,85]. Screening algae with defective motility or abnormal flagellar structure has been used to study the function of orthologous ciliary proteins, which were linked to human diseases. The second major advance leading to PCD gene identification was the collection of ciliogenesis-related transcriptomes and cilia proteomes that provided lists of cilia genes that could be linked to newly found disease mutations[86-89]. More recently, parallel sequencing to analyze regions of interests in the genome has allowed more rapid identification of multiple new mutations in cohorts of PCD subjects without prior knowledge of candidate genes. In addition, whole-exome sequencing has the potential to unravel the genetic causes of rare diseases and was recently successfully used to identify new candidate genes associated with PCD[11,90].

To date, mutations in 19 different genes have been linked to PCD (Table 1-1), and more candidates are being verified. Early searches for PCD-related mutations identified genes that encode proteins integral to axonemal structure and function; outer dynein arm: *DNAH5*, *DNAI1*, *DNAL1*, *DNAI2*, *TXNDC3*, and *DNAH11*[91-95]; inner dynein arm and axonemal organization: *CCDC39*, *CCDC40*, *CCDC164*[96-99]; central apparatus and radial spokes: *RSPH9*, *RSPH4A*, and *HYDIN*[100]. More recently, mutations in several genes coding for several cytoplasmic proteins not found in the axoneme have been linked to PCD. These

proteins are presumed to have roles in cilia assembly or protein transport, and mutations lead to ultrastructural abnormalities: *HEATR2*, *DNAAF1*, *DNAAF2*, *DNAAF3*, *CCDC103*, *LRRC6*, and *CCDC114*[60,101-106].

Most PCD-causing mutations have been identified in components of the ciliary axoneme and mutations in two genes in particular, dynein axonemal intermediate chain 1 (*DNAI1*; MIM 604366) and dynein axonemal heavy chain 5 (*DNAH5*; MIM 603335), which encode components of the outer dynein arm and account for more than 30% of all cases. *DNAI1* was the first disease-associated gene to be identified using a candidate gene approach, by screening algae for abnormal flagellar beat and outer dynein arm defects. *DNAI1* mutations were found in a large cohort at a prevalence of 9% of all identified PCD subjects. Mutations in *DNAH5*, another component of the outer dynein arm, were discovered using homozygosity mapping in large affected endogamous families, and later identified by sequencing in PCD subjects. Other examples of mutated axonemal proteins associated with PCD discovered using the candidate gene approach include intermediate dynein chain *DNAI2* (MIM 605483), which comprise about 2% of PCD patients, and *TXNDC3* (MIM 607421). Mutations in the dynein axonemal heavy chain 11 (*DNAH11*; MIM 603339) gene, which encodes an outer dynein arm protein, are not associated with an ultrastructural defect and cilia have normal (or more rapid) beat frequency. Mutations in other genes, such as coiled-coil domain containing proteins *CCDC39* (MIM 613798) and *CCDC40* (MIM 613799), produce inconsistent ultrastructural abnormalities characterized

by disordered microtubules in some but not all cilia.

Several nonstructural cilia-associated proteins have been found to be mutated in PCD individuals and result in the absence of outer and inner dynein arms. These mutations involve proteins that are considered to function in cilia assembly or "preassembly" pathways. Identification of the involvement of these proteins has spurred research into the mechanisms of cilia biogenesis. To understand the role of these mutations, cilia biogenesis can be conceptually divided into the following processes: intra-axonemal transport, transfer into the cilium, and cytoplasmic preassembly. How specific proteins are coded for precise delivery and assembly within the cilium and how the transition zone acts as a gate is not yet known.

1.3.3.1 PCD-causing preassembly proteins

Several gene mutations in preassembly proteins have been found to cause PCD. The first PCD-associated preassembly protein found was DNAAF2 (MIM 613190), which was identified in mutant *zebrafish* and later in PCD subjects who had complete absence of outer dynein arms. Localized within the apical region of the cell cytoplasm, DNAAF2 belongs to the proteins interacting with Hsp90 family and interacts with DNAI2 and the chaperone heat shock protein HSP70 to facilitate assembly or dynein complex transport into the cilia[60,61]. Similar to DNAAF2, MOT48 is a protein interacting with Hsp90 localized in the cell body that was identified in the Chlamydomonas to display motility defects and is associated with preassembly of both outer dynein arms and a subset of inner dynein arms, likely needed for the stability of dynein heavy chain components[61].

Mutations in the related proteins DNAAF1 (LRRC50; MIM 612517) and DNAAF3 (MIM 614566) caused outer dynein arm defects in subjects with PCD. Evidence for assembly roles of these proteins is substantiated in mutant cells where components of the inner dynein arm were found to accumulate in the cytoplasm of mutated cells and fail to move into the cilium[102,107]. These findings indicate the existence of a multistep cytoplasmic assembly pathway.

Another preassembly protein with mutations causative of PCD is HEATR2 (MIM 614864), which was recently implicated in dynein arm assembly. Similar to other preassembly factors, HEATR2 is localized to the cytoplasm of ciliated cells rather than in the apical region, which suggests that it either functions at different stages of dynein assembly or is part of a chaperone complex that facilitates transfer of different dynein complexes along an “assembly line.” The finding that HEATR2 mutations are associated with mislocalization of inner arm proteins supported this role[101].

Mutations in *LRRC6* (MIM 244400) also lead to PCD. A member of a protein family with diverse functions, including splicing factors and nuclear transport, LRRC6 is found in the cytoplasm and colocalizes with basal body markers. Mutations in LRRC6 were shown to downregulate expression of other dynein arm proteins and indicate an additional regulatory role[108]. Thus, dynein arm preassembly is intricately regulated by both positive and negative feedback mechanisms.

1.4 DYX1C1

A candidate gene in DYX1, subsequently named DYX1C1, was first identified through studies of a Finnish family in which a chromosomal rearrangement, a translocation involving chromosomes 2 and 15, co-segregated with reading and writing difficulties[109-111]. The chromosome 15 breakpoint of this translocation was located within the DYX1 region that mapped to the DYX1C1 gene[112].

1.4.1 DYX1C1 and Neuronal Migration

Wang and colleagues performed the first functional characterization of DYX1C1 where they utilized in utero knockdown of the rodent ortholog, Dyx1c1, of this gene in the embryonic rat neocortex. This knockdown led to the abnormal neuronal migration in the rat neocortex stalling the neurons in the intermediate zone, thus leading to accumulation of neurons in the multipolar stage of migration[114,124,125]. The effects of the knockdown were non-autonomous and also disturbed some other neighboring cells in addition to the cells that had been knocked down for Dyx1c1[126]. Overexpression of Dyx1c1 rescued migration, confirming that the knockdown was causing the aberrant phenotype; and it was found that the TPR domains were sufficient for this rescue [124].

1.4.2 DYX1C1 function and its known interactors

DYX1C1 is a 420 amino acid protein that is expressed ubiquitously in adult tissues including brain. The protein can be detected by immunocytochemistry in the nuclei and cytoplasm of neurons and glia in human neocortex. The protein

domains of DYX1C1 include an N-terminal p23 and three C-terminal TPR domains[112]. This combination of a p23 and TPR domains is shared with Sugtl, a protein known to play a role in kinetochore assembly in yeast, suggesting a potential role in cell division or cell dynamics. DYX1C1, when over-expressed in cell lines, can interact with Hsp70, Hsp90 and an E-3 ubiquitin ligase, Chip, suggesting that DYX1C1 may also be involved in the degradation of unfolded proteins[127,128]. At its C-terminal, there are three tetratricopeptide domains (TPR) which function in protein-protein interactions. Studies have shown that the rat orthologue of DYX1C1 interacts with estrogen receptors in primary rat neurons[129]. It has been thus proposed that DYX1C1 negatively regulates estrogen receptor levels in a dose-dependent manner, decreasing their transcriptional activity and stability. Variants in the promoter region of DYX1C1 have been suggested to mediate allele-specific binding of transcription factors (such as TFII-I and Sp1) and/or to be associated with different expression levels of the gene[130].

Follow-up study on the function of Dyx1c1 demonstrated that when neurons were subjected to embryonic knockdown of Dyx1c1 levels, they migrated past their expected laminar targets[114]. These over-migration observations have been confirmed in a subsequent investigation using live-cell imaging of human neuroblastoma cells, where knockdown of DYX1C1 led to increased migration rates compared with controls. This phenotype was dependent not only on the TPR domains but also on another novel highly conserved motif, referred to as a

DYX1 domain[131]. Analysis of changes in global gene expression levels after perturbation of DYX1C1, by overexpression or knockdown in these cell lines, uncovered a group of genes that was enriched for known functions, including 'cellular component movement', 'cell migration', and 'nervous system development', as well as a pathway involved in focal adhesion[131,132]. Tammimies and colleagues specifically assessed whether DYX1C1 can interact with other proteins implicated in neuronal migration and/or associated with dyslexia susceptibility, including DCDC2 and KIAA0319. It was found that DYX1C1 interacts with LIS1 (a protein implicated in lissencephaly, a rare brain disorder caused by severely disrupted neuronal migration) and DCDC2, but not with KIAA0319. Several new interactions with DYX1C1 were also reported, with a significant overrepresentation of proteins that are components of the cytoskeleton, three of which (TUBB2B, TUBA1, and Ataxin1) were further validated[131].

1.4.3 DYX1C1 and ciliary function

The literature mining approach utilized by Ivliev and colleagues revealed that the consensus ciliary signature included the dyslexia candidate genes DYX1C1, DCDC2 and KIAA0319. This finding was however surprising since no role of cilia has been identified to date in dyslexia[121]. Primary cilia are present on the surface of neurons and hence cilia are implicated in early brain patterning and homeostasis. As discussed earlier, a study has shown that overexpression of DCDC2 in neurons changes the morphology and function of the primary cilium. In sum, these studies raise a possibility that ciliary dysfunction might be associated

with dyslexia.

Recent work by Chandrashekar and colleagues demonstrated the developmental role of DYX1C1 using a zebrafish model. The zebrafish orthologue of DYX1C1 is expressed in many ciliated tissues, and its knockdown leads to multiple ciliopathy-related phenotypes such as body curvature, hydrocephalus, situs inversus and kidney cysts. The *dyx1c1* morphants also exhibited reduced cilia length in several organs including Kupffer's vesicle, pronephros, spinal canal and olfactory placode. Furthermore, electron microscopic analysis of cilia in *dyx1c1* morphants revealed loss of both outer (ODA) and inner dynein arms (IDA) that have been shown to be required for cilia motility. In sum, an essential role for *dyx1c1* was proposed in cilia growth and function[133].

1.5 Overview

Studies have been performed to evaluate the developmental role of Dyx1c1 in the brain due to its association with dyslexia. However, further characterization of the protein needs to be done to assess its role in development. A good approach to characterize the function of Dyx1c1 protein is to generate a transgenic mouse model that lacks the protein. The work herein highlights the role of Dyx1c1 in mouse development and disease. In chapter 2, I show that the Dyx1c1 protein is important for the function of motile cilia and the absence of Dyx1c1 leads to ciliopathy phenotypes of hydrocephalus and *situs inversus*. It is thus hypothesized to play a role in the assembly of the outer and inner dynein arms

that are responsible for the motility of the cilia.

In chapter 3, I describe the localization and interactors (direct or indirect) of Dyx1c1 in order to evaluate its role in the ciliary dynein assembly process. With co-immunoprecipitation and mass spectrometric analysis, I found that Dyx1c1 interacts with heat shock proteins Hsp70, Hsp90 as well as T-complex chaperones (CCTs). In addition to these proteins, an interesting interactor Septin2 was identified that has been previously shown to be a protein of the ciliary transition zone regulating the trafficking of proteins in and out of the cilium. These findings strengthen the hypothesis that Dyx1c1, a protein that localizes to the cytoplasm of ciliated cells, is required for the assembly and transport of the axonemal dyneins.

In chapter 4, I describe a novel mutation that has been identified in Dyx1c1 that is known to cause PCD in Druze patient population. Using western blot analysis on the patients, I found that Dyx1c1 protein is expressed at the correct molecular weight in these patients. The interactions of Dyx1c1 with Ktu and Septin2 are reduced in the Dyx1c1 mutant condition, thus indicating a critical role of Dyx1c1 in the ciliary dynein assembly process.

In chapter 5, I identify the role of Dyx1c1 in the pre-assembly of axonemal dyneins. By co-immunoprecipitation and western blot analysis, I show that Dyx1c1 interacts with the outer dynein arm light chain subunits Dnal1 and Dnal4

as well as intermediate chain subunits Dnai1 and Dnai2. However, in the cytoplasm of the Dyx1c1 knockout tracheal epithelial cells, the interaction of Dnal1 and Dnal4 is markedly reduced indicating a role of Dyx1c1 in the assembly of these two proteins. Using a heterologous expression system, I show that Dyx1c1 is essential for the association of Dnal1 and Dnal4; and this interaction requires both the p23 and TPR domains of Dyx1c1.

In chapter 6, I provide a summary of the work performed in this thesis. I will identify unanswered questions suggested by these works and propose follow up studies to address them.

2. CHARACTERIZATION OF THE DYX1C1 KNOCKOUT MOUSE

2.1 Abstract

Dyx1c1 was the first gene associated with dyslexia susceptibility *(Taipale et al 2003).* While the results of RNAi experiments suggest a role in neuronal migration *(Wang et al 2006)*, and protein interaction studies suggest possible roles in chaperonin function *(Chen et al 2009)* and estrogen receptor trafficking *(Massinen et al 2009)*, a genetic test for the required functions of Dyx1c1 has been lacking. In order to elucidate the required functions of Dyx1c1, we have analyzed the phenotype of a Dyx1c1 knockout mouse in which exons 2,3 and 4 were deleted. Western blot analysis confirmed that the mutation results in a complete loss of Dyx1c1 protein expression. In breeding experiments between heterozygous mice the ratio of homozygous KO, heterozygous, and WT mice was 1:4:2, indicating possible embryonic lethality. The surviving Dyx1c1 knockout mice display severe developmental abnormalities that include *Situs Inversus*, a reversal in the typical left-right asymmetry of thoracic and abdominal organs and early onset hydrocephaly. These two phenotypes are often associated with Primary Ciliary Dyskinesia in mice. We therefore examined cilia structure and motility in the ventricles of knockout mice. Immunostaining for acetylated tubulin, and gamma tubulin indicated that the cilia of ependymal cells lining the lateral, third, and fourth ventricles were intact and not appreciably decreased in number. In contrast, live cell imaging and an Indian ink flow assay indicated a lack of ciliary motility. In WT mice, a cilia beat frequency of 7.5 beats/second was

observed in lateral, third and fourth ventricles using DIC video microscopy of brain slices. However, in Dyx1c1 KOs cilia were completely immotile and displayed no apparent beating. In an additional assay for the motility of cilia in the lateral ventricles a small volume of Indian ink was applied to the surface of the ventricle and the dispersion and flow of ink was imaged. In wt mice an anteriorly directed flow was apparent with an approximate velocity of 96 mm/sec, while in the KO mice the Indian ink showed only a passive diffusion in all directions at a rate of 6 mm/sec. When the ultrastructure of the WT and KO cilia was examined, we found that the inner and outer dynein arms that are required for the ciliary motility were missing in the KO. In sum, the analysis of the Dyx1c1 KO thus indicates that Dyx1c1 is required for motility of cilia.

2.2 Introduction

Cilia, hair-like organelles projecting from the surface of nearly all polarized cell types, serve essential roles in cellular signaling and motility. The basic structure of motile cilia and the related organelle flagella is evolutionarily conserved. In most motile cilia, a ring of nine peripheral microtubule doublets surrounds a central pair apparatus of single microtubules that connect to the nine peripheral doublets by radial spokes (9+2 structure). Motile monocilia present at the mouse node during early embryogenesis are an exception, lacking the central pair apparatus (9+0 structure)[72,134]. Distinct multi-protein dynein complexes attached at regular intervals to the peripheral microtubule doublets contain molecular

motors that drive and regulate ciliary motility. Specifically, ODAs are responsible for beat generation, whereas both the IDAs and the nexin link–dynein regulatory complexes (N-DRCs) regulate ciliary and flagellar beating pattern and frequency. Identifying the proteins responsible for the correct assembly of this molecular machinery is critical to understanding the causes of motile cilia–related diseases[134].

PCD (MIM 244400), a rare genetic disorder affecting approximately 1 in 20,000 individuals, is caused by immotile or dyskinetic cilia. Loss of ciliary function in upper and lower airways causes defective mucociliary airway clearance and, subsequently, chronic inflammation that regularly progresses to destructive airway disease (bronchiectasis). Organ laterality defects are also observed, with approximately half of individuals with PCD exhibiting situs inversus and, more rarely, situs ambiguus, which can associate with complex congenital heart disease. Dysfunctional sperm tails (flagella) frequently cause male infertility in individuals with PCD. Another consequence of ciliary dysfunction, particularly evident in mouse models, is hydrocephalus caused by disrupted flow of cerebrospinal fluid through the cerebral aqueduct connecting the third and fourth brain ventricles. Although ciliary dysmotility is not sufficient for hydrocephalus formation in humans owing to morphological differences between the mouse and human brains, the incidence of hydrocephalus, secondary to aqueduct closure, is higher in individuals with PCD[85,90,135].

Genetic analyses of individuals with PCD have identified several autosomal recessive mutations in genes encoding axonemal subunits of the ODA

complexes and related components. In addition, recessive mutations in CCDC39[96] (MIM 613798) and CCDC40[97] (MIM 613799) have been linked to PCD with severe tubular disorganization and defective nexin links. Mutations in the radial spoke head genes RSPH4A and RSPH9 as well as in HYDIN can cause intermittent or complete loss of the central-apparatus microtubules[135]. Two X-linked PCD variants associated with syndromic cognitive dysfunction and retinal degeneration are caused by mutations in OFD1 (MIM 311200) and RPGR (MIM 312610), respectively. Another functional class of proteins emerging from the identification of PCD-causing mutations are proteins involved in the cytoplasmic preassembly of both ODAs and IDAs, including those encoded by DNAAF2[60] (also known as KTU; MIM 612517), DNAAF1[104] (also known as LRRC50; MIM 613190), DNAAF3[102] (also known as C19orf51; MIM 614566) and the recently identified LRRC6[103] (MIM 614930).

DYX1C1 (MIM 608706) was initially identified as a candidate dyslexia gene, owing to both a single balanced translocation t(2;15)(q11;q21) coincidentally segregating with dyslexia in a family and subsequent SNP association studies[112]. Follow-up gene association studies have provided both positive and negative support for association with dyslexia. Taipale et al. (2003) showed that DYX1C1 is expressed nearly ubiquitously in adult tissues, including brain, and that the protein can be detected by immunocytochemistry in the nuclei and cytoplasm of neurons and glia in human neocortex. The protein domains of DYX1C1 include an N-terminal p23 and three C-terminal TPR domains. DYX1C1, when over-expressed in cell lines, can interact with Hsp70, Hsp90 and an E-3 ubiquitin

ligase, CHIP, suggesting that the protein may also be involved in the degradation of unfolded proteins[127,128]. Wang and colleagues performed the characterization of the developmental function of DYX1C1 by employing in utero RNAi in embryonic rat neocortex. The results from this study indicate that DYX1C1 plays a role in the migration of neocortical neurons and more specifically is required for the transition out of the multipolar stage of migration. Dyx1c1 RNAi decreased the migration of neurons causing them to accumulate in a multipolar stage of migration. The impairment was rescued by overexpression of Dyx1c1, and the C-terminal TPR domains were sufficient to rescue migration. Using truncation mutants, they found that the C-terminus of DYX1C1 biases the cellular localization of DYX1C1 to the cytoplasm, while the N-terminus alone can localize to the nucleus and cytoplasm in cell lines and in developing neurons[124,125]. Molecular and cellular analyses of DYX1C1 have indicated potential functional roles in estrogen receptor trafficking, and recent proteomic and gene expression studies have suggested a possible role in cilia[121,129,133].

2.3 RESULTS

2.3.1 Generation of Dyx1c1-mutant mice

To elucidate the biological functions of DYX1C1, we performed a forward genetic experiment by producing an allele of Dyx1c1 in mice in which exons 2–4 were deleted (**Fig. 2-1a**). Homozygous mutant mice ($Dyx1c1^{\Delta/\Delta}$) expressed no detectable DYX1C1 protein by immunoblot analysis of all tissues tested,

including brain and lung (**Fig. 2-2b**).

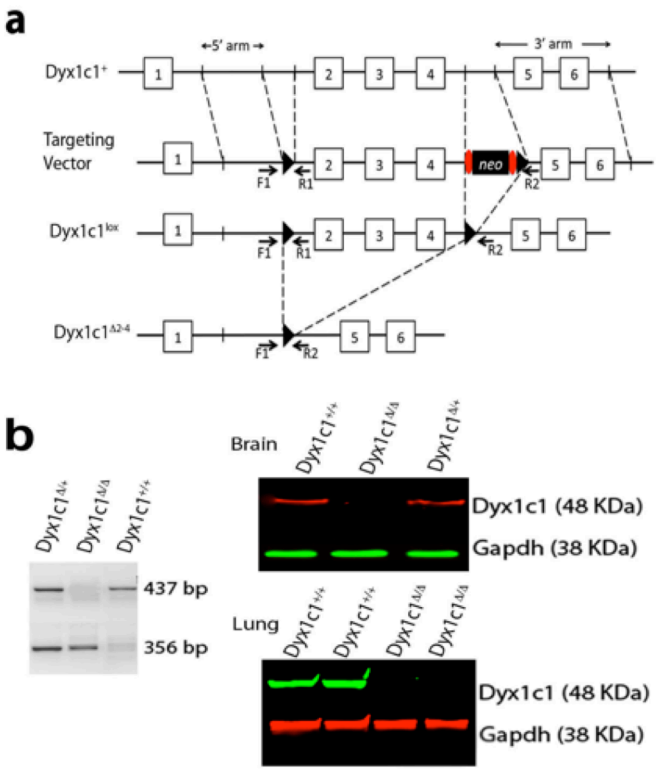

Figure 2-1: Targeted Deletion of Dyx1c1 *(**a**) Schematic of the strategy for producing the Dyx1c1 exon 2–4 deleted allele. A conditional knockout allele was inserted by homologous recombination and then exons 2–4 were deleted from the germline by breeding mice to an Hprt-Cre line of mice. (**b**) Left panel, PCR indicating the genotyping results from the wild-type (F1/R1, 437bp) and deleted alleles (F1/R2, 356bp). Right panels, Western blots show the presence of Dyx1c1 protein detected in brain and lung of wild-type (Dyx1c1$^{+/+}$), and heterozygous animals (Dyx1c1$^{\Delta/+}$), but missing from homozygous mutants (Dyx1c1$^{\Delta/\Delta}$).*

Mice heterozygous for the deletion allele were viable, fertile and not noticeably different from wild-type littermates. Homozygous mutant mice were recovered after birth from heterozygous breeding pairs at a rate deviating from the expected Mendelian ratio (295:570:87 for Dyx1c1$^{+/+}$:Dyx1c1 $^{\Delta/+}$:Dyx1c1$^{\Delta/\Delta}$, c = 128.017, P < 0.0001) but were recovered at early embryonic times (embryonic day (E)

6.5–12) at the expected Mendelian ratio (22:43:20, c = 0.105, P = 0.85), suggesting embryonic lethality of approximately two-thirds of homozygous mutants (**Fig. 2-2**).

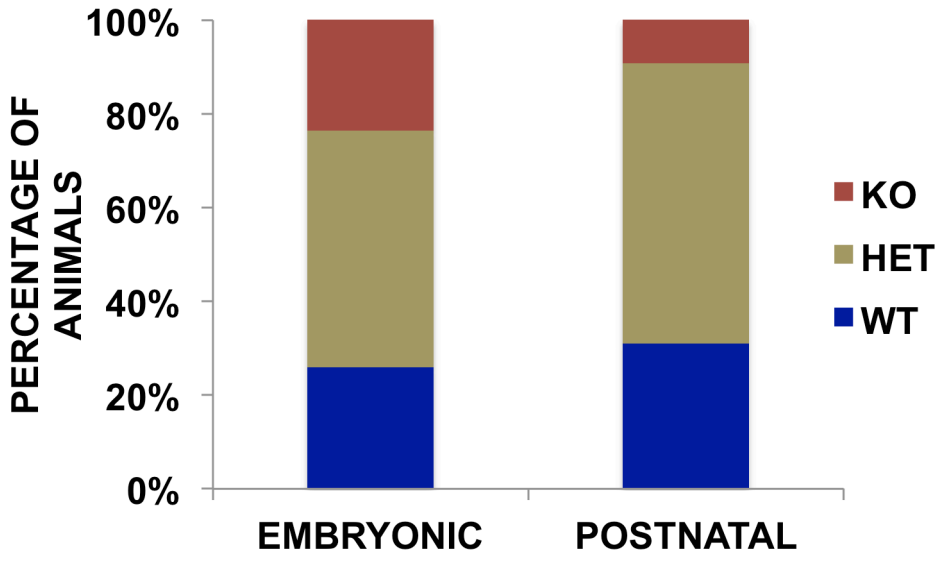

Figure 2-2 Recovery rates of the Dyx1c1 animals at embryonic and postnatal timepoints. *Graph shows the percentage survival of the wildtype, heterozygous and knockout animals.*

Homozygous mutants that survived after birth developed severe hydrocephalus by postnatal day (P) 16 (**Fig. 2-3**) and died by P21, similar to what has been described for other mouse mutants with defective motile cilia[3,39].

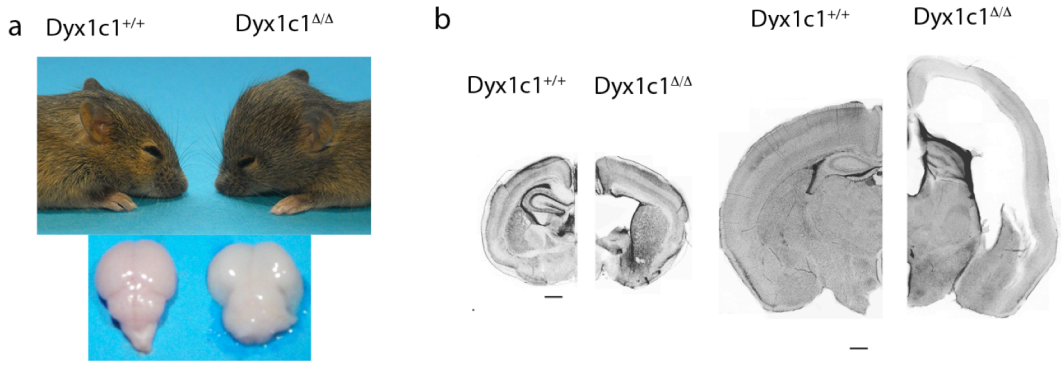

Figure 2-3: Dyx1c1 knockout mice exhibit hydrocephalus. *Characteristic domed crown in* Dyx1c1$^{\Delta/\Delta}$ *mice develops by P16 with the ventricles seen in coronal sections are greatly expanded in* Dyx1c1$^{\Delta/\Delta}$ *relative to* Dyx1c1$^{+/+}$ *mice. Scale bar, 250mm.*

In addition to hydrocephaly, postnatal homozygous mutant mice displayed laterality defects, with 59% of mutants (51/87) showing situs inversus totalis (a complete inversion of left-right asymmetry; **Fig. 2-4**), 17% (15/87) showing situs ambiguous with inverted heart and lung position relative to stomach and spleen or inverted stomach and spleen position relative to heart and lung, and 24% (21/87) showing situs solitus (normal left-right asymmetry).

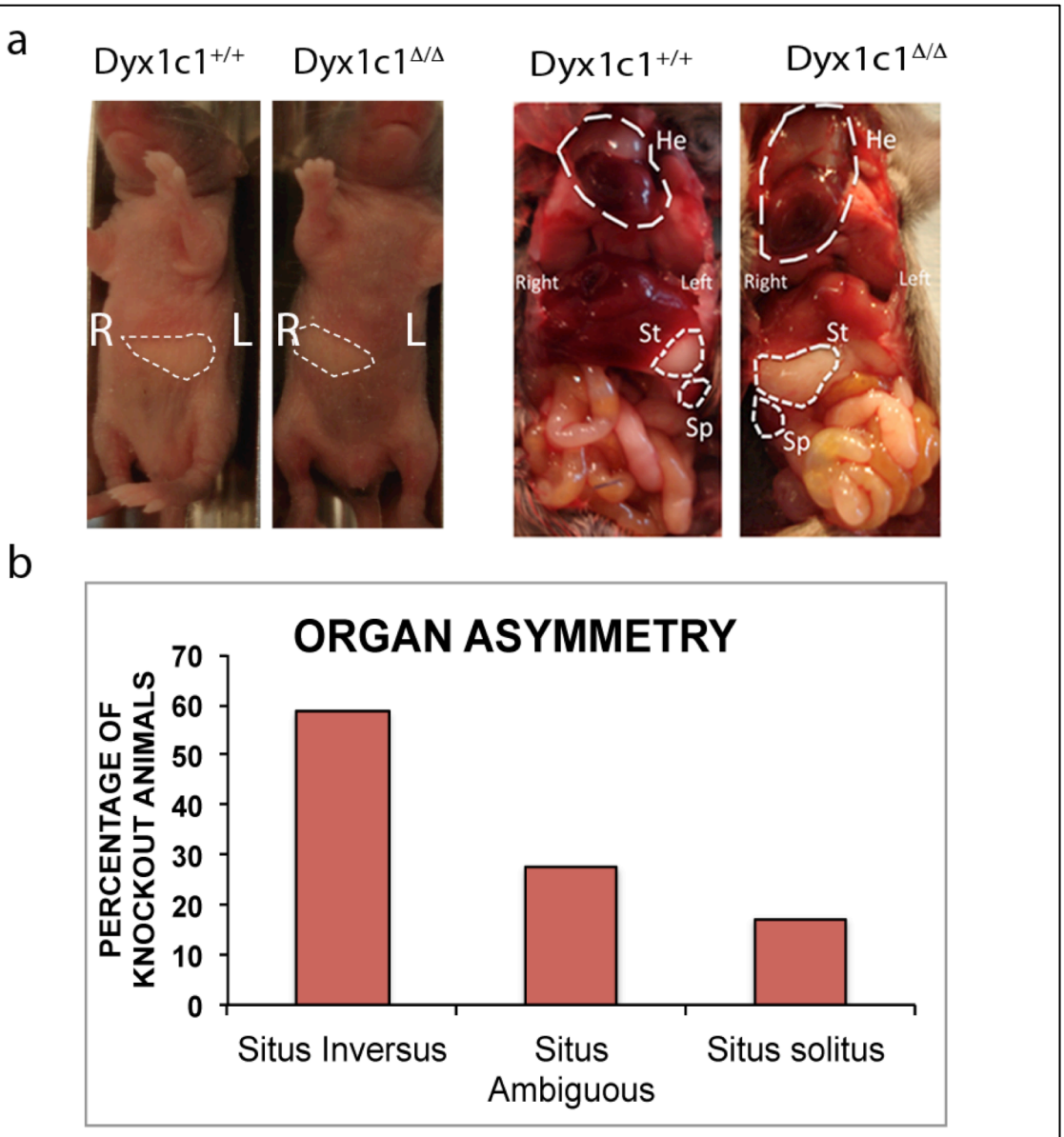

Figure 2-4: Dyx1c1 knockout mice exhibits situs inversus. *(a) Situs inversus in* Dyx1c1$^{\Delta/\Delta}$ *mice as seen in both the reversal of the milk filled stomach in neonates to the right side, and exposed viscera showing reversal of multiple organs including heart (He), stomach (St), and spleen (Sp). (b) Graph shows the organ symmetry of the knockout mice.*

Mutations that cause disruptions in left-right asymmetry in mice[40] are known to result from defects in the function of motile nodal monocilia and, more specifically, the loss of cilia-generated leftward flow across the node in early embryogenesis[40]. The typical phenotype for laterality mutants is a 1:1 ratio of situs inversus totalis and situs solitus, indicating a randomization of left-right patterning, although the inv mutant mouse has 100% of affected pups with situs inversus. Even if the ratio of situs inversus to situs solitus seen in surviving Dyx1c1-mutant mice deviates significantly from what would be expected for a 1:1 ratio of situs inversus to situs solitus (51:21, c = 12.5, P = 0.0004), this ratio was already observed in other mutants for left-right patterning, such as in Dnahc5-mutant mice[41].

2.3.2 Analysis of the nodal monocilia

Consistent with a role for DYX1C1 function in the embryonic node where left-right patterning is established in the mouse, it has been found by whole-mount in situ hybridization that Dyx1c1 expression in the early embryo (E7.5) was restricted to pit cells of the embryonic node. Recently, it was shown that knockdown of dyx1c1 results in phenotypes characteristically associated with cilia defects, such as body curvature, hydrocephalus, cystic kidneys and situs inversus[42]. In zebrafish, dyx1c1 is expressed in embryonic tissues that contain motile cilia[42], including Kupffer's vesicle, which is known to have an important role in establishing the left-right axis. We investigated the mutant mouse embryo at E7.5

and found no striking structural abnormalities compared to the wildtype embryo. However when we assessed the mutant mouse node, we found that some vesicle like structures were present on the node in addition to the monocilia (Fig 2-5). In contrast, the wildtype node did not show the presence of any vesicle like structures. The defective mouse node in the mutant could be due to the dysmotile cilia that cause aberrant flow of the extra-embryonic fluid containing morphogens required for the break of left-right asymmetry.

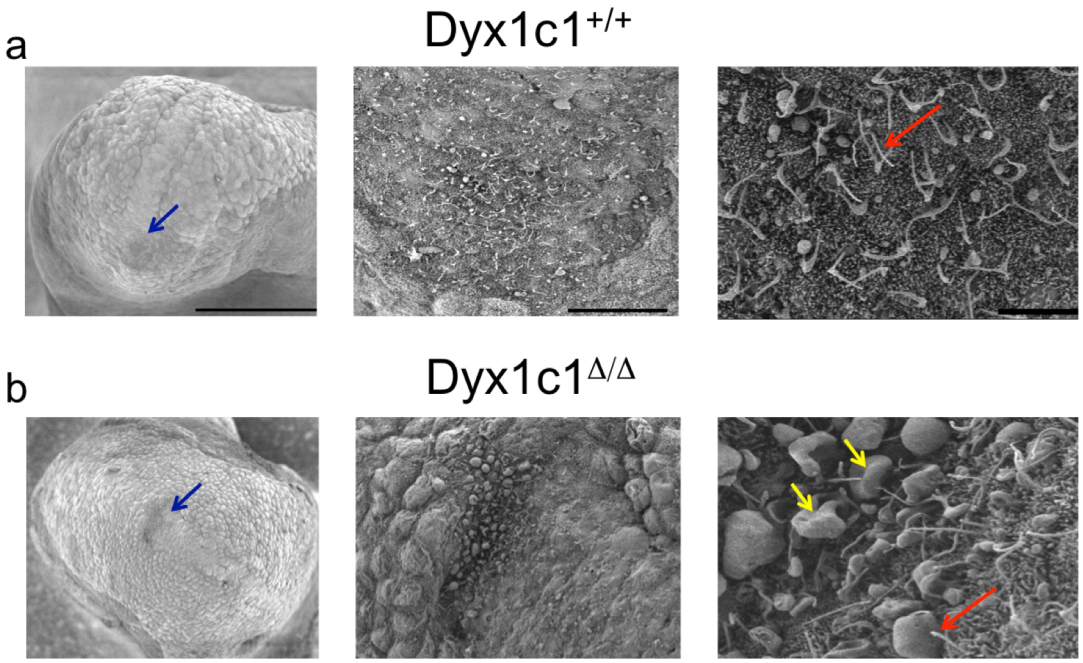

Figure 2-5 Dyx1c1 knockout mouse node is abnormal. Top panel (a) shows the wildtype E7.5 mouse embryo (left panel) and mouse node (middle, right panel). Bottom panel (b) shows the knockout E7.5 mouse embryo (left panel) and mouse node (middle, right panel). Blue arrows point to the node; red arrows point to the cilia; and yellow arrows point to vesicle-like depositions.

2.3.3 Analysis of ependymal cilia

Hydrocephalus and organ laterality defects are hallmarks of mutations that cause defects in ciliary motility in mice[1,3]. We therefore used light and electron microscopy as well as video-microscopy to determine whether DYX1C1 deficiency caused loss of motile cilia formation or loss of cilia. Cilia extending from mouse ependymal cells of the cerebral ventricles, visualized by light microscopy, appeared similar in length and distribution in Dyx1c1$^{\Delta/\Delta}$ and wild-type littermates (**Fig. 2-6a**). When immunofluorescence analysis on the was performed to look for the any abnormalities of the lateral ventricles; we found that markers for cilia (acetylated tubulin), cell margins (beta catenin) and basal bodies (gamma tubulin) were present on lateral ventricles of Dyx1c1$^{\Delta/\Delta}$ and wild-type littermates without any significant differences in structure (**Fig 2-6b**).

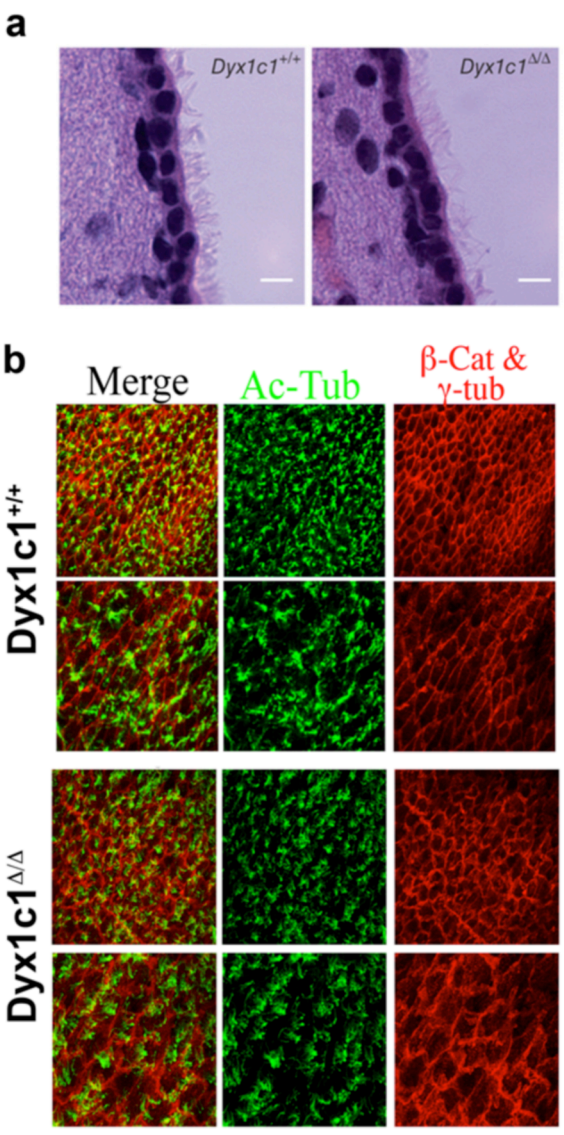

Figure 2-6 Cilia are present on the brain ependymal surface of the Dyx1c1 knockout mice. *(**a**) H&E stained sections of the cerebral ventricles show the presence of cilia on the surface of the ependymal cells in both* Dyx1c1$^{+/+}$ *and* Dyx1c1$^{\Delta/\Delta}$ *mice. (**b**) Immunofluorescence analyses of lateral ventricles stained for acetylated tubulin (green), and beta-catenin and gamma tubulin (red).*

We used live-cell imaging to directly assess cilia-mediated fluid flow and ciliary motility on the ependymal surface in Dyx1c1$^{\Delta/\Delta}$ mice. We prepared explants or slices of the lateral ventricular surfaces from Dyx1c1$^{\Delta/\Delta}$ and wild-type mice at P6. Ependymal cilia in wild-type mice continued to beat vigorously in these preparations and created a directional fluid flow across the surface that could be visualized by the displacement of a small volume of India ink pressure-injected onto the ependymal surface. This flow was present in all wild-type mice tested (n = 6; **Fig. 2-7a**) but was completely absent in tissue obtained from all Dyx1c1$^{\Delta/\Delta}$ mice tested (n = 4; **Fig. 2-7b**).

We next examined the motility of ependymal cilia in coronal brain slices of wild-type and Dyx1c1$^{\Delta/\Delta}$ mice by infrared differential interference contrast (DIC) videomicroscopy. Cilia at the ependymal surface in wild-type and heterozygous mice (n = 8) were found to beat at a frequency of approximately 9 beats/s (34 °C), whereas cilia on ependymal cells from all Dyx1c1$^{\Delta/\Delta}$ examined (n = 4) lacked ciliary beating (**Fig. 2-7b**).

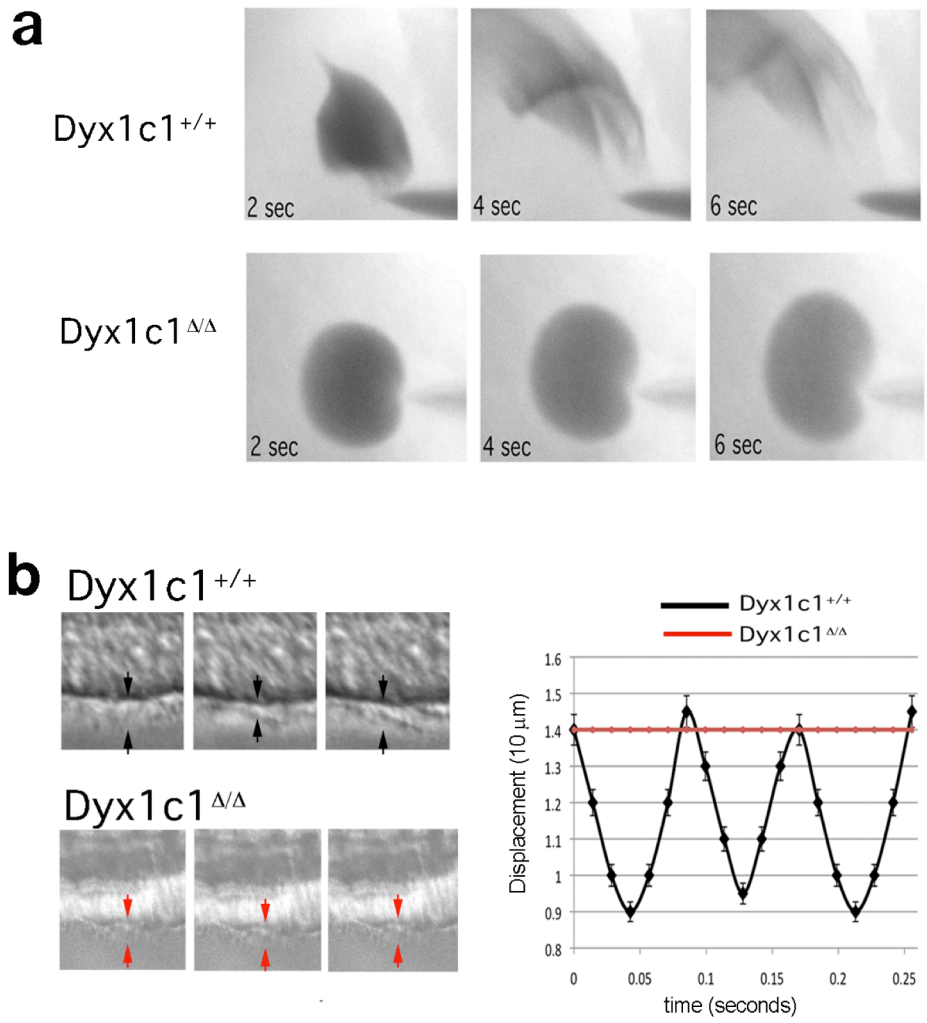

Figure 2-7: Motile cilia of the Dyx1c1 knockout mice are dysfunctional. (a) *Flow of fluid (Indian ink) across the ependymal surface in brain ventricle cup preparations from a* Dyx1c1$^{+/+}$ *and* Dyx1c1$^{\Delta/\Delta}$ *at mice P6. Directional flow was rapid across the surface of* Dyx1c1$^{+/+}$ *ependymal epithelia, while only non-directional passive diffusion was observed on ependymal surfaces in* Dyx1c1$^{\Delta/\Delta}$*. The starting point for the fluid is at the end of the pipette tip, seen bottom right. (b) Snapshots of the cilia motility in wildtype (top panel) and knockout (bottom panel). The right panel shows the displacement of the cilia.*

2.3.4 Analysis of Dyx1c1-mutant respiratory cilia

To assess the ultrastructure of respiratory cilia in mutants, we obtained transmission electron micrographs of tracheal cilia. As on the ependymal surface, tracheal cilia were abundant in both wild-type and Dyx1c1$^{\Delta/\Delta}$ epithelial cells (**Fig. 2-8a**), but, unlike tracheal cilia in wild- type mice, cilia in the Dyx1c1$^{\Delta/\Delta}$ trachea were surrounded by cellular debris and mucus (**Fig. 2-8a**). We further examined the ultrastructure of tracheal cilia in cross-sections by transmission electron microscopy (TEM). Using TEM, we observed that tracheal and brain ependymal cilia in wild-type and mutant mice had typical 9+2 microtubular structure with intact radial spokes (**Fig. 2-8b**). In contrast, cilia in Dyx1c1$^{\Delta/\Delta}$ mice lacked both ODA and IDA structures in respiratory cilia (**Fig. 2-8b**). Thus, the phenotype caused by loss of function of Dyx1c1 is a severe ciliary motility defect associated with absent axonemal ODA and IDA structures.

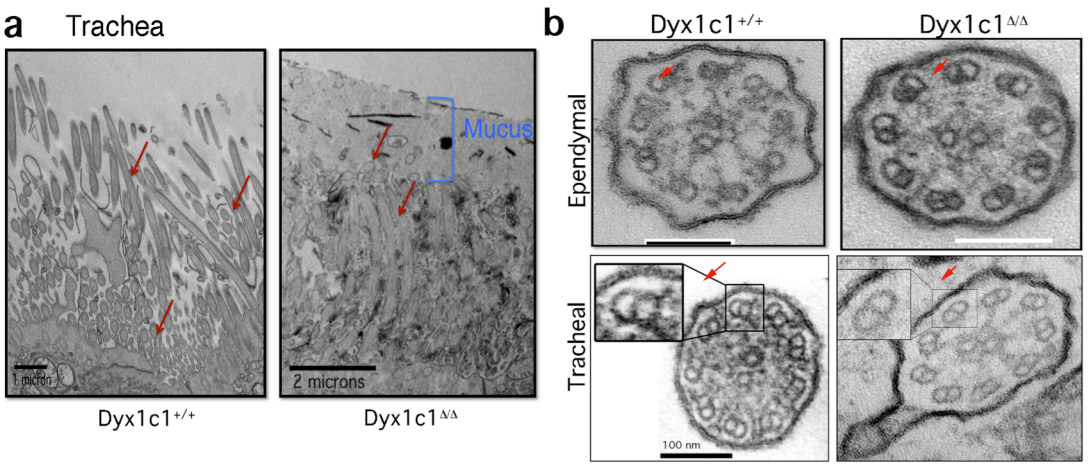

Figure 2-8: Dyx1c1 knockout motile cilia lack outer and inner dynein arms. *(a) TEM images of cross-sections through the trachea of wild-type and* Dyx1c1$^{\Delta/\Delta}$*. Abundant cilia were present in each, but cilia structures (red arrows) in the* Dyx1c1$^{\Delta/\Delta}$ *trachea are surrounded by cellular debris and mucus. (**b**) TEM cross-section images of ependymal and tracheal cilia in* Dyx1c1$^{+/+}$ *and* Dyx1c1$^{\Delta/\Delta}$ *mice. The 9+2 microtubular structure was well preserved in* Dyx1c1$^{\Delta/\Delta}$*, except that the outer and inner dynein arms were lacking in tracheal cilia. The scale bars represent in (**a**) 1µm (left panel) and 2µm (right panel) and in (**b**) 0.1 µm.*

2.4 Discussion

Dyx1c1 was previously identified as a candidate dyslexia susceptibility gene that plays an important role in the neuronal migration[124]. Studies performed to characterize the molecular function of Dyx1c1 in zebrafish showed that Dyx1c1 has a role in ciliary function[133]. Here we explore the role of Dyx1c1 during development, for which we generated a transgenic mouse wherein the exons 2,3 and 4 of the Dyx1c1 gene are deleted. The Dyx1c1 knockout mouse thus

generated was verified by genotyping to confirm the deletion of the exons 2,3 and 4. We further performed western blot analysis on the protein lysates obtained from the brain and lung tissues of the Dyx1c1 wildtype, heterozygous and knockout mice. We observed that the Dyx1c1 protein was detected at the molecular weight of 48KDa in the WT as well as heterozygous animals, however the KO mice lacked the expression of Dyx1c1. The KO mice were found to die perinatally, while those that survived after birth exhibited a deviation from the expected Mendelian ratio (3:6:1 for WT:HET:KO) but were recovered at embryonic times at the expected Mendelian ratio of (1:2:1 for WT:HET:KO).

Interestingly, the surviving KO mice exhibited two PCD-like phenotypes of hydrocephalus and *situs inversus*. 59% of the mutant mice display situs inversus totalis, 17% show situs ambiguous while 24% are situs solitus. The laterality defects are known to result from the defects in the structure or function of motile nodal monocilia especially due to the loss of the extra-embryonic nodal flow proposed to carry morphogens responsible for the break of left-right asymmetry patterning. When the E7.5 embryonic mouse node of the Dyx1c1 WT and KO mouse was examined, we found that monocilia were present on the surface of the epithelial cells of the node in both the conditions; however the KO displayed a deposition of vesicle-like structures on the nodal surface indicative of a faulty nodal flow and abnormal ciliary function.

The KO mice also developed severe hydrocephalus by P16 as evident from the thinning of the cortex and enlarged ventricles; these animals die by P21. Hydrocephalus could develop due to one or many of the following causes: i)

absence of cilia on the ependymal cells of the brain, ii) cilia are present but they are immotile, iii) abnormal production of the CSF, and iv) aqueductal stenosis. In order to understand the cause of hydrocephalus in the KO mice, we investigated whether the cilia were present on the ependymal cells of the ventricles and found by immunofluorescence analysis that tufts of cilia were present on the KO ependymal cells. However, live cell imaging and Indian ink assays showed that the KO ependymal cilia were non-motile. This phenotype of immotile cilia was consistent with the cilia of the tracheal epithelial cells of the KO, where we found an accumulation of mucus or debris on the surface of the cilia.

Motile cilia defects are observed most commonly due to the defects in the ciliary ultrastructure components such as the outer and inner dynein arms, radial spokes or nexin links[76]. Transmission electron microscopy performed on the KO ependymal and tracheal cilia revealed an absence of both the outer and inner dynein arms that are known to be critical for ciliary motility.

In summary, we show that the Dyx1c1 knockout mice exhibit PCD-like phenotypes, which resulted in axonemal defects of the dynein arms and ciliary dysmotility. The association between Dyx1c1 and PCD-like phenotypes was also recently reported in zebrafish, thus confirming the importance of Dyx1c1 in cilia structure and function[133,136,137]. Further studies are required to characterize the localization of the protein in ciliated cells in order to understand its role in ciliary motility. Also, identification of the interactor partners of Dyx1c1 would shed light on the functional pathway. Mutations in genes that are either axonemal dynein subunits of the ODA or IDA have been previously identified that cause PCD in

humans. Additionally, mutations in genes that are known to preassemble the outer and inner dynein arms in the cytoplasm, like DNAAF1, DNAAF2, and DNAAF3, or their transport to the basal bodies, similar to ODA16 have also been defined that are known to cause PCD[102,104,138,139]. Thus, Dyx1c1 can be added to the rapidly growing list of genes that when mutated cause PCD. Our data now suggest that Dyx1c1 is a novel dynein axonemal assembly factor Dnaaf4.

2.5 Methods

2.5.1 Gene targeting and genotyping of *Dyx1c1*$^{\Delta/\Delta}$ mice.

Mice carrying the *loxP*– exon 2–4–*loxP* conditional allele of *Dyx1c1* (*Dyx1c1*$^{flox2-4}$) were generated by the University of Connecticut Health Center Gene Targeting and Transgenic Facility. Embryonic stem cells harboring a *loxP*-flanked allele of exons 2–4 of *Dyx1c1* were produced by electroporating mouse embryonic stem (ES) cells (129S6) with a targeting construct designed to replace exons 2–4 and flanking intronic sequence through homologous recombination. We screened 96 ES cell clones by PCR for correctly targeted colonies. A single positive colony was expanded and used for embryo reaggregation to produce five chimeric mice. Three of these mice were shown to transmit the targeted allele through the germ line to offspring in a cross with C57BL/6J mice. The *PGK-Neo* cassette in the targeting construct was then removed by crossing these mice with *129S4/SvJaeSor-Gt(ROSA)26Sor*$^{tm1(FLP1)Dym}$*/J* mice (The Jackson Laboratory). These offspring were used to generate a colony of *Dyx1c1*$^{flox2-4/flox2-4}$ mice. To

generate *Dyx1c1*$^{del2–4/del2–4}$ (*Dyx1c1*$^{\Delta/\Delta}$) mice with a deletion of exons 2–4, we crossed *Dyx1c1*$^{flox2–4/flox2–4}$ mice with hypoxanthine-guanine phosphoribosyltransferase (*Hprt*)-*cre* mice, *C57B6/6-Hprtt*$^{m1(cre)Mnn}$*/J* (University of Connecticut Health Center). Genotyping was subsequently performed by PCR using two pairs of primers (Fig. 1a and Supplementary Table 4). Animal procedures were performed under protocols approved by the Institutional Animal Care and Use Committee of the University of Connecticut and conform to US NIH guidelines.

2.5.2 Immunohistochemistry of mouse tissue.

Mice were perfused transcardially with 0.9% saline followed by 4% paraformaldehyde (Electron Microscopy Science) in 1× PBS. Brains were removed, fixed overnight in the same fixative at 4 °C and washed in 1× PBS three times for 40 min the next day before cutting into 50-µm sections with a vibratome (VT-1000S, Leica). Nuclei were counterstained with Hoechst 33342 (2 µg/ml in PBS; Sigma). Stained sections were washed for 10 min in PBS, coverslips were applied using Prolong Gold Antifade (Invitrogen), and images were acquired on a Carl Zeiss Axiovert 200M inverted microscope with an ApoTome attachment and Axiovision 4.6 software (Carl Zeiss). Whole mounts of the entire lateral wall of the lateral ventricles were prepared as described previously[48], fixed overnight in 4% paraformaldehyde in PBS at 4 °C and washed in 1× PBS three times for 40 min the next day. They were then permeabilized with 0.1% Triton X-100 (Sigma) in PBS for 10 min, blocked in 10% goat serum

(Invitrogen) in PBS and 0.1% Triton X-100 for 1 h, and incubated with the following primary antibodies: mouse antibody to acetylated tubulin (1:500 dilution; Sigma, T6793), rabbit antibody to β-catenin (1:100 dilution; Cell Signaling Technology, 9562) and mouse antibody to γ-tubulin (1:500 dilution; Sigma, T6557). After washing three times in PBS, tissues were incubated with appropriate Alexa Fluor dye–conjugated secondary antibodies (Goat Anti-Rabbit 488 (A11008), Goat Anti-Mouse 488 (A11001), Goat Anti-Rabbit 568 (A11011) and Goat Anti-Mouse 568 (A11031), Invitrogen) at a dilution of 1:400 for 1 h. Tissues were washed in PBS and incubated for 5 min in 2 μg/ml Hoechst 33342 (Sigma) for counterstaining of nuclei. Secondary antibodies alone were used as a control. Whole mounts were placed onto depressed glass slides, and cover slips with CoverWell imaging chambers (Grace Bio-Labs) were applied. Samples were imaged either on a Carl Zeiss Axiovert 200M inverted microscope with an ApoTome attachment and Axiovision 4.6 software (Carl Zeiss) or on a Leica TCS SP2 confocal laser scanning microscope.

2.5.3 Transmission Electron Microscopy (TEM)

To collect brains, mice (12 d old) were perfused transcardially with 0.9% saline followed by 2% paraformaldehyde/2.5% glutaraldehyde in 0.1 mM phosphate buffer. Brain samples were further fixed by immersion overnight in 2% paraformaldehyde/2.5% glutaraldehyde in 0.1 mM phosphate buffer and were washed in phosphate buffer three times for 40 min per wash. Sections were postfixed with 2% OsO_4 in 0.1 mM phosphate buffer for 1.5 h and were dehydrated through a graded ethanol series. After dehydration, tissues were

washed twice in acetone and embedded in epoxy resin in capped inverted Beem capsules. Thin sections were cut with a diamond knife, placed onto Formvar-coated slot grids and heavy metal stained with uranyl acetate and lead citrate. Trachea tissues were directly dissected without perfusion and were fixed by immersion overnight in 2% paraformaldehyde/2.5% glutaraldehyde in 0.12 mM phosphate buffer. They were washed in phosphate buffer three times (60 min in total), postfixed in 1% OsO4 and 0.8% potassium ferricyanide in 0.12 M phosphate buffer for 1 h, dehydrated through a graded ethanol series, rinsed twice in acetone and embedded in epoxy resin. Thin sections were cut with a diamond knife, placed on copper grids and heavy metal stained with ethanolic uranyl acetate and Sato's lead citrate. Electron micrographs were captured using an FEI Tecnai 12 Biotwin TEM equipped with a side-mounted AMT XR-40 CCD camera.

2.5.4 Scanning electron microscopy

Wild-type and mutant mouse embryos (E7.5) were collected and fixed in 1.5% paraformaldehyde/1.5% glutaraldehyde in 0.10 M sodium cacodylate containing 0.05 M NaCl overnight at 4 °C. Samples were postfixed with 2% OsO4 in the same buffer overnight and were dehydrated using a graded ethanol series. Specimens were dried in a Polaron E3000 Critical-Point Dryer and mounted onto aluminum specimen mounts (Ted Pella) using carbon tape and silver paint (Ernest F. Fullam). Each mount was sputter coated with gold palladium (60% gold, 40% palladium) using a Polaron E5100 Sputter Coater. Samples were

examined and photographed using a LEO DSM982 field emission scanning electron microscope.

2.5.5 Protein blots of brain, lung and trachea lysates

Wild-type and mutant mouse brains and lungs were collected and lysed in RIPA Buffer (Sigma) supplemented with 1× Protease Inhibitor Cocktail (Sigma). For tracheal and lung preparation, tissues were dissected and carefully separated from the surrounding tissues. Samples were homogenized using a tissue homogenizer and cleared by centrifugation at 10,000*g* for 10 min. Proteins were separated on 10% SDS-PAGE minigels and then transferred to Immobilon (Millipore) membrane for protein blotting. For detecting DYX1C1 protein, the antibody to N-terminal DYX1C1 (Sigma, SAB4200128) was used at a dilution of 1:200; antibody to GAPDH (Sigma, G8795) was used at a 1:1,500 dilution as a loading control. LI-COR Odyssey infrared secondary antibodies (goat antibody to mouse 680 (926-32220), goat antibody to mouse 800 (926-32210) goat antibody to mouse 680 (926-32221) and goat antibody to mouse 800 (926-32211)) were used at dilutions of 1:10,000. All blots were imaged and analyzed using a LI-COR Odyssey Scanner and Software.

2.5.6 Videomicroscopy of ependymal flow and cilia in mice

P6–P10 wild-type and mutant mice were deeply anesthetized with isoflurane and were then decapitated. Brains were rapidly removed and immersed in ice-cold oxygenated (95% O2 and 5% CO2) dissection buffer containing 83 mM NaCl, 2.5 mM KCl, 1 mM NaH2PO4, 26.2 mM NaHCO3, 22 mM glucose, 72 mM sucrose,

0.5 mM CaCl2 and 3.3 mM MgCl2. The lateral wall of the lateral ventricle was dissected using a fine scalpel and forceps and was immediately observed in a chamber containing buffer at 37 °C. For visualization of flow, a small amount of India ink was placed on the surface of the lateral wall of the dissected ventricle. Movement of India ink was observed and recorded using infrared DIC microscopy (E600FN, Nikon) and a CCD camera (QICAM, QImaging, 120 frames per second (fps)). For direct observation of cilia movement, mouse brains were harvested as above, and coronal slices (400 μm) were cut using a vibratome (Leica, VT1200S). Slices from the third ventricle through the fourth ventricle were visualized using infrared DIC and a CCD camera. Images were analyzed with ImageJ software (NIH).

3. CELLULAR LOCALIZATION OF DYX1C1 AND IDENTIFICATION OF ITS INTERACTION PARTNERS

3.1 Abstract

Dyx1c1 knockout mice display Primary Ciliary Dyskinesia (PCD) like phenotypes that include *Situs Inversus* and early onset hydrocephaly. Live cell imaging and an Indian ink flow assay indicated a lack of ciliary motility in the knockout mice compared to the wildtype. Ultrastructural and immunofluorescence analyses of Dyx1c1 mutant motile cilia in mice showed disruptions of outer and inner dynein arms (ODAs and IDAs, respectively). Previous protein interaction studies suggest possible roles for Dyx1c1 in chaperonin function (Chen et al 2009). In this study, we determine the interaction partners of Dyx1c1 to understand its role in ciliary motility. Immunoprecipitation and mass spectrometric analysis experiments reveal that the Dyx1c1 interactome is enriched for proteins of the categories molecular chaperones as well as cytoskeletal proteins. We find by immunoprecipitation experiments that Dyx1c1 interacts with heat shock proteins and T-complex chaperones. Dyx1c1 also interacts with Septin2, a protein of the ciliary transition zone with implicated function in ciliary protein trafficking. Assessment of localization of Dyx1c1 identified that Dyx1c1 localizes to the cytoplasm of nasal respiratory epithelial cells. We performed tracheal deciliation to obtain axonemal and cilia-stripped tracheal fractions and further tested the lysates for the presence of the ODA and IDA subunits. Interestingly, we found that there was a reduction in the IDA subunit Dnali1 as well as ODA intermediate

chains Dnai1, Dnai2 and light chains Dnal4 and Dnal1. Our observations thus lead to the hypothesis that Dyx1c1 plays a role in cytoplasmic assembly of ciliary dyneins and/or their transport to the ciliary transition zone.

3.2 Introduction

Dyx1c1, a 420 amino acid protein, was first identified as a candidate dyslexia susceptibility gene[112]. The protein is ubiquitously expressed in brain, amongst other tissues, and is found to localize to the in the nuclei and cytoplasm of neurons and glia in human neocortex. The protein domains of DYX1C1 include an N-terminal p23 and three C-terminal TPR domains. This combination of a p23 and TPR domains is shared with Sugtl, a protein known to play a role in kinetochore assembly in yeast, suggesting a potential role in cell division or cell dynamics. DYX1C1, when over-expressed in cell lines, can interact with Hsp70, Hsp90 and an E-3 ubiquitin ligase, Chip, suggesting that DYX1C1 may also be involved in the degradation of unfolded proteins[127,128]. At its C-terminal, there are three tetratricopeptide domains (TPR) which function in protein-protein interactions.

To elucidate the biological functions of Dyx1c1, exons 2-4 of Dyx1c1 were deleted in mice. No detectable Dyx1c1 protein expression was observed by in all tissues tested, including brain and lung. The knockout mouse exhibited PCD-like phenotypes of situs inversus and hydrocephalus; both characterized by defects of motile cilia. Light microscopy revealed the presence of cilia on the surface of

the brain ependymal cells; however these cilia were completely immotile in the KO as evidenced by the videomicroscopy analysis. Analysis into the ultrastructural defects of the cilia exhibited an absence of both the inner and outer dynein arms (IDA and ODA) that are responsible for the motility of the cilia[140].

Nonstructural cilia-associated proteins have been found to be mutated in PCD individuals and result in the absence of outer and inner dynein arms. These mutations involve proteins that are considered to function in cilia assembly or "preassembly" pathways. Identification of the involvement of these proteins has prompted research into the mechanisms of cilia biogenesis especially into the following processes: intra-axonemal transport, transfer into the cilium, and cytoplasmic preassembly[56,141]. The first PCD-associated preassembly protein found was DNAAF2, the loss of which lead to complete absence of outer and inner dynein arms. Localized within the apical region of the cell cytoplasm, DNAAF2 interacts with Hsp90 and DNAI2 to facilitate assembly or dynein complex transport into the cilia[138]. Mutations in the proteins DNAAF1 and DNAAF3 caused outer dynein arm defects in patients with PCD[102,104]. Evidence for assembly roles of these proteins is substantiated in mutant cells where components of the dynein arm complex were found to either accumulate or deplete from the mutant cytoplasm leading to a failure in their transport into the ciliary axoneme. Mutations in *LRRC6*, a protein that is found in the cytoplasm but colocalizes to the basal bodies, also lead to PCD[142].

Identification of the localization of Dyx1c1 will help us understand which of the cilia biogenesis processes such as intra-axonemal transport, transfer into the cilium, or cytoplasmic preassembly it is involved in. Also the previously defined assembly factors function by interacting with the chaperones and the axonemal dynein subunits of the dynein arms themselves. It is hence required to identify the interaction partners of Dyx1c1 to detail its role in the ciliary motility. In this study, we perform immunofluorescence analysis to find that Dyx1c1 localizes to the apical cytoplasm of the ciliated cells. Furthermore, mass spectrometric analysis identified the interactome of Dyx1c1, wherein the chaperone category of proteins was enriched followed by the cytoskeletal proteins. We confirmed the interaction of Dyx1c1 with the mass spectrometry (MS)-identified proteins like the heat shock proteins Hsp70 and Hsp90; CCTs and Septin 2. We found that the TPR domains of Dyx1c1 are necessary for mediating the interaction between Hsp70 and CCTs; whereas the Hsp90 interaction was mediated via the p23 domain. We thus hypothesize that Dyx1c1 acts as a co-chaperone assisting in the cytoplasmic preassembly of the axonemal dyneins and their subsequent transport to the base of the cilium at the transition zone.

3.3 Results

3.3.1 Sub-cellular localization of Dyx1c1

To characterize the functional role of Dyx1c1 in ciliary motility, it is necessary to analyze the expression of Dyx1c1 in the ciliated tissues. Also, the phenotypes

described above as well as previously reported interactions between exogenously expressed DYX1C1 protein and molecular chaperones suggested to us that DYX1C1 might function as a newly identified axonemal dynein assembly factor. We found by immunofluorescence that mouse Dyx1c1 protein was located in the cytoplasm of respiratory epithelia (**Fig. 3-1**).

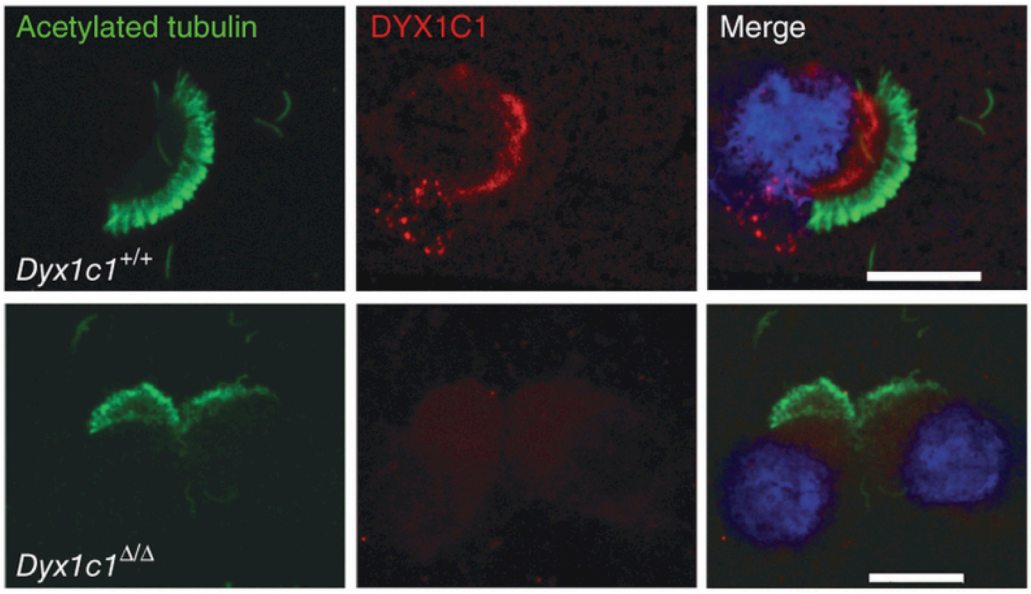

Figure 3-1: Dyx1c1 localizes to the cytoplasm of ciliated epithelial cells. *Immunofluorescence analyses of mouse nasal epithelial cells stained for acetylated tubulin (green) and Dyx1c1 (red). In* Dyx1c1$^{+/+}$ *mice, Dyx1c1 localizes to the cytoplasm of the epithelial cells and partly to the basal bodies but is absent in the cilia. In the mutant, Dyx1c1 is absent from the cytoplasma. Nuclei were stained with Hoechst 33342 (blue).*

In order to confirm the cytoplasmic localization of Dyx1c1; we developed a protocol for separation of the ciliary axonemes from the trachea of Dyx1c1

wildtype and knockout mouse. After harvesting tracheas in cold PBS, they were then incubated in chilled buffer containing 20mM calcium that induces deciliation of the trachea. The mechanism underlying Ca^{++} induced deciliation involves a calcium-binding protein centrin, which is a part of the stellate fibers of the transition zone, contraction of which causes the severing of microtubules at the transition zone. The region of the detached cilia seals over, minimizing the protein leakage out of the cell body[87]. The tracheas were then separated from the buffer containing the ciliary axonemes, and incubated in lysis buffer to obtain the cytoplasmic fraction that contains the trachea stripped of the axonemes. The axonemal fraction was further spun down at low speed to pellet any cellular debris. The pellet is discarded and the axoneme-containing buffer is further spun down at high speed for about 30 min to pellet the axonemes, which are then incubated in lysis buffer to get the axonemal lysate.

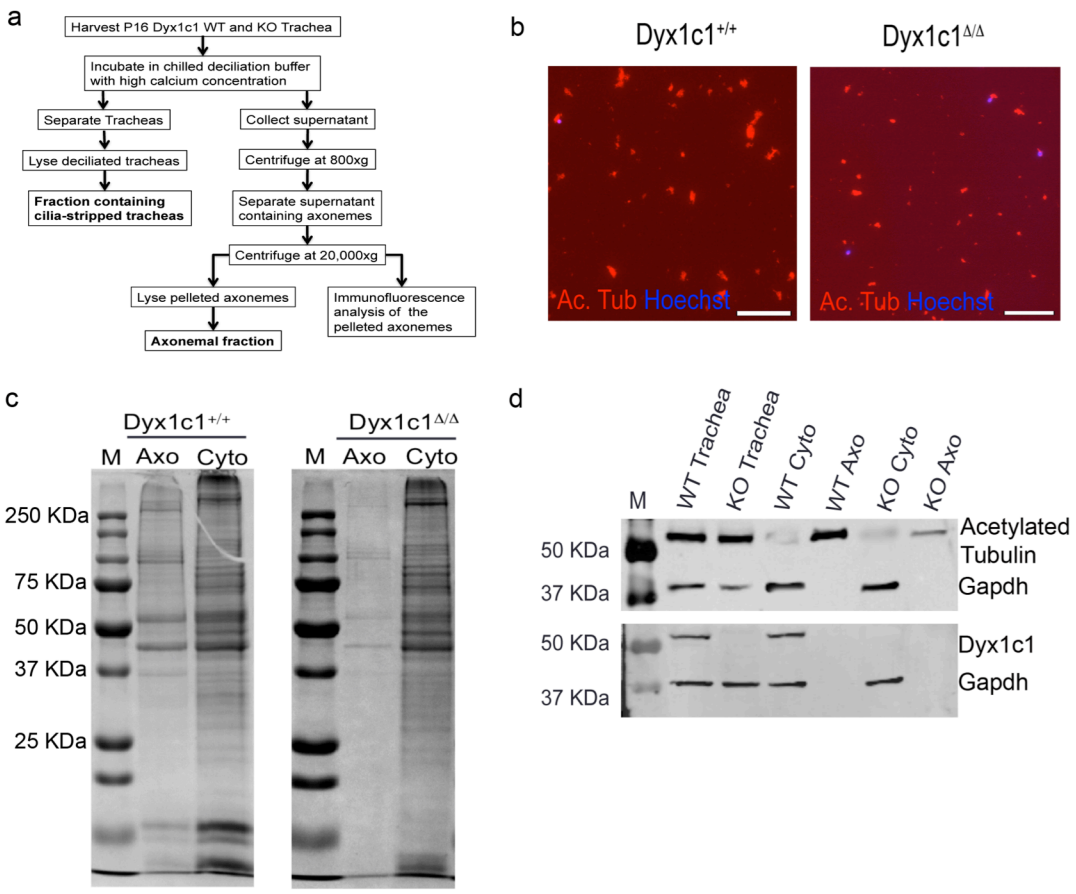

Figure 3-2: Deciliation of Dyx1c1 wildtype and knockout trachea (a) Deciliation workflow. (b) Immunofluorescence analysis of the axonemal fraction of the wildtype (left panel) and knockout (right panel) using anti-acetylated tubulin (cilia, red) and Hoechst (nuclear stain, blue). (c) Coomassie stained gel showing the axonemal and deciliated tracheal lysates of the wildtype and knockout. (d) Western blot probed with acetylated tubulin, Gapdh (control) and Dyx1c1. Axo: axonemal fraction; Cyto: cytoplasmic fraction.

We thus obtain two fractions after the deciliation workflow (**Fig. 3-2a**): i) cytoplasmic fraction containing the trachea stripped off the ciliary axoneme and ii) axonemal fraction consisting of the ciliary axoneme. The separated axonemes were analyzed for their purity by using immunofluorescence analysis (**Fig. 3-2b**). It was observed that there was little to no contamination of the cells in the axonemal preparation. The deciliation was confirmed by Coomassie staining (**Fig. 3-2c**) and western blot (**Fig. 3-2d**). Western blot was performed using lysates of the whole trachea, cytoplasmic extract, and axonemal extract of both the Dyx1c1 wildtype and knockout, and the blot was stained with acetylated tubulin (a marker for cilia), Gapdh, as well as Dyx1c1 (**Fig. 3-2d**). We found that the wildtype and knockout axonemal fraction expressed acetylated tubulin with little contamination of the Gapdh-containing cytoplasmic fraction and vice-versa; whereas the whole trachea from the Dyx1c1 wildtype and knockout mice showed the presence of both Gapdh and acetylated tubulin. We also showed that Dyx1c1 is present in the cytoplasmic fraction of the wildtype trachea and absent from the wildtype axonemal and knockout cytoplasmic as well as axonemal fraction. Gapdh was used as the marker for the cytoplasmic fraction (**Fig. 3-2d**).

3.3.2 Identification of the interaction partners of Dyx1c1

To categorize the molecular function of Dyx1c1 more completely in respiratory tissue, we defined the protein interactome of Dyx1c1 in mouse trachea by co-immunoprecipitation and tandem mass spectrometry. We prepared input extracts for co-immunoprecipitation from the tracheal tissue of either wildtype or mutant mice and found that these appeared similar in protein composition, as evaluated

by Coomassie staining after SDS-PAGE. After co-immunoprecipitation with antibodies to Dyx1c1, Coomassie-stained protein bands were apparent in preparations from wild-type extracts but not in those generated from mutant extracts. We cut 14 matched pairs of gel pieces covering the range from approximately 20 to 200 kDa, with many pieces containing multiple bands, from wild-type and mutant co-immunoprecipitations and subjected them to tryptic digestion and tandem mass spectrometry analysis for protein identification. In all, we identified 702 proteins in immunoprecipitates from wild-type trachea and 29 proteins in gel slices from the immunoprecipitates from trachea expressing mutant protein (Supplementary Table 1).

To determine whether the identified Dyx1c1 protein interactome was enriched for particular molecular or biological functions, we used the Database for Annotation, Visualization and Integrated Discovery (DAVID) to determine the presence of enriched Panther Gene Ontology terms in the Dyx1c1 interactome and proteins identified in the knockout control. Using a mouse lung proteome as background, we found several molecular functional categories enriched in the Dyx1c1 interactome, and several of these were in categories containing molecular chaperones (MF00077: chaperone, $P < 0.001$; MF00091: cytoskeletal proteins, $P < 0.001$; BP00062: protein folding, $P < 0.01$; BP00072: protein complex assembly, $P < 0.05$; and MF00078: chaperonin, $P = 0.05$; Table 3-1). All four of these chaperone-containing categories were not significantly enriched in the protein set identified in the immunoprecipitates with mutant protein (Table 3-1).

Table 3-1: Complete list of PANTHER Gene Ontology enrichment terms from Dyx1c1 wild-type subtracted by knockout control with a lung proteome as a background. Thick horizontal line separates statistically significant terms ($p < 0.05$) from non-statistically significant terms ($p > 0.05$).

Term	Count	%	P-Value	Benjamini
MF00077:Chaperone	**23**	**3.9**	**1.20E-06**	**1.80E-04**
MF00091:Cytoskeletal protein	55	9.4	1.40E-04	9.80E-03
BP00001:Carbohydrate metabolism	39	6.7	8.50E-05	1.20E-02
MF00250:Serine protease inhibitor	12	2.1	4.10E-04	1.20E-02
MF00126:Dehydrogenase	29	5	2.70E-04	1.30E-02
MF00102:Protease inhibitor	15	2.6	3.80E-04	1.40E-02
MF00123:Oxidoreductase	48	8.2	5.80E-04	1.40E-02
BP00062:Protein folding	**20**	**3.4**	**5.00E-04**	**3.60E-02**
BP00071:Proteolysis	41	7	1.50E-03	3.60E-02
BP00072:Protein complex assembly	**11**	**1.9**	**1.30E-03**	**3.80E-02**
MF00153:Protease	27	4.6	1.80E-03	3.80E-02
BP00020:Fatty acid metabolism	18	3.1	2.00E-03	4.10E-02
MF00078:Chaperonin	**7**	**1.2**	**3.10E-03**	**5.00E-02**
MF00156:Other hydrolase	17	2.9	4.90E-03	6.90E-02
BP00008:Tricarboxylic acid pathway	9	1.5	7.50E-03	1.20E-01
MF00262:Non-motor actin binding protein	18	3.1	1.30E-02	1.50E-01
MF00154:Metalloprotease	11	1.9	1.90E-02	1.90E-01
MF00168:Mutase	5	0.9	2.40E-02	2.20E-01
BP00129:Endocytosis	17	2.9	1.90E-02	2.40E-01
BP00209:Blood circulation and gas exchange	8	1.4	2.00E-02	2.40E-01
BP00019:Lipid, fatty acid and steroid metabolism	30	5.1	2.50E-02	2.40E-01
BP00292:Other carbon metabolism	9	1.5	2.50E-02	2.50E-01
BP00125:Intracellular protein traffic	46	7.9	2.40E-02	2.60E-01
BP00148:Immunity and defense	41	7	3.60E-02	3.00E-01
BP00021:Fatty acid biosynthesis	5	0.9	3.90E-02	3.10E-01
BP00140:Other protein targeting and localization	5	0.9	5.70E-02	3.80E-01
BP00007:Pentose-phosphate shunt	3	0.5	6.60E-02	3.90E-01
BP00176:Blood clotting	7	1.2	6.30E-02	4.00E-01
BP00126:Exocytosis	10	1.7	7.20E-02	4.10E-01
MF00166:Isomerase	14	2.4	7.40E-02	4.30E-01
MF00024:Ion channel	8	1.4	6.60E-02	4.40E-01
MF00293:Transmembrane receptor regulatory/adaptor protein	6	1	7.00E-02	4.40E-01
MF00079:Other chaperones	7	1.2	6.10E-02	4.60E-01
MF00265:Tubulin	3	0.5	6.50E-02	4.60E-01
MF00071:Translation factor	9	1.5	9.50E-02	4.70E-01
MF00118:Synthase and synthetase	15	2.6	8.90E-02	4.80E-01
MF00256:Intermediate filament	7	1.2	9.40E-02	4.80E-01
BP00178:Stress response	10	1.7	9.80E-02	5.00E-01

The DYX1C1 interactome contained a total of 28 proteins in the chaperone or chaperonin category, including 6 of 8 subunits in the T-complex chaperonin

complex and multiple heat-shock proteins. In addition to the chaperones, another interesting family of proteins, Septins, was identified as a part of the Dyx1c1 interactome.

Septins are evolutionarily conserved family of small GTPases that form hetero-oligomers, which assemble into filaments, rings and spirals. In mammals, Septins have been linked to scaffolding functions with the cytoskeleton especially through their interactions with actins. Sept2 interacts with MAP4 that positively regulates the polymerization/stability of cytoplasmic microtubules. Map4 directly binds and bundles microtubules in turn regulates the Septin-microtubule interactions. Septins organize lateral membrane diffusion barriers between the ciliary compartment and the surrounding plasma membrane in the sperm flagellum[143], primary cilium[3] and motile cilia. The transition zone includes the region where the basal body is docked onto the cellular membrane, and extends distally to link microtubule doublets to the ciliary membrane by Y-shaped molecular links. Septins form a ring-shaped structure at the base of cilia. Sept2 is also required for ciliogenesis, thereby linking septins to ciliary function and morphogenesis[3,143]. The mass spectrometric analysis performed on the wildtype immunoprecipitates identified Septin2 and Septin 7 as a part of the Dyx1c1 interactome.

Cytoplasmic dyneins are thought to be involved in linking dynein to cargos and to adapter proteins thus regulating dynein function. Cytoplasmic dynein also acts as a motor for the intracellular retrograde motility of vesicles and organelles along microtubules. The intermediate chains of the cytoplasmic dyneins are known to

mediate the binding of dynein to dynactin via the 150 kDa component of DCNT1; thus functioning in membrane-transport. Our MS/MS screen identified the intermediate chain of the cytoplasmic dyneins, Dync1i1.

We confirmed the interaction of Dyx1c1 with Hsp70, Hsp90, Cct3, Cct4, Cct5, Cct8, Sept2 and Dync1i1 by co-immunoprecipitation and western blot analysis (Fig. 3-3).

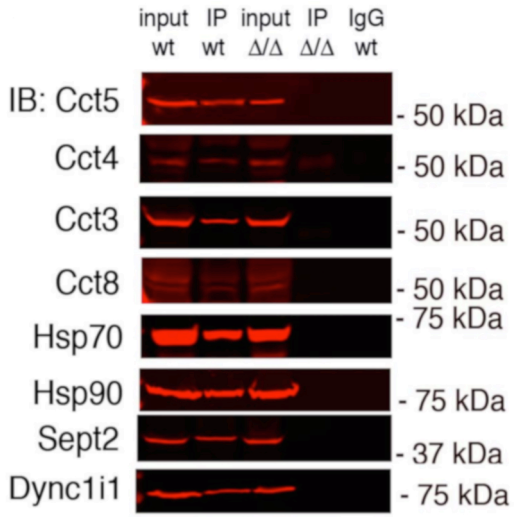

Figure 3-3: Identification of interaction partners of Dyx1c1. *Co-immunoprecipitations and western blot analyses show the interaction of Dyx1c1 with the chaperones Cct3, Cct4, Cct5, Cct8, Hsp70 and Hsp90. Dyx1c1 also interacts with cytoplasmic dynein 1 intermediate chain 1 (Dync1i1) protein as well as Septin-2 (Sept2).*

3.3.3 Interaction of Dyx1c1 with the interaction partners in HEK cells

Dyx1c1 protein contains N-terminal heat shock protein family domain and C-terminal TPR domains that are known to mediate protein-protein interactions. TPR-containing proteins have been previously studied for their roles in molecular

protein complexes, anaphase promoting complexes, transcription repression complexes, and the organization of protein import complexes[128].

3.3.3.1 Interaction of Dyx1c1 with heat shock proteins Hsp70 and Hsp90

Dyx1c1 is known as a co-chaperone due to its previously identified interactions with the heat shock proteins Hsp70 and Hsp90. It is known that Dyx1c1 interacts with Hsp70 via its TPR domains while the p23 is sufficient for the interaction of Hsp90 and Dyx1c1. Our MS/MS data identified chaperones Hsp70 and Hsp90 in the interactome of Dyx1c1; we confirmed that Dyx1c1 interacts with both Hsp70 and Hsp90 (Fig 3-3). We decided to investigate this interaction in a heterologous expression system. We transfected HEK cells with the full-length, N-terminal truncation and C-terminal truncation constructs of Dyx1c1 all fused to GFP; and decided to investigate the interaction of full-length and truncation constructs of Dyx1c1 with endogenous Hsp70 or Hsp90 (Fig. 3-4). We found that Dyx1c1 full-length protein co-immunoprecipitated with both Hsp70 and Hsp90. The TPR domains mediated the interaction of Hsp70 while the p23 domain aided that of Hsp90.

3.3.3.2 Interaction of Dyx1c1 with the T-complex chaperones

Chaperonins are large double-ring complexes of ~800−900 kDa that function by enclosing substrate proteins up to ~60 kDa for folding. Group I chaperonins (also known as HSP60s in eukaryotes and GroEL in bacteria) have seven-membered rings in bacteria, mitochondria and chloroplasts, and functionally cooperate with HSP10 proteins (GroES in bacteria), which form the lid of the folding cage. The

most complex group II chaperonin is however the eukaryotic cytosolic chaperonin containing TCP1 [CCT, also termed TRiC (TCP1 ring complex)], which is composed of eight different subunits (CCTα, β, γ, δ, ε, ζ, η and θ in mammals, CCT1–8 in yeast) organized in a unique intra- and inter-ring arrangement. They are independent of HSP10 factors[144-147]. They are known to be involved in the quality control of cytoskeletal proteins and also tubulin biogenesis.

Our MS/MS screen identified four of the eight CCTs Cct3, Cct4, Cct5 and Cct8. We confirmed by co-immunoprecipitation and protein blot analysis the interactions of these four six chaperones with DYX1C1 (**Fig. 3-3**). We also further confirmed the interaction of Dyx1c1 with these Ccts heterologously. We used HEK cell lysates transfected with full-length Dyx1c1, N-terminal and C-terminal truncation constructs of Dyx1c1 to pull down Dyx1c1 protein; and further blotted with the Cct antibodies to test for the interaction of Dyx1c1 with the Ccts. We found that all the Ccts interacted with Dyx1c1 via the TPR domains (**Fig. 3-4**).

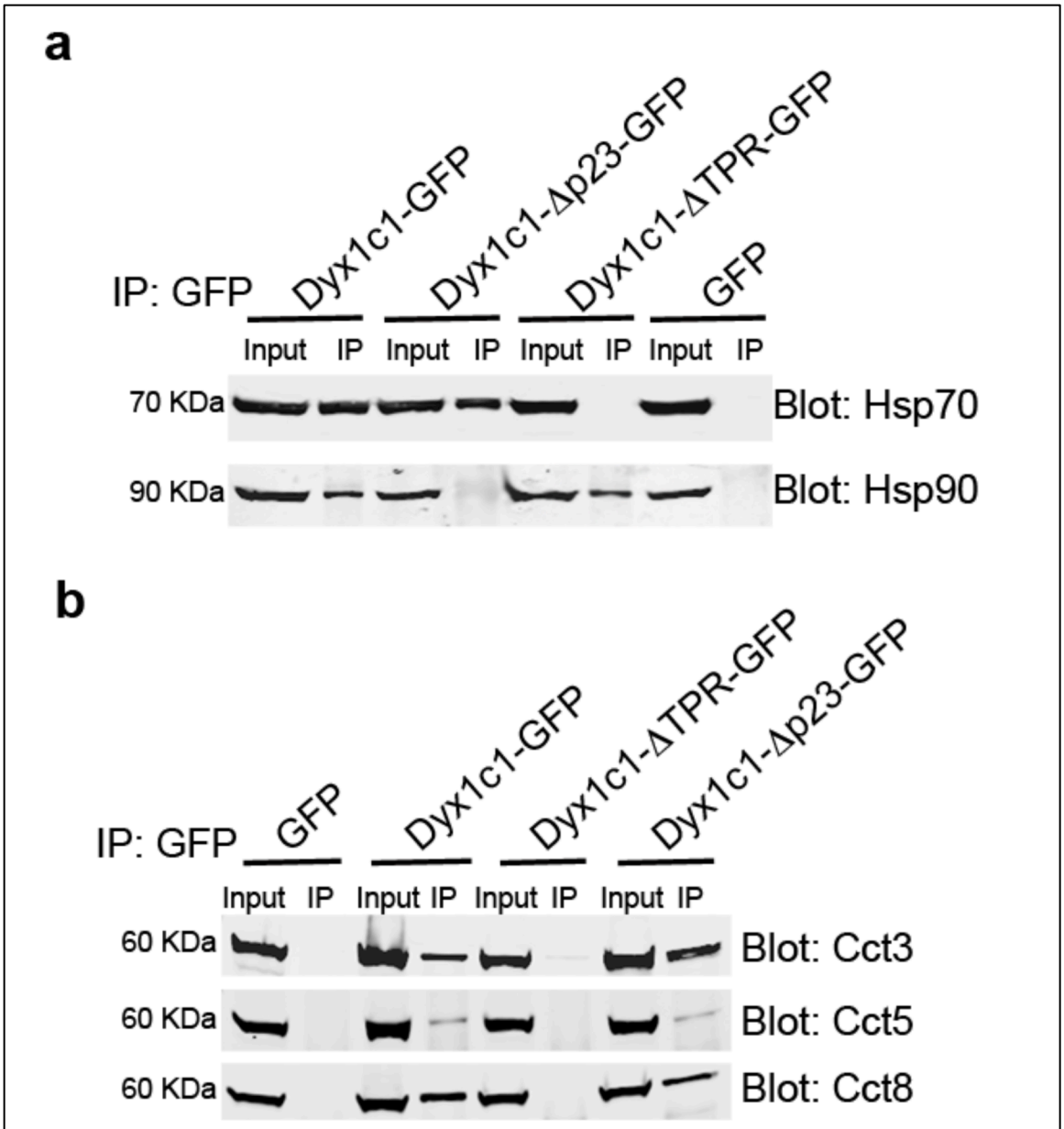

Figure 3-4: Dyx1c1 interacts with the chaperones. *(a) Co-immunoprecipitation and western blot analysis shows that transfected Dyx1c1-GFP interacts with endogenous HSp70 and Hsp90; Dyx1c1-Δp23-GFP interacts with Hsp70; while Dyx1c1-ΔTPR-GFP interacts with Hsp90. (b) Co-immunoprecipitation and western blot analysis shows that transfected Dyx1c1-GFP interacts with endogenous Cct3, Cct5 and Cct8. Dyx1c1-Δp23-GFP interacts with the CCTs. GFP condition acts as a control.*

3.3.4 Cytoplasmic abundance of dynein subunits of IDA and ODA

Previous studies have shown that Chlamydomonas can disassemble and subsequently reassemble their flagella once each cell cycle while maintaining a cytoplasmic pool of flagellar dynein subunits enough to assemble half-length of the flagella in the absence of any protein synthesis[148,149]. The dynein assembly mutations could either prevent the dynein complex from preassembling in the cytoplasm or block the IFT-mediated transport of the assembled complex into the flagella. In order to understand the Dyx1c1 aided assembly process it is hence important to examine the cytoplasmic pool of axonemal proteins by biochemical analysis. Loss of function of the previously studied assembly factors Ktu and Lrrc50 reduces the abundance of some ODA HC subunits while increasing the abundance of the ODA IC subunits in the cytoplasm. In the Lrrc6 mutant cytoplasm, the ODA HCs are retained at wildtype levels while the IC subunit Dnai2 is hyperabundant, which suggests that the Lrrc6 mutation has an effect on the assembly of heavy chains with intermediate chains[56,102,150].

In order to assess the cytoplasmic abundance of the dynein subunits in the cytoplasm of the Dyx1c1 mutant, we performed deciliation of the trachea obtained from wildtype and knockout Dyx1c1 mice. We confirmed the cytoplasmic localization of Dyx1c1 in the wildtype extracts and the deciliation was confirmed by the presence of acetylated tubulin only in the axonemal fraction with little to no expression in the cytoplasmic extract using Gapdh as the control for the cytoplasmic fraction. Having confirmed the deciliation, we then decided to

investigate the abundance of the dynein subunits in the cytoplasmic fraction obtained from the WT and KO trachea.

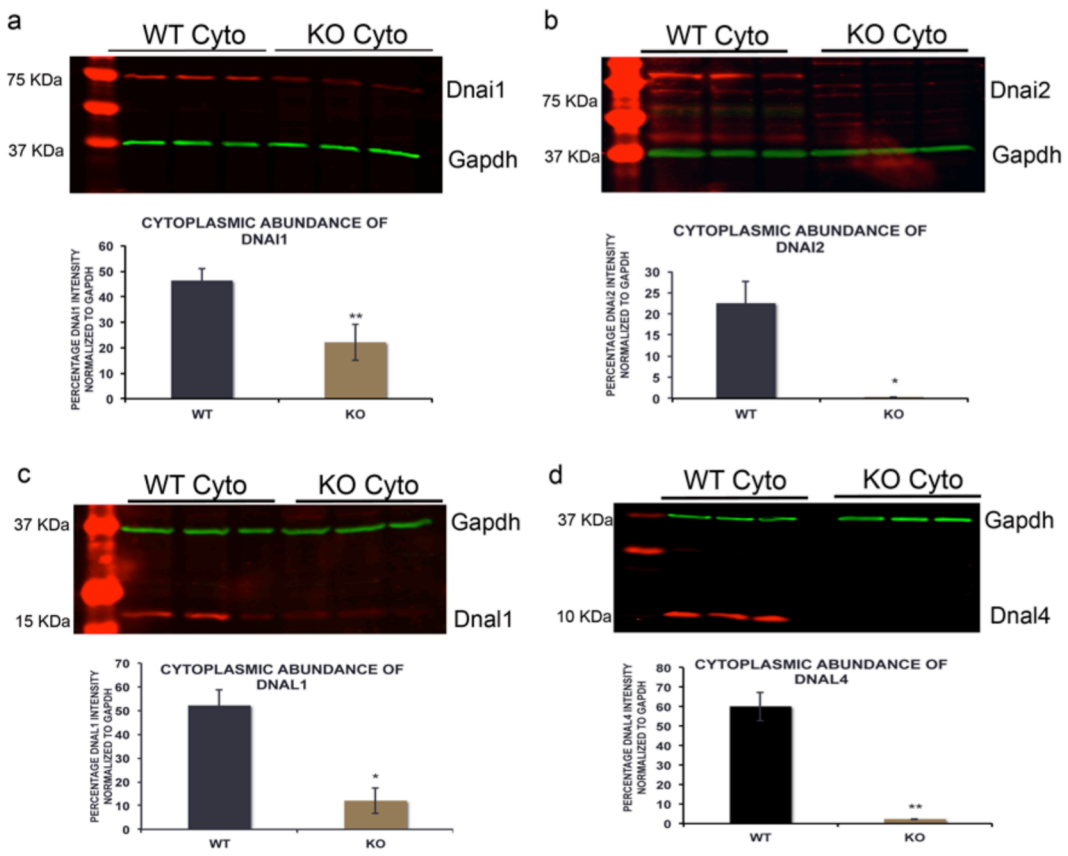

Figure 3-5: Outer dynein arm intermediate and light chain subunits are reduced in the Dyx1c1 knockout tracheal cytoplasm. *Western blot analysis (top panel) and quantification (bottom) of the dynein subunits shows reduced cytoplasmic abundance of Dnai1 (red) (a), Dnai2 (red) (b), Dnal1 (red) (c), and Dnal4 (red) (d). Gapdh is used as a loading control and for normalization. Student's T-test, P-value<0.01(*); P-value <0.05 (**).*

Western blots of cytoplasmic extracts showed that in the Dyx1c1 knockout cytoplasm, the abundance of ODA intermediate chains Dnai1 (Fig. 3-5a) and Dnai2 (Fig. 3-5b) was reduced. Compared to the wildtype cytoplasm, the levels of Dnai1 were decreased by about half whereas the levels of Dnai2 were

reduced by 99% in the knockout cytoplasm. In addition to the intermediate chains, the abundance of some of the light chains was altered as well in the knockout cytoplasm. There was a seven-fold decrease in the abundance of the light chain Dnal1 (Fig. 3-5c), while a 98% reduction in abundance of Dnal4 (Fig. 3-5d) in the knockout cytoplasm when compared to the wildtype cytoplasm. Thus, the Dyx1c1 mutation suggests a defect in assembling the intermediate chains and/or light chains of the ODA complex or the maintenance of these axonemal dyneins.

Since ultrastructural studies of the cilia from the Dyx1c1 knockout mice show the absence of both the inner and outer dynein arms as well as the immunocytochemistry indicates the lack of expression of the IDA subunit Dnali1 from the mutant ciliary axoneme, we looked at the abundance of the IDA light intermediate chain subunit Dnali1 (Fig. 3-6). We found that the cytoplasmic abundance of the light intermediate chain Dnali1 was also reduced to about 4% in the knockout cytoplasm compared to the wildtype.

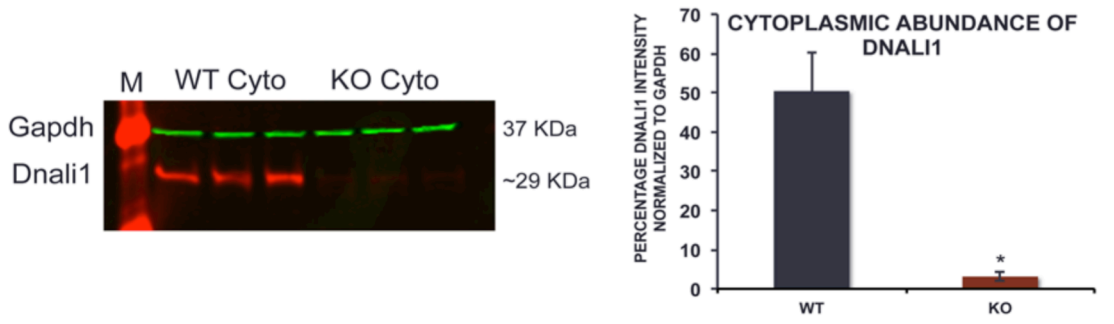

Figure 3-6: ***Inner dynein arm light intermediate chain Dnali1 is reduced in the Dyx1c1 knockout tracheal cytoplasm.*** *Western blot analysis (left panel) and quantification (right panel) of Dnali1 shows reduced cytoplasmic abundance. Gapdh is used as a loading control and for normalization. Student's T-test, P-value<0.01(*).*

The results suggest that, in the cytoplasm of the Dyx1c1 knockout tracheal cells, the ODA intermediate chain subunits Dnai1 and Dnai2; the ODA light chain subunits Dnal1 and Dnal4; as well as the IDA light intermediate chain subunit Dnali1 might be undergoing rapid degradation due to the lack of their incorporation into the ODA or IDA complex. Thus we propose that Dyx1c1 is indeed required for the cytoplasmic preassembly of the ciliary dyneins and the absence of which leads to protein degradation due to the defect in the assembly process.

3.4 Discussion

To identify the function of Dyx1c1 in ciliary motility, it was important to first characterize the subcellular localization of the protein. Since the loss of Dyx1c1 is known to cause an absence of ODA and IDA in the ciliary axoneme, it could localize to the ciliary axoneme and play in role in attachment of the ODA and IDA to the microtubules; or Dyx1c1 could be a cytoplasmic protein functioning in the assembly of the ODA and/or IDA or subsequent transport of the assembled motor complexes to the base of the cilia.

When immunofluorescence analysis was performed on the acutely dissociated nasal respiratory cells, we identified a cytoplasmic localization for Dyx1c1. Three other proteins, termed as assembly factors of axonemal dyneins, DNAAF1, DNAAF2 and DNAAF3 are identified that localize to the cytoplasm and are involved in the pre-assembly of the axonemal dyneins before their transport into the ciliary axoneme. Due to the cytoplasmic localization of Dyx1c1, we proposed

that Dyx1c1 probably functions like the assembly factors mentioned above.

Dyx1c1 has identified as a co-chaperone due to its interaction with the heat shock proteins Hsp70 and Hsp90. In addition, Dyx1c1 is also implicated in protein quality control due to its interaction with the E3 ubiquitin ligase, CHIP. To characterize the function of Dyx1c1 in greater detail, we next identified the interactome of Dyx1c1 by immunoprecipitation and mass spectrometric analysis. We identified previously known interactors like the heat shock proteins Hsp70 and Hsp90; in addition to these, we also found a group of chaperonins (T-complex chaperones) that interact with Dyx1c1. We further identified that the TPR domains of Dyx1c1 are critical for the interaction of the Hsp70 and CCTs with Dyx1c1, while the p23 domain of Dyx1c1 mediates the interaction with Hsp90. These results validate the function of Dyx1c1 in chaperone-mediated processes or especially as a co-chaperone. In addition, Dyx1c1 interactome also consisted of proteins that are a part of the proteasomal degradation pathway. Due to these findings, we speculate that Dyx1c1 might be involved in the quality control or stability of the unfolded protein complexes. It might however also be involved in the degradation of the misfolded protein complexes due to its association with the proteasomal pathway subunits as well as its previously known interaction with CHIP.

Interestingly, the newly identified interaction partner of Dyx1c1, Sept2, hints at a role of Dyx1c1 at the transition zone of the cilium. We have hypothesized that Dyx1c1 is involved in the cytoplasmic preassembly of ciliary dyneins. Once these ciliary dyneins have assembled in the cytoplasm, they need to be transported to

the transition zone before entering the axoneme. Dyx1c1 might be responsible for the stability of the assembled dynein arm complexes and hence might be transporting this complex to the Sept2-containing transition zone, where the motor complex then gets docked onto the intraflagellar transport (IFT) complex.

The cytoplasm of the ciliated epithelial cells generates a precursor ODA and IDA motor complex, hence investigation into the cytoplasmic abundance of the ODA and IDA dynein subunits will give us insights into the biochemical function of Dyx1c1. We performed deciliation of the trachea obtained from the WT and KO to assess the abundance of the ODA and IDA subunits in the deciliated tracheal lysates. Interestingly, we found that the ODA intermediate chain subunits Dnai1 and Dnai2 were depleted from the KO cytoplasm; as were the ODA light chain subunits Dnal1 and Dnal4. The light intermediate chain subunit of the IDA complex, Dnali1, was also reduced in the KO cytoplasm compared to the control. These results suggest that Dyx1c1 is probably required for the proper folding of these subunits in the KO; in the absence of Dyx1c1, the subunits fold abnormally leading to their rapid degradation. Alternatively, the axonemal dynein subunits might be folded correctly, but due to the lack of Dyx1c1 their incorporation as an ODA or IDA is affected. Since the subunits are not assembled accurately, they might be degenerating at a faster rate in the KO than the WT. A third possibility is that Dyx1c1 plays a role in the transcriptional regulation of the axonemal dynein subunits and loss of Dyx1c1 affects the synthesis of the proteins.

In summary, we hypothesize that Dyx1c1 plays a role in the cytoplasmic preassembly of the axonemal dyneins mediated by its interaction with the

chaperones. It might also assist in the stability of the individual dynein subunits or the assembled ODA/IDA complex. Due to the interaction of Dyx1c1 with Sept2, we also predict that Dyx1c1 is required for the transport of the assembled ODA or IDA complex to the transition zone, which is the checkpoint for the assembled motor complex to enter the axoneme.

3.5 Materials and Methods

3.5.1 Immunofluorescence of dissociated mouse nasal epithelial cells

Nasal epithelial cells were harvested from mouse septa by acute dissociation on a 4-well slide in 1:1 PBS/HBSS. Slides were dried to let the cells adhere to the wells, and cells were immediately fixed with 4% paraformaldehyde for 2 min at room temperature. Cells were then washed twice with 1× PBS for 2 min for each wash. Blocking buffer (10% goat serum and 0.1% Triton X-100 in 1× PBS) was added for 15 min at room temperature. Slides were incubated with rabbit polyclonal antibody to DYX1C1 (Sigma, SAB4200128) at a 1:500 dilution and mouse monoclonal antibody to acetylated tubulin (Sigma, T7451) at a 1:1,000 dilution in the same blocking buffer for 30 min at room temperature. After three washes with 1× PBS for 5 min each, slides were incubated with Alexa Fluor 488–conjugated goat antibody to rabbit (Invitrogen, A11034; 1:5,000 dilution) and Alexa Fluor 568–conjugated goat antibody to mouse (Invitrogen, A11031; 1:1,000 dilution) for 20 min at room temperature. Slides were washed twice with 1× PBS for 5 min each, and nuclear stain Hoechst 33342 (Invitrogen, H3570) at a 1:2,500 dilution was added for 15 min at room temperature. Slides were dried,

and cover slips were applied with Prolong Gold Antifade (Invitrogen, P36930). Cells were imaged on a Leica TCS Sp2 laser scanning microscope.

3.5.2 Basic peptide identification by tandem mass spectrometry

After separation by SDS-PAGE, proteins were stained with Coomassie dye. Fourteen gel pieces were excised from the gels that contained bands in the immunoprecipitates with wild-type Dyx1c1 or were adjacent to these bands in the lane containing immunoprecipitates with mutant Dyx1c1. Bands were in-gel digested with trypsin, and resulting peptides were analyzed using liquid chromatography tandem mass spectrometry on a Thermo Scientific LTQ-Orbitrap XL mass spectrometer equipped with Waters nanaoACQUITY ultra-high-pressure liquid chromatographs (UPLCs) for peptide separation. The liquid chromatography tandem mass spectrometry data were searched with an in-house Mascot algorithm for uninterpreted tandem mass spectrometry spectra after using the Mascot Distiller program to generate Mascot compatible files. Charge states of +2 and +3 were preferentially located with a signal-to-noise ratio of 1.2 or greater, and a peak list was generated for database searching. NCBInr, a mouse- specific database (in FASTA format), was used for searching.

3.5.3 Tandem mass spectrometry and gene ontology enrichment analysis

Raw tandem mass spectrometry peptide sequencing results for the wild-type and control analyses obtained from the Yale W.M. Keck Foundation Proteomics Resource were stringently filtered to ensure a low false positive protein identification rate. Specifically, proteins were considered identified only if they

contained two or more unique peptides with expectation values of <0.01. Resulting unique protein GI accession numbers for the wild-type and controls were separately used as inputs for the DAVID bioin- formatics resource with the mouse proteome selected as the background[49,50]. To detect enrichment in gene ontology terms associated with the input pro- teins, the PANTHER biological process and PANTHER molecular function annotations were selected, and functional annotation charts were generated. To further account for high-abundance proteins commonly observed in tandem mass spectrometry analyses, a list of 1,000 mouse protein Swiss-Prot accession numbers was obtained from the Global Proteome Machine web site and was used as an alternate background in the DAVID gene ontology analysis of DYX1C1 interactors.

3.5.4 Deciliation of the trachea

The tracheas harvested from postnatal day 16 (P16) Dyx1c1 wildtype and knockout mice were washed with cold phosphate-buffered saline to remove mucus and cell debris. Animal procedures were performed under protocols approved by the Institutional Animal Care and Use Committee of the University of Connecticut and conform to US NIH guidelines. The dissected tracheas were transferred to a separate tube containing deciliation buffer containing 10mM Tris-HCl (pH 7.5), 50mM NaCl, 20mM CaCl2, 1mM EDTA, 0.1% TritonX-100, 7mM betamercaptoethanol, and 1% volume of protease inhibitor mixture; incubated for 10 min with intermittent mild vortexing. The supernatant was collected in a separate tube, and the procedure was repeated twice. The tracheas were then separated from the supernatant, the three washings were pooled, and after

pelleting cell debris at 800x*g*, the ciliary axonemes were collected by centrifugation at 20,000xg. Ciliary axonemal pellets were resuspended gently in 30 mM Hepes (pH 7.3), 1 mM EGTA, 0.1 mM EDTA, 25 mM NaCl, 5 mM $MgSO_4$, 1 mM dithiothreitol, and 1% volume of protease inhibitor mixture (Sigma). Triton X-100 was added (0.5%) to the suspension, and the axonemes were incubated for 15 min on ice, followed by centrifugation. The lysates containing the axonemal fraction were then frozen at -80°C. The cilia-stripped-tracheas were incubated in RIPA buffer (Sigma) on ice for 20 min. Samples were homogenized using a tissue homogenizer and cleared by centrifugation at 10,000g for 10 min to obtain the protein lysate of the cytoplasmic fraction of the trachea. Protein concentrations were estimated using the BCA reagent (Pierce).

3.5.5 Protein blots of whole trachea, cytoplasmic and axonemal lysates

For whole tracheal preparation, tracheal tissues were dissected from wildtype and knockout mice, and carefully separated from the surrounding tissues. After incubation in RIPA Buffer supplemented with 1× Protease Inhibitor Cocktail (Sigma), samples were homogenized using a tissue homogenizer and cleared by centrifugation at 10,000g for 10 min. The cytoplasmic and axonemal fractions of the trachea were prepared as described above. Proteins were separated on 12% SDS- PAGE minigels and then transferred to Immobilon (Millipore) membrane for protein blotting. For detecting DYX1C1 protein, the antibody to N-terminal DYX1C1 (Sigma, SAB4200128) was used at a dilution of 1:200; antibody to acetylated tubulin (Sigma, T6793) was used at a dilution of 1:2000; and antibody to GAPDH (Sigma, G8795) was used at a 1:1,500 dilution as a loading control.

LI-COR Odyssey infrared secondary antibodies (goat antibody to mouse 680 (926-32220), goat antibody to mouse 800 (926-32210), goat antibody to rabbit 680 (926-32221) and goat antibody to rabbit 800 (926-32211)) were used at dilutions of 1:15,000. All blots were imaged and analyzed using a LI-COR Odyssey Scanner and Software.

3.5.6 Cell culture and transfection

Human embryonic kidney (HEK293T) cells were grown to confluence in DMEM supplemented with 10% FBS, 1% non-essential amino acid (NEAA) and 1% penicillin-streptomycin antibiotics (Invitrogen). Cultures were plated at a density of 10^6 cells on a 10-cm petridish. DNA (24 µg) was added to the petridish with 75 µl of Lipofectamine 2000 reagent (Invitrogen) in OptiMEM-1. The transfection mix was added to cells in normal growth media and incubated for 48 h at 37 °C. To obtain the protein lysates from the cells, the normal growth media was removed and the cells were washed with PBS. The cells were then collected, centrifuged to pellet the cells and the pellet was incubated in RIPA buffer supplemented with 1X Proteinase Inhibitor Cocktail for 20 min on ice. The lysates were then centrifuged at 2000xg to pellet the debris. Protein blots were also performed on the transfected cells as described above.

4. CHARACTERIZATION OF MUTANT DYX1C1 PROTEIN AND ITS INTERACTIONS

4.1 Abstract

Defects in motile cilia cause primary ciliary dyskinesia (PCD), characterized by chronic airway disease, infertility, and left-right laterality disturbances. Dyx1c1 (DNAAF4) was identified as a candidate PCD gene, mutations in which resulted in loss of the outer and inner dynein arms. 12 biallelic PCD-causing mutations were identified in Dyx1c1, which were speculated to cause either protein degradation or a truncated protein product lacking the TPR domains of Dyx1c1. Interestingly, a novel missense mutation p.Leu19Glu was identified in a Druze cohort that coincidentally segregated with PCD. The patients suffer from the classical PCD symptoms and the patient cilia show an absence of inner dynein arms. Here, we show that the DYX1C1 protein is produced in the patients at the correct molecular weight. The ODA intermediate chain, DNAI2 and IDA light intermediate chain, DNALI1 are reduced in the patients. The interactor proteins of Dyx1c1, Sept2 and Ktu, were not reduced in abundance in the patients. Interaction of Dyx1c1 between Sept2 and Ktu was studied heterologously to demonstrate a reduction in their association with Dyx1c1 mutant protein. Thus, DYX1C1 is an essential ciliary protein required for the cytoplasmic preassembly of both the ODAs and IDAs.

4.2 Introduction

Primary ciliary dyskinesia (PCD [MIM 244400]) is a genetically heterogeneous

autosomal-recessive disorder affecting 1 in 15,000–30,000 births and is caused by abnormal function of motile cilia and flagella. Abnormal motility is associated with axonemal ultrastructural defects, giving rise to symptoms including pulmonary disease, which is due to impaired mucociliary transport in the airways. Mutations that cause PCD have been reported in 19 genes, all of which are associated with various ultrastructural defects, mutations in which might contribute to syndromic PCD. These 19 genes include those encoding axonemal proteins of the ODA or its docking complex (DNAH5, DNAH11, DNAI1, DNAI2, DNAL1, TXNDC3, and CCDC114), the radial spoke heads (RSPH4A and RSPH9), the central-pair apparatus (HYDIN), or the nexin-dynein regulatory complexes (CCDC164, CCDC39, and CCDC40). A distinct set of six proteins altered in PCD are either solely localized to the cytoplasm or found in both the cytoplasm and the axoneme: DNAAF1 (LRRC50), DNAAF2 (KTU), DNAAF3, CCDC103, HEATR2, and LRRC6. These are most likely involved in the cytoplasmic preassembly of dynein-arm complexes prior to their movement into the axoneme and/or in axonemal transport and attachment processes for the dynein-arm complexes.

Our results described in Chapter 2 and 3 suggest that Dyx1c1 can also be considered as an axonemal dynein assembly factor due to its cytoplasmic localization and its involvement in ciliary motility. Studies performed using the morpholino-mediated knockdown approach in zebrafish, confirmed an evolutionarily conserved role of Dyx1c1 in the ciliary function. Morpholino-mediated knockdown of zebrafish dyx1c1 resulted in hydrocephalus, kidney cysts

and body-axis curvature, phenotypes consistent with ciliary dysfunction in zebrafish. Morpholino-mediated knockdown of dyx1c1 also produced laterality defects in dyx1c1-morphant embryos at 48 h post-fertilization[140].

Owing to the conservation of function of Dyx1c1 in mice and zebrafish, studies were initiated to search for mutations in DYX1C1 in humans with PCD. DYX1C1, located on chromosome 15q21.3, comprises ten exons (translation starts in exon 2) and encompasses 77.93 kb of genomic DNA. A total of nine human DYX1C1 mutations were identified as shown in **Fig. 4-1a**. Apart from a 3.5-kb deletion and a splice-site mutation, the other seven mutations were predicted to cause premature protein termination and clustered toward the middle of the 420-amino-acid sequence, between amino acids 128 and 195 (**Fig. 4-1b**). Thus, seven of the nine identified mutations are predicted to result in a truncated DYX1C1 protein that would lack more than half of the protein, including the C-terminal tetratricopeptide-repeat (TPR) domain. The TPR domains in DYX1C1 have been shown previously to be functionally important domains required for the activities of DYX1C1 in neuronal motility, its cellular localization and its interaction with molecular chaperones. All the 12 individuals with biallelic DYX1C1 mutations suffered from classical symptoms of PCD, including recurrent upper and lower airway disease and bronchiectasis. Thus, DYX1C1 deficiency in humans causes disruption of left-right body asymmetry, similar to the findings observed in mice and zebrafish.

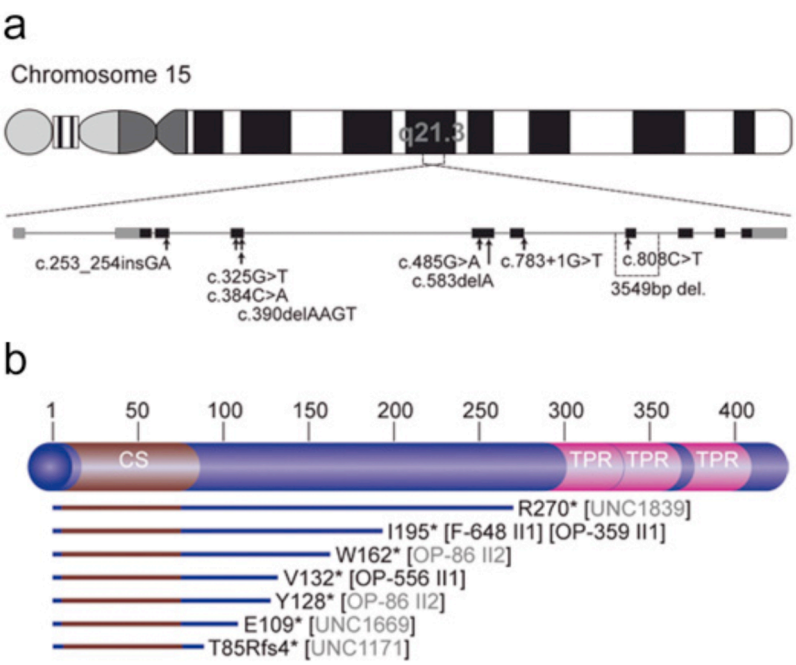

Figure 4-1: DYX1C1 mutations in PCD patients. *(**a**) Schematic presentation of chromosome 15 and the genomic structure of* DYX1C1*. The positions of 8 identified mutations are indicated by black arrows, the position of the 3.5kb deletion is indicated by a rectangle. (**b**) Schematic showing the relative positions of seven* DYX1C1 *nonsense mutations identified in PCD patients and families in the* DYX1C1 *coding sequence. All mutations are clustered in the middle of* DYX1C1 *coding sequence and each mutation predicts to cause a premature stop prior to the tetricopeptide repeat domains (TPR) at the C-terminus of DYX1C1 (CS: p23-like C-terminal CHORD-SGT1 domain). (Adapted from Tarkar et al. 2013)*

In addition to the above already published data regarding the mutations identified in DYX1C1 causing PCD in humans, our collaborators identified a novel mutation in DYX1C1 p.L19Q (unpublished). This mutation was recently identified in an in-bred family belonging to the Druze community of the Golan Heights in Israel. The patients with this mutation suffer from the classical PCD symptoms of recurrent upper and lower respiratory tract infections. This point mutation p.L19Q leads to the substitution of Glutamine for Leucine in the p23 domain of DYX1C1, which is

a domain belonging to the heat shock protein family. This mutation leading to non-polar to polar switch of amino acid, might disrupt the intermolecular contacts leading to altered native structure of the Dyx1c1 protein. It might also potentially have an effect on the interactions of Dyx1c1 protein mediated by the p23 domain. It is hence critical to evaluate the protein expression of Dyx1c1 in the patients as well as assess the interactions of Dyx1c1 with its known interactors, to gain insights into the function of Dyx1c1.

4.3 Results:

4.3.1 Expression profile of Dyx1c1 protein in the Druze mutant

Mutations in DYX1C1 have been identified that are known to cause PCD in humans; however all the previously known human mutations are postulated to generate either a truncated protein product lacking the C-terminal TPR domains or led to non-sense mediated decay. The novel DYX1C1 mutation p.L19Q is identified in the p23 domain of Dyx1c1, and hence it is interesting to evaluate whether this mutation leads to degradation or a truncated Dyx1c1 protein product. In order to characterize the mutation heterologously, we obtained a plasmid construct of Dyx1c1 harboring this mutation (Dyx-Mut). To assess for the protein expression, we transfected this construct in HEK cells and performed western blot analysis. We thus confirmed that Dyx-Mut construct produced Dyx1c1 protein product at the correct size as evident from the two controls: a control Dyx1c1 plasmid and the tracheal lysate from Dyx1c1 wildtype mouse (Fig. 4-2a).

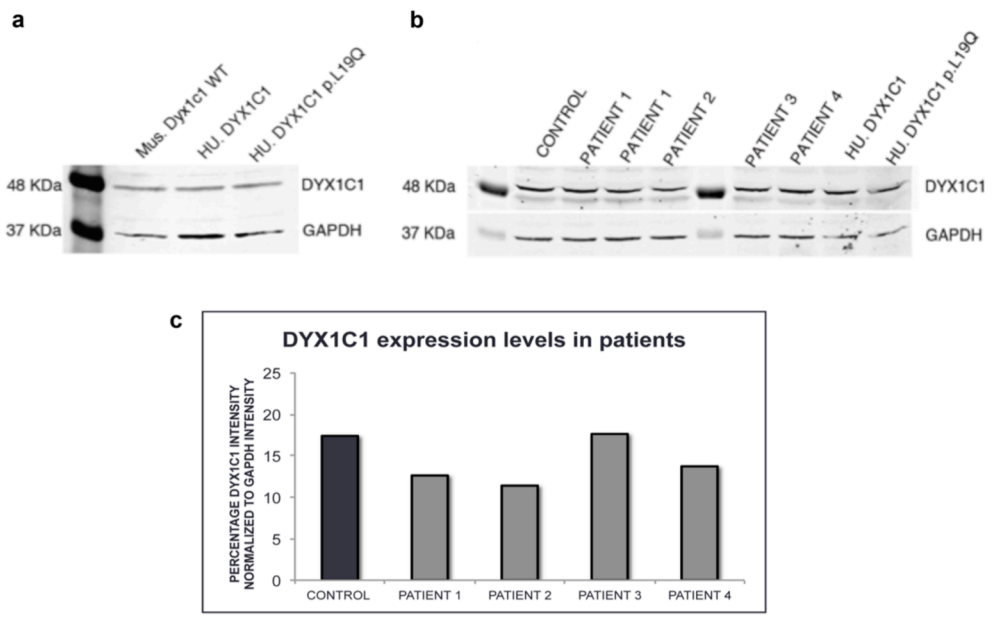

Figure 4-2: DYX1C1 protein is produced in the PCD patients. *(a) Western blot analysis shows DYX1C1 protein is expressed in the p.L19Q mutant condition at 48KDa. (b) Western blot analysis on the patient lysates shows that DYX1C1 is expressed in the patients. (c) Quantification of the expression levels of DYX1C1 normalized to GAPDH. GAPDH was used as a loading control.*

We obtained the respiratory epithelial cells of the patients and control from our collaborators. These cells were pelleted and lysates were prepared according to the procedures described in methods section of this chapter. Immunoblot analysis on the patient lysates showed that Dyx1c1 protein was produced in the patients and the Dyx1c1 protein band was observed at the correct molecular weight of 48KDa compared to the control patient **(Fig 4-2b)**. We also quantified the abundance of DYX1C1 by normalizing the expression of DYX1C1 to that of GAPDH **(Fig. 4-2c)**. These results suggest that the Dyx1c1 protein produced in the patients might be folded incorrectly that might affect its downstream

interactions with other proteins.

4.3.2 Expression profile of axonemal dyneins and the known interactors of Dyx1c1

Mutations in the cytoplasmic assembly factors lead to absence of the outer and inner dynein arms in the mutant cilia. In some mutant cilia, these arms are completely absent in the axoneme; whereas some others show a reduction in the number of both outer and inner dynein arms. It is thought that the cytoplasmic abundance of the axonemal dyneins might provide useful information on the assembly of the dynein arms. Studies show that in case of a defect in the dynein arm assembly, there is either a decrease or increase in the abundance of the axonemal dyneins in the cytoplasm of the mutant compared to the control. The chaperones work with the assembly factors to aid in the correct assembly of the dynein motor complexes. However, due to defects in the assembly process, the dynein arms do not get assembled and thus are not transported into the axoneme of the cilia[56,141].

We investigated the expression of the ODA intermediate chain subunit DNAI2 (Fig. 4-3a) and the IDA light intermediate chain subunit DNALI1 (Fig. 4-3a) in the lysates obtained from the patient samples, using Gapdh as a loading control. It was interesting to find that both the axonemal dynein subunits DNAI2 and DNALI1 were reduced in the patients compared to the control (Fig. 4-3b). The change in the axonemal dynein abundance was quantified by normalizing with

GAPDH. The reduction in the abundance of the dynein subunits indicates a defect in the preassembly of the axonemal dyneins in the cytoplasm or their subsequent transport.

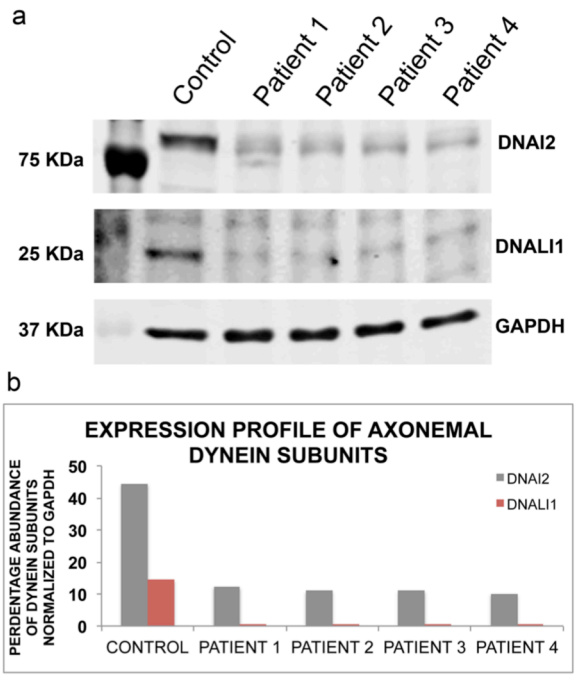

Figure 4-3: Reduction in the levels of the ODA subunit DNAI2 and IDA subunit DNALI1 from the patients. *(a) Western blot analysis performed using anti-DNAI2 and anti-DNALI1 exhibit reduction in the abundance of these subunits. GAPDH was used as a loading control. (b) Quantification of the abundance of DNAI2 and DNALI1 normalized to GAPDH.*

We have previously shown that Dyx1c1 interacts with an assembly factor DNAAF2/ Ktu[140], which is known to play a role in the assembly of the dynein arms by acting as a co-chaperone and assisting in either folding or stabilization of the dynein subunits. The dynein assembly is a multi-step process requiring the axonemal dyneins, assembly factors and the chaperones. This is an orchestrated

process wherein the interactions of all the components are critical for the dynein arm generation. After the dynein arm is assembled, it is transported to the Septin-containing transition zone where the quality control of the dynein arm is performed. Our mass spectrometric results (described in Chapter 3) show that Dyx1c1 interacts with one protein of the Septin family, Septin2. The entire process of assembly and transport of the dynein arms is crucial for the ciliary motility, and any defect in either of these processes can adversely affect the function of cilia.

We investigated the expression profile of the above two interactors of Dyx1c1, Ktu and Sept2, to assess for their altered abundance in the Druze patient samples. Intriguingly, we found that both Ktu and Sept2 were expressed at the same levels in the patients compared to the control and were detected at the correct size (Fig 4-4a,b).

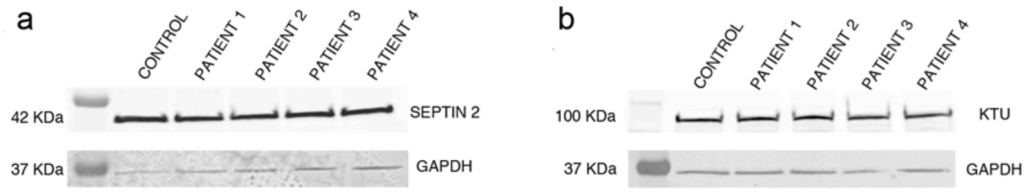

Figure 4-4: Expression profile of SEPTIN2 and KTU in the patient samples. *Western blot analysis of the patient samples using anti-SEPT2 (a) and anti-KTU (b) antibodies show that the levels of these proteins are unchanged in the patients compared to the control. GAPDH was used as a loading control.*

4.3.3 Interaction analysis of Dyx1c1 with known interactors

Our results suggest that the Dyx1c1 protein in the Druze patient population is probably misfolded that could potentially alter the interactions of Dyx1c1 with other proteins in turn affecting the assembly of the dynein arms. We hence investigated the interactions of Dyx1c1 mutant construct with its previously identified interactors Ktu and Sept2 in heterologous expression system. These proteins are known to function in ciliogenesis and/or dynein assembly and transport. We co-transfected HEK cells with either the myc-tagged wildtype or mutant construct of Dyx1c1 along with flag-tagged Sept2 or Ktu. We performed immunoprecipitation experiments using anti-Dyx1c1 antibody to pull down Dyx1c1 and probed for either Sept2 or Ktu. Even though the expression levels of Ktu and Sept2 in the patients were not altered, we found that the interaction of Dyx1c1 with Sept2 and Ktu was reduced in the mutant condition compared to the control (Fig 4-5a,b).

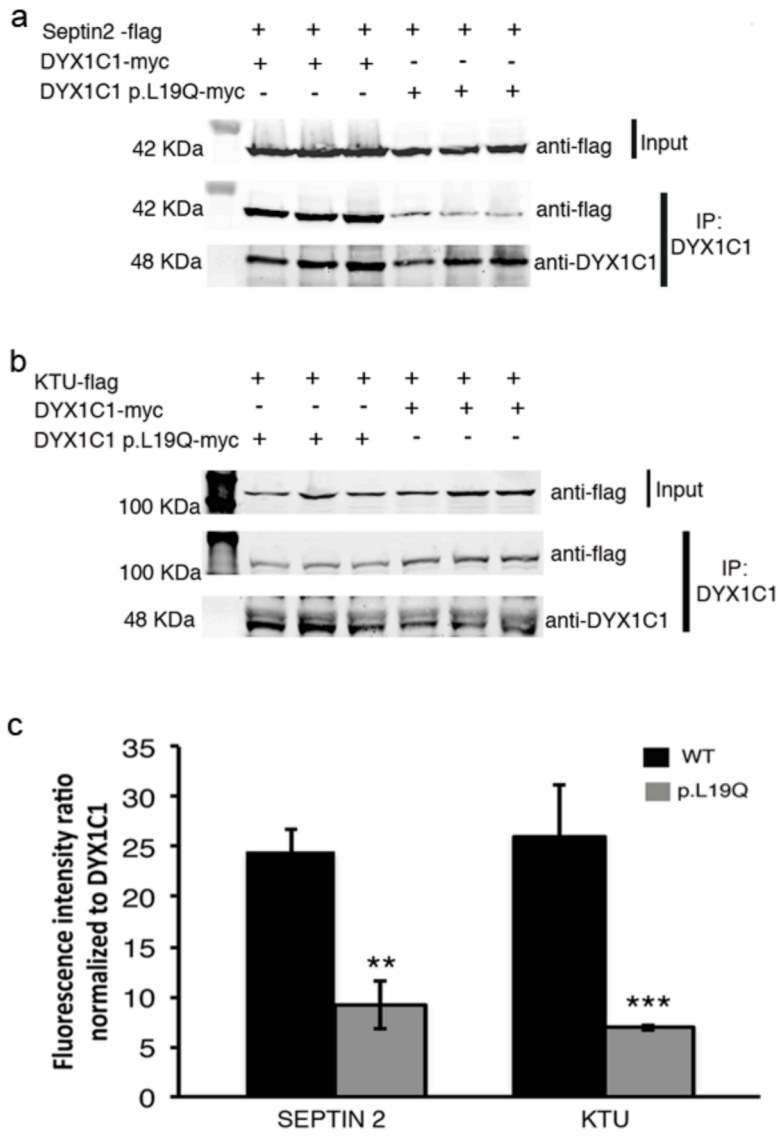

Figure 4-5: Interaction of DYX1C1 with SEPT2 and KTU is reduced in the mutant condition. *(a) Co-immunoprecipitation and western blot analysis shows weaker interaction of DYX1C1-p.L19Q-myc and SEPT2 compared to the control DYX1C1-myc condition. (a) Co-immunoprecipitation and western blot analysis shows weaker interaction of DYX1C1-p.L19Q-myc and KTU compared to the control DYX1C1-myc condition. (c) Quantification of interaction of SEPT2 and KTU with DYX1C1 normalized to the immunoprecipitated DYX1C1. Student's T-test, P-value <0.05 (**); P-value <0.001 (***).*

In order to quantify the interaction of Dyx1c1 and Ktu or Sept2, we first got the percentage ratio of the intensity of Sept2 or Ktu in the immunoprecipitates to the intensity of Sept2 or Ktu in the input and then normalized that to the percentage of Dyx1c1 protein that was immunoprecipitated. We found a 60% reduction in the interaction of Dyx1c1 to Sept2 in the mutant condition compared to the control; while the interaction of Dyx1c1 to Ktu exhibited a 75% decrease in the interaction (Fig. 4-4c). Thus, we speculate that the Dyx1c1 function in the cilia is probably mediated by its interactions with Ktu and Sept2. These proteins constitute a group of proteins of the ciliary cytoplasm; hence it strengthens our hypothesis that Dyx1c1 functions as a cytoplasmic assembly factor.

4.4 Discussion

In the present study, a novel mutation in Dyx1c1 (p.L19Q) that is causative of PCD in humans is characterized. The Dyx1c1 gene is conserved among mice, zebrafish and humans. Dyx1c1 is identified as a protein essential for the motility of cilia; the absence of which leads to absence of inner and outer dynein arms in the ciliary axoneme. The phenotypic similarity of the Dyx1c1 mutants in three organisms examined suggests that Dyx1c1 functions for dynein arm pre-assembly. We initially assessed whether the Dyx1c1 protein was produced in the nasal respiratory epithelial cells of the patients harboring this mutation. Intriguingly, we found that Dyx1c1 protein was expressed in the patients at the appropriate molecular weight (48KDa). The plasmid construct with this mutation, when transfected into HEK cells also expressed the DYX1C1 protein.

Ciliary axonemes of the PCD patients with this mutation exhibited a loss of the outer and inner dynein arms. The mutant cilia lacked the expression of the ODA heavy chain DNAH5 as well as the IDA light intermediate chain DNALI1 in the axoneme. We characterized the protein expression levels of the ODA and IDA subunits DNAI2 and DNALI1 respectively in the patient samples and observed reduced abundance of these two proteins in the mutant samples compared to the control. Densitometric analysis exhibited a 72% reduction in the expression of DNAI2, while a 99% decrease in DNALI1. The reduction in the abundance of the axonemal dynein subunits has been implicated in a faulty assembly of the dynein arms in the mutant cilia due to the loss of the subunit incorporation into the dynein motor complex or altered rates of degradation. We thus gathered additional evidence of the role of DYX1C1 in the cytoplasmic preassembly of the ciliary dyneins due to the reduction in the subunit abundance.

Our biochemical analyses provided additional insight into the proposed function of Dyx1c1 as a facilitator of dynein pre-assembly, by revealing defects in the association of mutant Dyx1c1 with Sept2 and Ktu. The finding of reduced ODA intermediate chain and IDA light intermediate chain abundance in the mutant is consistent with an altered pre-assembly process. Intriguingly, no change in the expression pattern of Sept2 and Ktu was observed in the mutant when compared to the wildtype. Furthermore, immunoprecipitation demonstrated an interaction between Dyx1c1 and Ktu as well as Sept2 in the control condition however, a substantial reduction in the interaction was observed in the mutant condition. Because Hsp70 and Hsp90 were found to be interacting proteins of Dyx1c1 and

Ktu, Dyx1c1 could work as a co-chaperone to localize general functions of molecular chaperones (holding, assembling and protecting of proteins from degradation) to dynein arm formation with the help of Ktu. The reduced interaction might implicate decreased transfer of the correctly assembled dynein arms in to the axoneme. Although much progress has been made in understanding the mechanisms of IFT responsible for the transport of the dynein arms, very little is known about the cytoplasmic process for pre-assembly of dynein complexes. Dyx1c1 point mutant will thus aid in understanding this cytoplasmic process.

4.5 Methods:

4.5.1 Protein lysates for human respiratory epithelial cells

Human respiratory cells were obtained by nasal brushing. The suspension containing the nasal respiratory cells were centrifuged at 20,000xg at 4^{o}C for 10 min to pellet the cells. The cells were then washed 2 times with PBS to remove any mucus or storage buffer. The cells were again centrifuged 20,000xg at 4^{o}C for 10 min and the pellet was incubated in RIPA lysis buffer containing protease inhibitor cocktail. The lysates were incubated on ice for 20 min, following which the lysates were spun down to pellet the debris. The concentration of the protein lysates was obtained by BCA assay.

4.5.2 Plasmids

The DYX1C1-WT and DYX1C1-p.L19Q plasmids were obtained from Dr. Hannah Mitchision. DYX1C1-WT and DYX1C1-p.L19Q sequences were further amplified

using primers incorporating myc epitope tagged sequence and then subcloned into pCAG vector to create pCAG- DYX1C1-WT-myc and pCAG-DYX1C1-p.L19Q-myc plasmids. The Sept2-flag plasmid was constructed as described previously (Chapter 3). The flag-tagged DNAAF2 plasmid was a gift from Dr. Heymut Omran. The sequence of all plasmids was confirmed by sequencing.

4.5.3 Cell culture and transfection

Human embryonic kidney (HEK293T) cells were grown to confluence in DMEM supplemented with 10% FBS, 1% non-essential amino acid (NEAA) and 1% penicillin-streptomycin antibiotics (Invitrogen). Cultures were plated at a density of 10^6 cells on a 10-cm petridish. DNA (24 µg) was added to the petridish with 75 µl of Lipofectamine 2000 reagent (Invitrogen) in OptiMEM-1. The transfection mix was added to cells in normal growth media and incubated for 48 h at 37 °C. To obtain the protein lysates from the cells, the normal growth media was removed and the cells were washed with PBS. The cells were then collected, centrifuged to pellet the cells and the pellet was incubated in RIPA buffer supplemented with 1X Proteinase Inhibitor Cocktail for 20 min on ice. The lysates were then centrifuged at 2000xg to pellet the debris. Protein blots were also performed on the transfected cells as described above.

4.5.4 Western blotting

Proteins were separated on 10% SDS-PAGE minigels and then transferred to Immobilon (Millipore) membrane for protein blotting. For detecting DYX1C1 protein, the antibody to N-terminal DYX1C1 (Sigma, SAB4200128) was used at a

dilution of 1:200; antibody to GAPDH (Sigma, G8795) was used at a 1:1,500 dilution as a loading control; monoclonal antibody to DNAI2 (Abnova, M01, clone 1C8; 1:500 dilution), c-myc antibody (Sigma, C3956, 1:500 dilution), c-myc antibody mouse monoclonal (Sigma, M4439, 1:750 dilution), antibody to flag produced in rabbit (Sigma, SAB1306078, 1:1000 dilution), and mouse monoclonal anti-flag antibody (Sigma, F4042, 1:500 dilution). LI-COR Odyssey infrared secondary antibodies (goat antibody to mouse 680 (926-32220), goat antibody to mouse 800 (926-32210) goat antibody to mouse 680 (926-32221) and goat antibody to mouse 800 (926-32211)) were used at dilutions of 1:10,000. All blots were imaged and analyzed using a LI-COR Odyssey Scanner and Software.

4.5.5 Immunoprecipitation

Immunoprecipitation assays were performed using the Dynabeads Protein G Immunoprecipitation kit (Invitrogen). Briefly, Dynabeads were resuspended in the vial and separated on a magnet from solution. Antibody to Dyx1c1 (Sigma, SAB4200128), (5 µg) was diluted in 200 µl of Washing and Binding Solution and incubated with rotation for 120 min at room temperature. Bead-antibody complexes were separated on the magnet, washed by gentle pipetting and separated. Protein lysates were incubated with the bead-antibody complexes overnight at 4 °C. Bead-antibody-antigen complexes were then washed using the washing solution three times. Complexes were then incubated with elution buffer for 10–15 min to dissociate them. Beads were separated on a magnet, and

supernatant containing the proteins was separated by SDS-PAGE and analyzed by protein blotting using monoclonal antibody to antibody to flag produced in rabbit (Sigma, SAB1306078, 1:1000 dilution), and mouse monoclonal anti-flag antibody (Sigma, F4042, 1:500 dilution). Rabbit IgG was used as a control.

5. DYX1C1 (DNAAF4) IS REQUIRED FOR ASSEMBLY OF LIGHT AND INTERMEDIATE CHAIN AXONEMAL DYNEINS IN TRACHEAL EPITHELIAL CELLS

5.1 Abstract:

Genetic evidence indicates that cytoplasmic preassembly of axonemal dyneins requires proteins encoded by the genes DNAAF1/LRRC50, DNAAF2/KTU, DNAAF3 and DYX1C1/DNAAF4. These assembly factors are thought to act as co-chaperones that promote the assembly of large macromolecular axonemal dynein complexes in the cytoplasm prior to transport into the cilia. In this study, we have investigated the role of Dyx1c1 in preassembly of components of the outer dynein arm (ODA) complex. Dyx1c1 interacts with intermediate and light chain subunits of the ODA complex in the cytoplasm of tracheal epithelial cells. Light and intermediate chains fail to form complexes in the cytoplasm of tracheal epithelial cells of Dyx1c1 mutants. Dyx1c1 increases by four fold the association of Light chain subunits Dnal1 and Dnal4 in heterologously expressing HEK 293-T cells. Finally, a novel Primary Ciliary Dyskinesia (PCD) patient associated missense mutation in Dyx1c1 is impaired in its ability to assembly Dnal1 and Dnal4. In conclusion, we identify a step in ODA pre-assembly in which Dyx1c1 facilitates formation of light and intermediate chain dynein complexes.

5.2 Introduction:

Failure to assemble the outer and inner dynein arms of motile cilia causes Primary Ciliary Dyskinesia (PCD), a ciliopathy characterized by defects in multiple organ systems. The axonemal dynein assembly factors identified largely

through genetic studies have been classified into three general categories: i) cytoplasmic proteins required for the preassembly of outer and inner dynein complexes (e.g. DNAAF1, DNAAF2, DNAAF3 and DNAAF4/DYX1C1)[102,104,138,140]; ii) adaptor proteins involved in the transport of the assembled 2MDa dynein motor complex (ODA16)[58,62]; and iii) proteins of the axoneme that assist in the docking of the assembled dynein arms to the microtubular scaffold at appropriate sites (e.g. DC)[106,151,152]. The molecular details of axonemal dynein assembly, especially the stages in the cytoplasmic preassembly process, that each of the DNAAF proteins serve is not yet completely defined.

The outer dynein arms (ODAs) of motile cilia are composed of either two (e.g. mammals and sea urchins) or three (e.g. Chlamydomonas and Tetrahymena) dynein heavy chain (HC) molecules; two WD-repeat intermediate chains (ICs) and multiple light chains (LCs)[32,33,36,58]. In Chlamydomonas, one distinct type of ODA complex is known to contain three HCs (alpha, beta and gamma-HC), two ICs, nine LCs and three docking complex proteins. Based on homolog searches, five ODA HC orthologs of Chlamydomonas beta and gamma chains have been identified in humans. In humans and mice DNAI1, DNAI2 and TXNDC3 are the three known IC subunits, and DNAL1, TCTE3, DYNLRB1/2, DYNLL1/2, DYNLT1/2 and DNAL4 form the group of LC subunits of the ODA. Genetic studies have shown that mutations in several ODA complex dynein subunits cause PCD: i) DNAI1[153], OMIM ID: 604366, ii) DNAH5[154], OMIM ID: 603335, iii) DNAH11[92], OMIM ID: 603339, iv) thioredoxin domain containing 3[95] (TXNDC3,

OMIM ID: 607421), v) DNAI2[93], OMIM ID: 605483 and vi) DNAL1[155], OMIM ID: 610062. Mutations in DNAI1, DNAI2, DNAL1 and DNAH5 cause an ODA deficiency in PCD patients leading to ciliary immotility. In contrast, DNAH11 mutations did not result in ultrastructural defects in cilia and TXNDC3 mutant cilia exhibited both normal and ODA-deficient cross sections. TXNDC3 is proposed to function as one of the two distinct ODAs in humans.

Cytoplasmic preassembly of the ODA complex is thought to be a sequential process wherein the intermediate chain subunits first assemble, followed by assembly of the heavy chain subunits, and finally light chains are incorporated to form a functional ODA motor complex that is competent for attachment to the ciliary doublet microtubules. The docking complex comprising 3 proteins helps assemble the motor complex on the doublet microtubules. In addition to the individual dynein chain, the process requires both chaperones and the specialized assembly factors, DNAAFs[56,156]. Mutations in most dynein chains interfere with the association of the remaining subunits into a complex in the cytoplasm and block subsequent transport of this complex into the axoneme. Mutations identified in assembly factors (DNAAF1/Lrrc50, DNAAF2/Ktu, DNAAF3 and DNAAF4/Dyx1c1) lead to the absence of ODAs from the mutant axoneme due to a faulty assembly of the ODA motor complex in the mutant cytoplasm. A mutation in the assembly factor DNAAF1/Lrrc50/Oda7, a leucine-rich repeat protein that localizes to the cell body, caused decrease in the abundance of one of the heavy chain subunits in the cytoplasm without affecting levels of other heavy chains and intermediate chain subunits. A partial co-assembly of the

remaining heavy and the intermediate chains was observed in Oda7 mutants[58,157,158]. Ktu/PF13/DNAAF2, a cytoplasmic assembly factor belonging to the PIH protein group, is hypothesized to act as a co-chaperone in dynein assembly within the cytoplasm as it interacts with Hsp70. Studies show that all three ODA heavy chain subunits are depleted from pf13 mutants, while the intermediate chains are overabundant. Immunoprecipitation experiments show that intermediate and light chains preassemble in the pf13 mutants, however heavy chains are not assembled suggesting that KTU may be involves in heavy chain assembly but not light and intermediate chain assembly[60,61,156]. A third dynein assembly factor DNAAF3/Pf22 is specifically required for the proper folding of the individual HCs for their subsequent association into larger, multi-subunit complexes with the ICs and LCs[46,102]. DNAAF1, DNAAF2 and DNAAF3 thus appear to facilitate folding of the dynein heavy chains that are then assembled into an ODA complex in the presence of chaperones. Factors that similarly contribute to assembly of light and intermediate chains have yet to be defined.

Mutations in Dyx1c1 are identified that cause PCD in humans and PCD-like phenotypes in mouse and zebrafish. Immunofluorescence analysis revealed that Dyx1c1 localizes to the cytoplasm of mouse respiratory epithelial cells. DYX1C1 interacts with the E3 ubiquitin ligase CHIP, HSP70, HSP90, and KTU/DNAAF2 consistent with function as a cytoplasmic assembly factor[128,129]. Together, these findings suggested that DYX1C1/DNAAF4 is an essential component of the ciliary dynein cytoplasmic pre-assembly process[159]. Dyx1c1 mutant ciliary

axoneme exhibit the lack of the ODA components DNAH9, DNAH5 and DNAI2[160]; but the assembly state of heavy, light and intermediate chain dyneins in the cytoplasm of the Dyx1c1 mutants has not been previously defined.

In this study we provide evidence that DYX1C1 promotes assembly of axonemal light chains in the cytoplasm of tracheal epithelial cells. We find that Dyx1c1 interacts with the ODA intermediate chain subunits Dnai1 and Dnai2 and light chain subunits Dnal1 and Dnal4 in tracheal epithelial cells. Tracheal epithelial cells in mutants have reduced levels of light and intermediate chains, and light and intermediate chains fail to assemble in mutants. To further test whether DYX1C1 specifically promotes assembly of light chains we co-expressed DYX1C1 or other DNAAFs in HEK293 cells along with axonemal dynein light chains. DYX1C1 promoted the highest level of light chain association in Hek293 cells compared to all other DNAAFs, and this activity was reduced by DYX1c1 mutations. Based on this data, we propose a model wherein Dyx1c1 assembles the light chain subunits Dnal1 and Dnal4 in an early step in ODA preassembly.

5.3 Results:

5.3.1 Dyx1c1 interacts with axonemal dynein subunits of the ODA complex in the cytoplasm of tracheal epithelial cells

Previous studies have suggested that mutations in dynein assembly factors could either prevent the dynein arm complex from preassembling in the cytoplasm and that dynein assembly factors might play a role in the assembly of the dynein subunits; either by directly interacting with them, or in an indirect, chaperone-

mediated fashion. More direct biochemical analysis of Dyx1c1 function depends on the cytoplasmic pool of the axonemal dyneins. In order to identify the role of Dyx1c1 in the cytoplasm, we developed a protocol for separation of the ciliary axonemes from the trachea of Dyx1c1 wildtype and knockout mouse. We thus obtain two fractions after the deciliation workflow: i) cytoplasmic fraction containing the trachea stripped off the ciliary axoneme and ii) axonemal fraction consisting of the ciliary axoneme. We found that the wildtype and knockout axonemal fraction had little or no contamination of the cytoplasmic fraction and vice-versa.

We investigated the role of Dyx1c1 in the ODA pre-assembly in the tracheal cytoplasm. Since some of the assembly factors associate with one or more of the axonemal dynein subunits themselves, we found it important to evaluate for an interaction of Dyx1c1 with the intermediate and light dynein chain subunits of the outer dynein arm complex (Fig. 5-1). We investigated the interaction of Dyx1c1 with the dynein subunits in the cytoplasmic fraction obtained from the WT and KO trachea. We performed immunoprecipitations using the anti-Dyx1c1 antibody to pull down the Dyx1c1 protein from the wildtype and knockout Dyx1c1 tracheal cytoplasmic fractions. Since the Dyx1c1 protein is not expressed in the KO mouse trachea, the immunoprecipitation from the KO cytoplasm acts as the control. We looked for the interaction of Dyx1c1 with the ODA light chain subunits Dnal1 and Dnal4; and found that Dyx1c1 interacts with both the dynein light chain subunits Dnal1 and Dnal4. When we tested for the interaction of the Dyx1c1 with the intermediate chain subunits of the ODA Dnai1, Dnai2 and

Txndc3, we found that Txndc3 does not co-immunoprecipitate with Dyx1c1. However, the two other dynein intermediate chain subunits Dnai1 as well as Dnai2 co-precipitate with Dyx1c1 (Fig. 5-1). We thus show that Dyx1c1 needs to associate with intermediate and light chain dynein subunits for its function as a dynein cytoplasmic assembly factor.

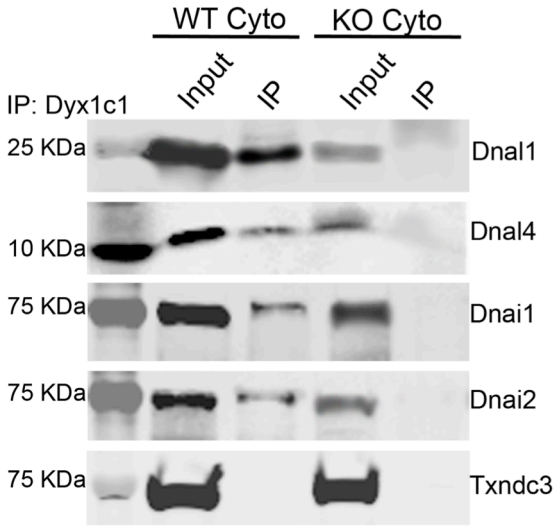

Figure 5-1 Interaction of Dyx1c1 with intermediate and light chain subunits of the outer dynein arm. *Co-immunoprecipitation and western blot analysis indicates that Dyx1c1 interacts with ODA light chains Dnal1 and Dnal4; ODA intermediate chains Dnai1 and Dnai2; but not with Txndc3.*

5.3.2 Dyx1c1 require C-terminal TPR containing domains to interact with ODA light chains Dnal1 and Dnal4

We assessed the interactions of Dyx1c1 with the ODA light chains Dnal1 and Dnal4 in a heterologous expression system. The Dyx1c1 protein has an N-terminal p23 domain similar to the heat shock protein family domains and C-terminal TPR domains that are known to mediate protein-protein interactions.

Biallelic mutations identified in Dyx1c1 that caused PCD in humans were found between amino acids 128 and 195 of the 420-amino acid Dyx1c1 protein. These mutations are thus predicted to lead to a truncated protein product devoid of the TPR domains. Studies characterizing the role of Dyx1c1 in the developing rat neocortex showed that knockdown of Dyx1c1 leads to abnormal neuronal migration and this phenotype can be rescued by overexpressing the TPR domain-containing region of Dyx1c1. Additionally the TPR domains have been shown to be important for interaction of Dyx1c1 with the chaperones.

We tested three Dyx1c1 constructs fused with GFP; one full-length; one N-terminal deletion missing the p23 domain; and the other C-terminal deletion construct lacking the TPR domains; as shown in the schematic in Fig. 5-2a for the interaction with Dnal1 and Dnal4 by co-immunoprecipitation. Dnal1 and Dnal4 were incorporated into the vector with chicken actin gene promoter with flag and myc epitope-tags (pCAG-Dnal1-flag and pCAG-Dnal4-myc) respectively. To test for the interaction of Dyx1c1 with the light chains Dnal1 and Dnal4, we co-transfected HEK 293T cells with full-length Dyx1c1 (pCAG-Dyx1c1-GFP) construct with either pCAG-Dnal1-flag or pCAG-Dnal4-myc. We also co-transfected either of the light chains with pCAG-GFP plasmid as a control. We immunoprecipitated the Dyx1c1 protein using the anti-GFP antibody and probed with Dnal1 or Dnal4 antibody. We found that Dyx1c1 interacts with Dnal1 and Dnal4 both independently co-precipitate with Dyx1c1 (Fig. 5-2b, d). We found a 9-fold increase in the interaction between Dnal1 and Dyx1c1, whereas a 5-fold increase was observed in the association of Dnal4 and Dyx1c1 compared to the

GFP control condition. We further investigated the interaction of the Dnal1 and Dnal4 with the truncation constructs of Dyx1c1. We co-transfected the dynein light chains Dnal1 or Dnal4 with one of the following: full-length, N-terminal or C-terminal truncation constructs of Dyx1c1. We then performed immunoprecipitation experiments using anti-GFP antibody and probed for Dnal1 or Dnal4 (Fig 5-2c, e). The interaction of both Dnal1 and Dnal4 with the p23 domain of Dyx1c1 was reduced by about 75% when normalized to their association with full-length Dyx1c1. Interestingly, both the Dnal1 and Dnal4 were found to co-precipitate with the TPR domain-containing construct of Dyx1c1. The TPR domains of Dyx1c1 are thus necessary and sufficient for the interaction of Dyx1c1 with the light chain dyneins Dnal1 and Dnal4.

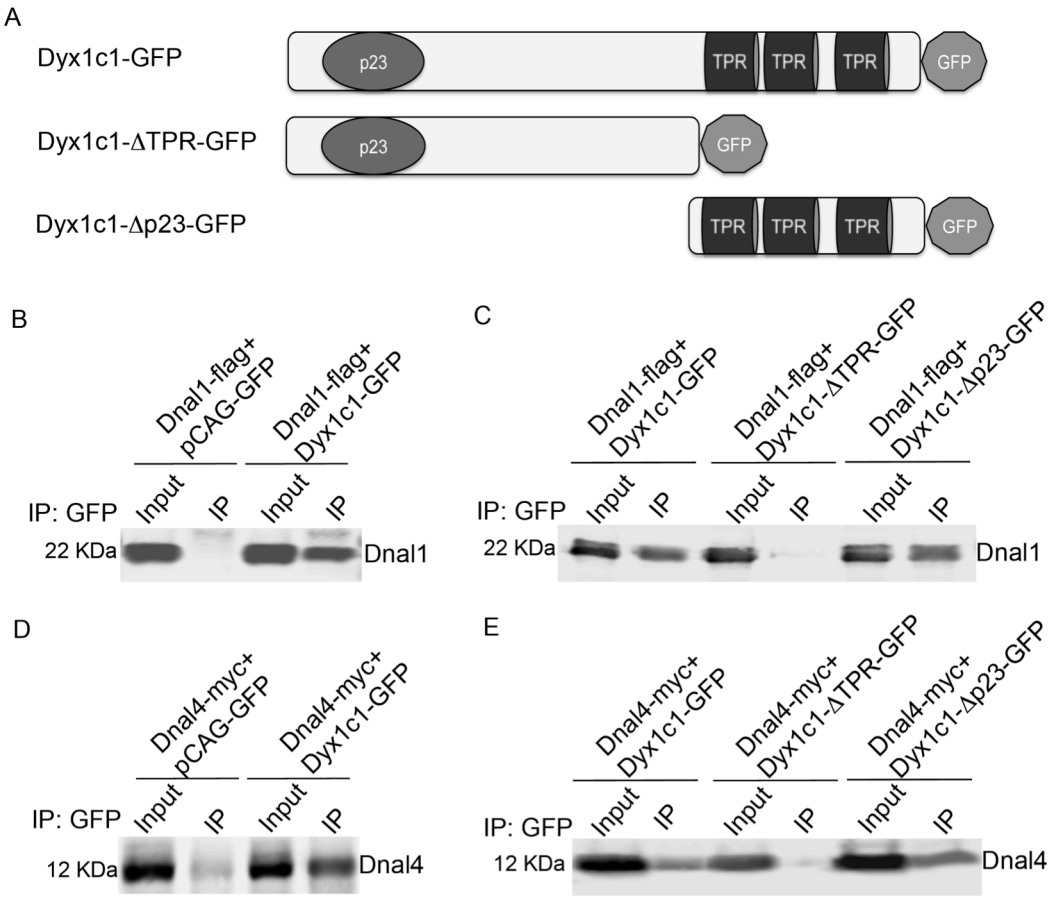

Figure 5-2: Heterologous interaction of Dyx1c1 with ODA light chain subunits Dnal1 and Dnal4. *(a) Schematic of Dyx1c1 full-length and truncation constructs fused to GFP. Co-immunoprecipitation and western blot analysis shows that Dyx1c1 interacts with Dnal1 (b) and Dnal4 (d). Co-immunoprecipitation and western blot analysis shows that Dyx1c1 interacts with Dnal1 (c) and Dnal4 (e) through the TPR domains of Dyx1c1.*

5.3.3 Light and intermediate dynein subunits of the ODA complex fail to assemble in the Dyx1c1 knockout tracheal epithelial cell cytoplasm

The mutant cilia of the previously identified axonemal dynein assembly factors (DNAAF1, DNAAF2, DNAAF3) have all shown absence of the outer and inner dynein arms in the axoneme due to a defect in the chaperone-dependent cytoplasmic preassembly of the ODA or IDA complex. Since Dyx1c1 localizes to the cytoplasm of the ciliated respiratory epithelial cells and interacts with the heat shock proteins Hsp70 and Hsp90, it is hypothesized to play a role in promoting axonemal dynein subunit preassembly. We thus investigated the assembly state of the ODA complex in the cytoplasm of the Dyx1c1 knockout trachea. To assess the association of the light chain subunits Dnal1 and Dnal4, we co-immunoprecipitated the light chain subunit Dnal1 using anti-Dnal1 antibody and probed for Dnal4 as well as Dnal1. We found that Dnal4 co-precipitated with Dnal1 in the WT cytoplasm, while it failed to interact in the KO cytoplasm. In order to evaluate the interaction of Dnal1 to Dnal4 quantitatively, we analyzed the percentage intensity ratio of immunoprecipitated Dnal4 to its input and normalized that to the percentage intensity ratio of immunoprecipitated Dnal1 to its input. The interaction between Dnal1 and Dnal4 was reduced by ~85% in the knockout cytoplasm indicating a faulty assembly of the light chain subunits (Fig. 5-3a).

We further assessed the interaction amongst the intermediate chain subunits of the ODA complex for which we immunoprecipitated one of the IC subunits and

blotted for the presence of the other IC subunit. Here we investigated the interaction between the IC subunits Dnai1 and Dnai2 as well as Txndc3 and Dnai2. We immunoprecipitated the IC subunit Dnai2 from the WT and KO cytoplasmic extracts and probed with Dnai1 and Txndc3 to analyze their interaction with Dnai2. Dnai1 and Dnai2 interact in the WT cytoplasm while this interaction is diminished in the KO cytoplasm. After quantitative analysis of the interaction of Dnai1 and Dnai2 as previously described, we identified that interaction was reduced to ~1% in the KO cytoplasm compared to the 34% association in the WT cytoplasm (Fig. 5-3b). Txndc3 and Dnai2 were found to assemble in the WT cytoplasm and failed to associate in the KO. The interaction between these two subunits was reduced by almost 99% in the KO cytoplasm when compared to the WT (Fig. 5-3c). We have shown that Txndc3 fails to associate with Dyx1c1 (Fig. 5-1d) but the interaction of Txndc3 with the intermediate chain subunit Dnai2 is altered in the mutant cytoplasm. Dyx1c1 seems to be crucial for the interaction of the intermediate chain subunits Dnai1, Dnai2 and Txndc3 in the cytoplasm, even though it does not directly interact with Txndc3.

Next, we examined the assembly state of the LC-IC complex of the ODA by assessing the interaction between IC subunit Dnai2 and LC subunit Dnal4. We performed immunoprecipitation of Dnal4 using anti-Dnal4 antibody from the WT and KO cytoplasmic extracts and probed for Dnai2. Dnai2 co-precipitated with Dnal4 in the WT cytoplasm, but showed reduced association in the KO cytoplasm. Upon quantitative analysis of the interaction, we found a 76%

decrease in the association of Dnai2 to Dnal4 in the KO (Fig. 5-3d). These results demonstrate the defect in the assembly of the light chain subunits with the intermediate chain subunits in the Dyx1c1 mutant cytoplasm. We thus found that Dyx1c1 is critical for the assembly of the ODA light chain and intermediate chain dynein subunits in the cytoplasm.

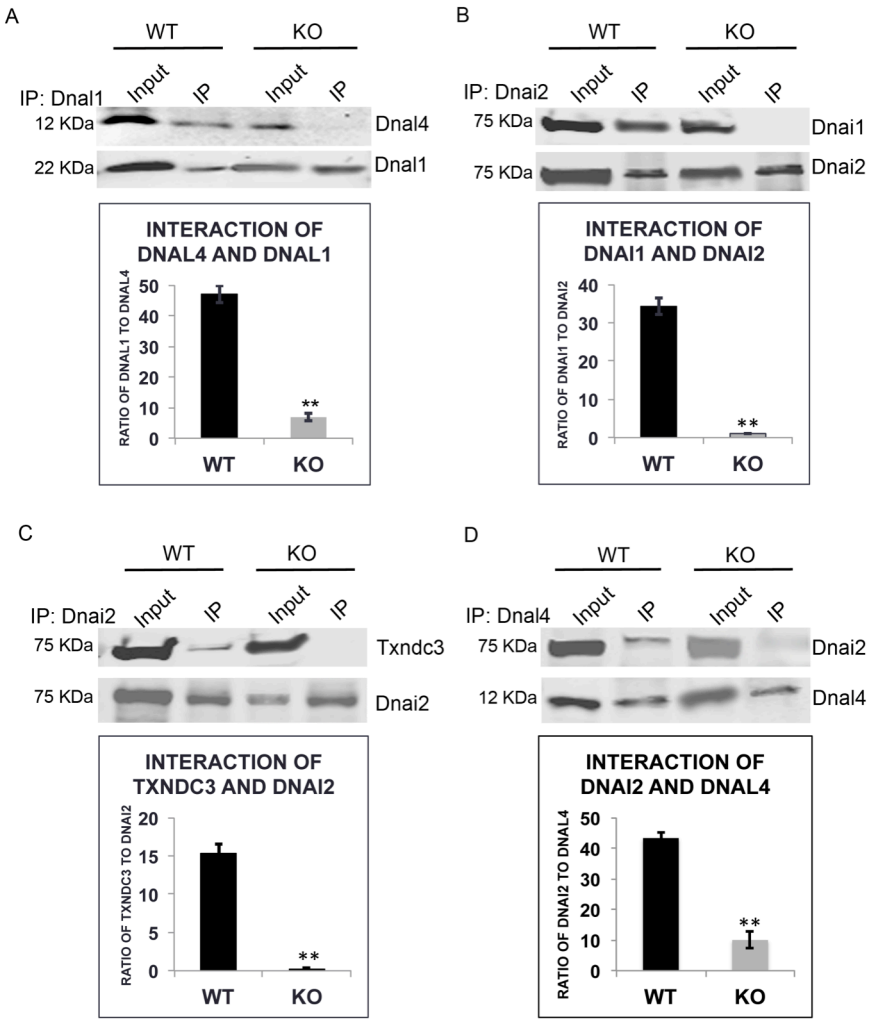

Figure 5-3: Outer dynein arm fails to assemble in the Dyx1c1 knockout tracheal cytoplasm. *(a) Co-immunoprecipitation and western blot analysis shows that Dnal4 interacts with Dnal1 (top panel); quantification of interaction (bottom panel). (b) Co-immunoprecipitation and western blot analysis shows that Dnai1 interacts with Dnai2 (top panel); quantification of interaction (bottom panel). (c) Co-immunoprecipitation and western blot analysis shows that Txndc3 interacts with Dnai2 (top panel); quantification of interaction (bottom panel). (d) Co-immunoprecipitation and western blot analysis shows that Dnai2 interacts with Dnal4 (top panel); quantification of interaction (bottom panel).*

5.3.4 Dyx1c1 induces the assembly of axonemal light chain subunits of Dnal1 and Dnal4

We have shown earlier in Fig. 5-3a that the dynein light chain subunits Dnal1 and Dnal4 interact in the wildtype cytoplasm and this interaction is weakened in the Dyx1c1 KO cytoplasm. To obtain an insight into the function of Dyx1c1 pertaining to light chain assembly, we tested for the association of Dnal1 and Dnal4 in HEK cells. HEK cells are immortalized kidney derived cell line that possesses primary cilia. Since HEK 293-T cells do not normally express the axonemal dyneins or motile-cilia specific genes, it was interesting to evaluate whether Dyx1c1 would be sufficient for the association of Dnal1 and Dnal4 in these cells. We co-transfected HEK cells with pCAG-Dnal1-flag and pCAG-Dnal4-myc with pCAG-Dyx1c1-GFP or pCAG-GFP constructs. We then performed immunoprecipitation using anti-Dnal1 antibody to pull down the Dnal1 and its interacting proteins and probed with Dnal4, to test for Dnal1-Dnal4 interaction. We also probed the blots for Dnal1 for normalization and subsequent analysis of the association. In the absence of full-length Dyx1c1, Dnal1 and Dnal4 fail to assemble heterologously; interestingly Dnal1 and Dnal4 interact robustly in the presence of Dyx1c1 (Fig. 5-4a). To obtain a quantitative measure of the interaction, we acquired percentage of intensity ratio of immunoprecipitated Dnal4 to its wildtype expression level and normalized that to the intensity ratio of immunoprecipitated Dnal1 to its wildtype expression level. We observed that there was a 8-fold increase in the association of Dnal1 and Dnal4 in the presence of Dyx1c1 compared to the GFP control condition (Fig. 5-4b).

We showed that the C-terminal TPR-containing domains of Dyx1c1 mediate the interaction Dyx1c1 with the individual axonemal dynein light chain subunits Dnal1 and Dnal4. To assess the domain of Dyx1c1 required for the association of Dnal1 and Dnal4, we co-transfected with both pCAG-Dnal1-flag and pCAG-Dnal4-myc constructs with either N-terminal or C-terminal truncation constructs of Dyx1c1. Using the anti-Dnal1 antibody, we pulled down Dnal1 protein and performed western blot to look for the expression of Dnal4. Unexpectedly, we found that Dnal1 and Dnal4 associate with each other in both the conditions (Fig. 5-4a) and just the TPR-domains are not sufficient for the assembly. Compared to the full-length Dyx1c1, the Dnal1-Dnal4 association was reduced to half in the presence of the Dyx1c1 truncation constructs (Fig. 5-4b); indicating that both the domains of Dyx1c1 are required for the light chain assembly.

We further investigated whether the interaction of Dnal1 and Dnal4 was altered in the presence of the novel missense mutant Dyx1c1 p.L19Q (Dyx-Mut). We co-transfected HEK cells with the pCAG-Dnal1-flag and pCAG-Dnal4-myc along with point mutant construct Dyx-Mut. We then performed co-immunoprecipitation experiments and analysis as described earlier and found that the association of Dnal1 and Dnal4 was considerably reduced in the Dyx-Mut condition (Fig. 5-4a). Analysis of the Dnal1-Dnal4 assembly in the mutant condition exhibited a reduction of 62.5% when compared to the full-length Dyx1c1 condition (Fig. 5-4b).

We next assessed whether any of the other three cytoplasmic assembly factors DNAAF1/Lrrc50, DNAAF2/Ktu and DNAAF3 could aid in the association of the light chains Dnal1 and Dnal4. HEK cells were co-transfected with pCAG-Dnal1-

flag and pCAG-Dnal4-myc along with one of the above-mentioned assembly factors. After the co-immunoprecipitation and western blot analysis, we found that Dnal1 and Dnal4 do not associate in the presence of DNAAF1 or DNAAF3. Interestingly, they are found to interact in the presence of the assembly factor DNAAF2 (Fig. 5-4a), which is previously shown to interact with Dyx1c1. When normalized to Dnal1-Dnal4 assembly in the presence of full-length Dyx1c1, it was observed that the association was decreased by 50% in the presence of DNAAF2/Ktu (Fig. 5-4b). We thus show that Dyx1c1 induces the assembly of the dynein light chain subunits Dnal1 and Dnal4 in a heterologous expression system. We conclude that both the TPR and p23 domains of Dyx1c1 are required for the promoting the assembly of the light chain subunits.

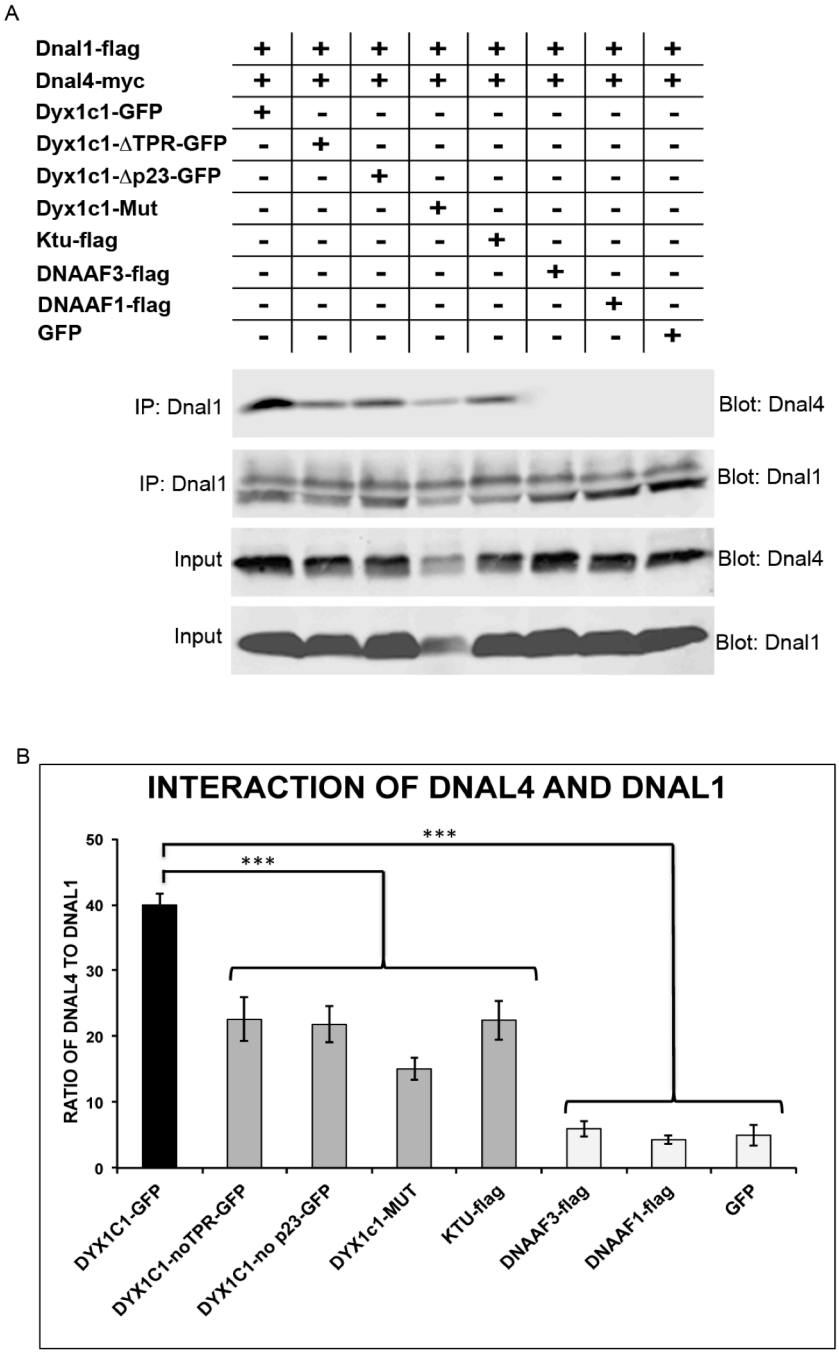

Figure 5-4: Dyx1c1 facilitates the assembly of Dnal1 and Dnal4. *(a) Interaction of Dnal1 and Dnal4 in the presence of full-length Dyx1c1, truncation constructs of Dyx1c1, Dyx-Mut and assembly factors DNAAF1, DNAAF2 and DNAAF3. (b) Quantification of the association of Dnal4 to Dnal1 when normalized to Dnal1. Posthoc analysis, P-value<0.001 (***).*

5.4 Discussion

Defects in the assembly of the outer and inner dynein arm complexes due to mutations in either the dynein subunits themselves, or the assembly factors that aid in the formation of the dynein complexes, lead to PCD. It has been proposed in previous studies performed in Chlamydomonas that the dynein arms are preassembled in the cytoplasm as three complexes: a heavy chain-intermediate chain (HC-IC) complex; a light chain complex (LC) and a docking complex (DC)[56]. According to this model, the heavy and the intermediate chain subunits exist as a complex in the cytoplasm and the lack of either the heavy or light chain subunit would lead to a defective dynein complex. The light chains would then be assembled onto the HC-IC complex, which would later be docked on the DC before being loaded on the IFT particle. Detailed characterization of the cytoplasmic preassembly process is required to understand ciliary motility that might help in the better diagnosis of PCD. Deciphering the multi-step assembly pathway and the proteins involved could also potentially lead to identification of pharmacological targets that might help PCD patients.

Dyx1c1 has been previously identified as a cytoplasmic pre-assembly factor of the axonemal dyneins, the lack of which leads to the absence of both the inner and the outer dynein arms in the axoneme of the patients. Despite the functional conservation of Dyx1c1 amongst the organisms examined (mouse, humans and zebrafish) evident from the similar phenotypes observed, it was still unclear how Dyx1c1 functions in the dynein arm assembly process. It was hypothesized that due to the cytoplasmic localization of Dyx1c1, it plays a role in the assembly of

the dynein arm complex through its interactions with the heat shock proteins and/or its subsequent transport from the cytoplasm to the transition zone or the base of the cilia. The data presented in this study suggest that the assembly of the outer dynein arm complex requires at least the following steps: a first step in which the subunits are folded and stabilized; a second step wherein the subunits are aggregated by one or more assembly factors; and the final step that generates a functional complex competent for transport and binding to the microtubules.

Our biochemical analyses provide an important insight into the proposed function of Dyx1c1 as a facilitator of dynein preassembly in the cytoplasm by identifying the defect in the assembly of the dynein light and intermediate chain subunits in the absence of Dyx1c1. It has been shown that the assembled dynein arms form a pool of cytoplasmic precursor that is then transferred to a loading zone around the basal body from where it is transported into the axoneme via IFT. Since the dynein arm assembly process takes place in the cytoplasm, it was critical to perform fractionation of the trachea into cytoplasmic extract and axonemal extract. We evaluated the interaction of Dyx1c1 with the light and intermediate chain dynein subunits by co-immunoprecipitation and western blot analysis. We found that Dyx1c1 fails to interact with IC subunit Txndc3, but associated with the other IC chains Dnai1 and Dnai2 as well as LC subunits Dnal1 and Dnal4. The interaction of Dyx1c1 with the IC and LC subunits is considerably reduced in the Dyx1c1 KO tracheal cytoplasm; thus indicating that Dyx1c1 is important for the assembly of the intermediate and light chain axonemal dynein subunits in the

cytoplasm. We also verified the interaction of the light chain subunits Dnal1 and Dnal4 with Dyx1c1 heterologously. Furthermore, we identified that the TPR domains of Dyx1c1 are critical for the light chain interaction.

We found that the ODA complex fails to assemble in the Dyx1c1 mutant cytoplasm. We observed that the light chain subunits Dnal1 and Dnal4 that associated in the WT cytoplasm fail to assemble in the KO cytoplasm. Similarly, the IC subunits Dnai2 and Dnai1 as well as Dnai2 and Txndc3 that interact in the WT cytoplasm are found to not assemble in the KO cytoplasm. Interestingly, the IC-LC assembly of Dnai2 and Dnal4 was also absent in the mutant cytoplasm indicating a role of Dyx1c1 in the assembly of the IC-IC, LC-LC as well as IC-LC subunits of the ODA complex. We also observed reduced abundance of the light and intermediate chain subunits in the Dyx1c1 knockout cytoplasm, which is consistent with an altered preassembly process. Since the light chain subunits Dnal1 and Dnal4 interact with each other in the Dyx1c1 wildtype cytoplasm, we assessed whether Dyx1c1 was sufficient for their association in HEK cells. Interestingly, Dyx1c1 induces the assembly of Dnal1 and Dnal4 and the association of these two light chains requires both the p23 and TPR domains of Dyx1c1. A novel missense mutation identified in Dyx1c1 reduces the interaction between the light chains by about 60%. Previous evidence has also shown that in spite of the overabundance of one the heavy chain dynein subunits in the cytoplasm of the Ktu mutant, this subunit fails to co-precipitate with the other dynein subunits, suggesting an aberrant assembly process[61]. We also tested the interaction of Dnal1-Dnal4 in the presence of Ktu, an interactor of Dyx1c1, as

well as the other assembly factors Dnaaf1 and Dnaaf3. The association of the light chains was impaired in the presence Dnaaf1 and Dnaaf3, while Ktu assisted weakly in the assembly of the light chains.

In conclusion, we have shown an essential role for Dyx1c1 (Dnaaf4), a conserved dynein assembly factor in the pre-assembly of multiple ciliary axonemal dyneins. Dyx1c1 function seems to be different from the other recently identified PCD proteins Dnaaf1, Dnaaf2, Dnaaf3 and Mot48[61] in that it is essential for the assembly of the light chain and intermediate chain subunits (Fig. 5-5). We propose that Dyx1c1 assembles the intermediate chains in the cytoplasm onto which the heavy chains get assembled. The light chains are assembled in the cytoplasm in the presence of Dyx1c1, which are then potentially targeted to the correct dynein subunit in the presence of other assembly factors. In summary, Dyx1c1 defines a step in the multi-stage pathway that is essential for the cytoplasmic assembly of the ciliary dyneins. Further characterization of Dyx1c1 in the assembly process is required to determine whether Dyx1c1 is involved in the chaperone-mediated folding of the individual subunits, or their association into the multi-subunit dynein arm complex. Because there are many dynein subunits and their isoforms that are required for the normal ciliary function, and the current assembly factors do not contribute to the formation of all the dynein complexes, there is a need for additional future studies to identify more assembly factor proteins.

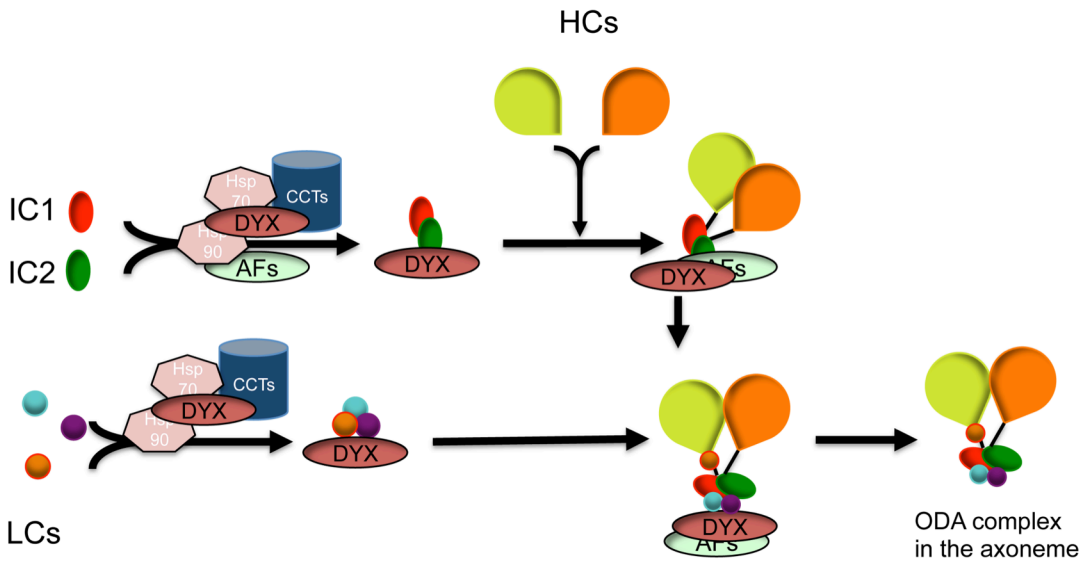

Figure 5-5: Proposed role of Dyx1c1 in the cytoplasmic assembly pathway. *Dyx1c1 interacts with the chaperones and intermediate as well as light chain dynein subunits in the cytoplasm. The heavy chains are added onto the intermediate chains and the light chains are further incorporated into the outer dynein arm complex in the presence of Dyx1c1 and other assembly factors.*

5.5 Materials and Methods

5.5.1 Deciliation of the trachea

The tracheas harvested from postnatal day 16 (P16) Dyx1c1 wildtype and knockout mice were washed with cold phosphate-buffered saline to remove mucus and cell debris. Animal procedures were performed under protocols approved by the Institutional Animal Care and Use Committee of the University of Connecticut and conform to US NIH guidelines. The dissected tracheas were

transferred to a separate tube containing deciliation buffer, and incubated for 10 min with intermittent mild vortexing. The supernatant was collected in a separate tube, and the procedure was repeated twice. The tracheas were then separated from the supernatant, the three washings were pooled, and after pelleting cell debris at 800x*g*, the ciliary axonemes were collected by centrifugation at 20,000xg. Ciliary axonemal pellets were resuspended gently in 30 mM Hepes (pH 7.3), 1 mM EGTA, 0.1 mM EDTA, 25 mM NaCl, 5 mM $MgSO_4$, 1 mM dithiothreitol, and 1% volume of protease inhibitor mixture (Sigma). Triton X-100 was added (0.5%) to the suspension, and the axonemes were incubated for 15 min on ice, followed by centrifugation. The lysates containing the axonemal fraction were then frozen at -80°C. The cilia-stripped-tracheas were incubated in RIPA buffer (Sigma) on ice for 20 min. Samples were homogenized using a tissue homogenizer and cleared by centrifugation at 10,000g for 10 min to obtain the protein lysate of the cytoplasmic fraction of the trachea. Protein concentrations were estimated using the BCA reagent (Pierce).

5.5.2 Protein blots of whole trachea, cytoplasmic and axonemal lysates

For whole tracheal preparation, tracheal tissues were dissected from wildtype and knockout mice, and carefully separated from the surrounding tissues. After incubation in RIPA Buffer supplemented with 1× Protease Inhibitor Cocktail (Sigma), samples were homogenized using a tissue homogenizer and cleared by centrifugation at 10,000g for 10 min. The cytoplasmic and axonemal fractions of the trachea were prepared as described above. Proteins were separated on 12% SDS- PAGE minigels and then transferred to Immobilon (Millipore) membrane for

protein blotting. For detecting DYX1C1 protein, the antibody to N-terminal DYX1C1 (Sigma, SAB4200128) was used at a dilution of 1:200; antibody to acetylated tubulin (Sigma, T6793) was used at a dilution of 1:2000; and antibody to GAPDH (Sigma, G8795) was used at a 1:1,500 dilution as a loading control. LI-COR Odyssey infrared secondary antibodies (goat antibody to mouse 680 (926-32220), goat antibody to mouse 800 (926-32210), goat antibody to rabbit 680 (926-32221) and goat antibody to rabbit 800 (926-32211)) were used at dilutions of 1:15,000. All blots were imaged and analyzed using a LI-COR Odyssey Scanner and Software.

5.5.3 Plasmids

To construct Dnal1 and Dnal4 expression plasmids, cDNAs of Dnal1 and Dnal4 respectively were amplified by PCR (Platinum Hi-Fidelity *Taq*DNA polymerase, Invitrogen) from cDNA clones (BioSource). Dnal1 and Dnal4 sequences were further amplified using primers incorporating flag and myc epitope tagged sequences respectively and then subcloned into pCAG vector to create pCAG-Dnal1-flag and pCAG-Dnal4-myc plasmids. The GFP fused full length (pCAG-Dyx1c1-GFP) and deletion constructs of Dyx1c1 (pCAG-ΔTPR-GFP and pCAG-Δp23-GFP) were constructed as described previously[124]. The pCAG-GFP plasmid was used as a control. The flag-tagged DNAAF1, DNAAF2 and DNAAF3 plasmids were a gift from Dr. Heymut Omran. The sequence of all plasmids was confirmed by sequencing.

5.5.4 Cell culture and transfection

Human embryonic kidney (HEK293T) cells were grown to confluence in DMEM supplemented with 10% FBS, 1% non-essential amino acid (NEAA) and 1% penicillin-streptomycin antibiotics (Invitrogen). Cultures were plated at a density of 10^6 cells on a 10-cm petridish. DNA (24 µg) was added to the petridish with 75 µl of Lipofectamine 2000 reagent (Invitrogen) in OptiMEM-1. The transfection mix was added to cells in normal growth media and incubated for 48 h at 37 °C. To obtain the protein lysates from the cells, the normal growth media was removed and the cells were washed with PBS. The cells were then collected, centrifuged to pellet the cells and the pellet was incubated in RIPA buffer supplemented with 1X Proteinase Inhibitor Cocktail for 20 min on ice. The lysates were then centrifuged at 2000xg to pellet the debris. Protein blots were also performed on the transfected cells as described above.

5.5.5 Immunoprecipitation

Immunoprecipitation assays were performed using the Dynabeads Protein G Immunoprecipitation kit (Invitrogen). Briefly, Dynabeads were resuspended in the vial and separated on a magnet from solution. Antibody to Dyx1c1 (Sigma, SAB4200128), Dnal1 (Proteintech, 15809-1-AP), Dnal4 (Proteintech, 10388-1-AP), DNAI2 (Abnova, M01, clone 1C8) or GFP (Life Technologies, A11122) (5 µg) was diluted in 200 µl of Washing and Binding Solution and incubated with rotation for 120 min at room temperature. Bead-antibody complexes were separated on the magnet, washed by gentle pipetting and separated. Protein lysates were incubated with the bead-antibody complexes overnight at 4 °C. Bead-antibody-antigen complexes were then washed using the washing solution

three times. Complexes were then incubated with elution buffer for 10–15 min to dissociate them. Beads were separated on a magnet, and supernatant containing the proteins was separated by SDS-PAGE and analyzed by protein blotting using monoclonal antibody to DNAI2 (Abnova, M01, clone 1C8; 1:500 dilution), antibody to DNAI1 (Proteintech, 12756-1-AP; 1:500 dilution), antibody to Hsp70 (BD Biosciences, 610607; 1:1,000 dilution), antibody to Txndc3 (Proteintech, 13586-1-AP, 1:500), antibody to Hsp90 (BD Biosciences, 610418; 1:1,000 dilution), antibody to CCT4 (Aviva Systems Biology, ARP34271_P050; 1:500 dilution), antibody to CCT3 (Proteintech, 10571-1-AP; 1:500 dilution), anti- body to CCT5 (Proteintech, 11603-1-AP; 1:500 dilution), antibody to CCT8 (Proteintech, 12263-1-AP; 1:500 dilution), c-myc antibody (Sigma, C3956, 1:500 dilution), c-myc antibody mouse monoclonal (Sigma, M4439, 1:750 dilution), antibody to flag produced in rabbit (Sigma, SAB1306078, 1:1000 dilution), and mouse monoclonal anti-flag antibody (Sigma, F4042, 1:500 dilution). Rabbit IgG was used as a control.

6. SUMMARY

This dissertation is focused on characterization of the developmental role of Dyx1c1. In this chapter, I will summarize the significance of my results and discuss the role of Dyx1c1 in the axonemal dynein preassembly process, followed by a detailed discussion of the unanswered questions.

6.1 Summary of Chapters 2,3 and 4

In the present study, reverse genetics approach has been successfully applied to assess the function of a candidate dyslexia gene Dyx1c1. We identified that Dyx1c1 knockout mice generated by the deletion of exons 2, 3 and 4 of Dyx1c1 causes an absence of the Dyx1c1 protein. The mutation in Dyx1c1 in mice leads to PCD-like symptoms of hydrocephalus and situs inversus. Investigation of the mutant embryonic node revealed abnormalities as evident from the deposition of vesicle-like structures on the nodal surface in addition to monocilia; indicative of ciliary dysmotility. The ependymal cilia of the brain ventricles were examined by videomicroscopy and Indian ink assay to find mutant cilia completely immotile. Ultrastructural analysis of these mutant cilia further revealed the absence of two components of the motile cilia critical for ciliary motility, outer and inner dynein arms, missing from the mutant ciliary axoneme. Similar PCD-associated phenotypes were found in the Dyx1c1 mouse mutant, zebrafish knockdown and human PCD patients[160]. Thus, Dyx1c1 is an evolutionarily conserved protein essential for the motility of cilia. This gene is speculated to be important for formation of the outer and inner dynein arms in the cytoplasm, or their transport and binding to the microtubules in the axoneme.

Given the loss of identifiable IDA and ODA in Dyx1c1 mutant cilia, we analyzed the subcellular localization of Dyx1c1 and observed that Dyx1c1 localized to apical cytoplasm of the respiratory epithelial cells. These results led us to the hypothesis that Dyx1c1 is required for the cytoplasmic pre-assembly of axonemal dyneins. The Dyx1c1 mutation affected the localization of axonemal components of motile cilia. No expression of ODA DNAI2 and DNAH5 was detected by immunofluorescence in Dyx1c1 mutant cilia of the mice and PCD patients. To obtain insights into Dyx1c1 function, we further defined the interactome of Dyx1c1 by immunoprecipitation and mass spectrometric analysis. Endogenous Dyx1c1 complexes were isolated by immunoprecipitation from wildtype tracheal lysates and tandem MS/MS analysis was performed on the immunoprecipitates to find that the Dyx1c1 interactome was enriched for the proteins in the categories of chaperones and cytoskeletal proteins. Previously known interactors of Dyx1c1 such as Hsp70 and Hsp90 were identified by MS screen. In addition, a group of T-complex chaperones (CCTs), with a known role in ciliogenesis, were also identified as interaction partners of Dyx1c1. Furthermore, Dyx1c1 interacted with a protein of the transition zone, Sept2, known to mediate the control of protein trafficking into and out of the ciliary axoneme. Immunoprecipitation and immunoblot analysis confirmed the interaction of Dyx1c1 with these newly identified interaction partners. The interactions were also validated in heterologous expression system; and it was further demonstrated that the TPR domains mediated the interaction of Dyx1c1 with the Hsp70 and CCTs, while the p23 domain was sufficient for interaction with Hsp90.

The cytoplasm of the ciliated cells supposedly accumulates the assembled precursor ODA/IDA motor complex prior to its transport into the axoneme. Information about the assembly state of the ODA/IDA in the Dyx1c1 mutant would thus be apparent by analyzing the cytoplasmic extract of the mutant cytoplasm. Hence we performed deciliation of the wildtype and knockout trachea to obtain axonemal fraction and deciliated tracheal fraction and assessed the cytoplasmic abundance of the dynein arm subunits. Western blot analysis with antibodies against components of outer dynein arms (DNAI1, DNAI2, DNAL1, DNAL4) and inner dynein arms (DNALI1) exhibited a reduction in the abundance of these subunits in the knockout tracheal cytoplasmic fraction compared to the wildtype. The decrease in the dynein subunits is suggestive of a faulty dynein arm assembly in the cytoplasm due to either altered degradation of the unassembled dynein subunits or decreased synthesis of the subunits. These results suggested a role of Dyx1c1 in the chaperone-dependent assembly of the dynein arms by assisting in the folding and stability of the individual dynein arm subunits or aiding in the incorporation of the subunits into a functional motor complex. Alternatively, the data suggest that Dyx1c1 might be required for the stability of the assembled dynein motor complex and trafficking to the base of the cilium at the transition zone.

A novel PCD-causing mutation in Dyx1c1 (p.L19Q) was recently identified in an inbred Druze population of Israel. This mutation was identified in the p23 domain of the Dyx1c1 protein and hence it was interesting to characterize this mutant biochemically. The patients suffered from the above-mentioned classic PCD

symptoms and lacked the expression of the ODA intermediate chain DNAI1 as well as the IDA chain DNALI1 from the mutant axoneme. Immunoblot analysis of the patient respiratory epithelial protein lysates demonstrated that the Dyx1c1 protein was expressed in the PCD patients at the correct size as were the proteins Sept2 and Ktu. However, intriguingly the interaction of Dyx1c1 with Setp2 and Ktu was reduced by more than half in the presence of the mutant compared to the control condition. Additional analysis of the dynein subunit abundance exhibited decreased expression of the ODA subunits DNAI2 and IDA subunit DNALI1; indicative of a defective pre-assembly of the dynein arms, thus strengthening our claim that Dyx1c1 is a cytoplasmic pre-assembly factor.

Outer arm dynein assembly is a multistep process that involves preassembly of subunits in the cytoplasm, movement of complexes into flagella, and assembly of these complexes into a functional dynein arm (Fig. 6-2).

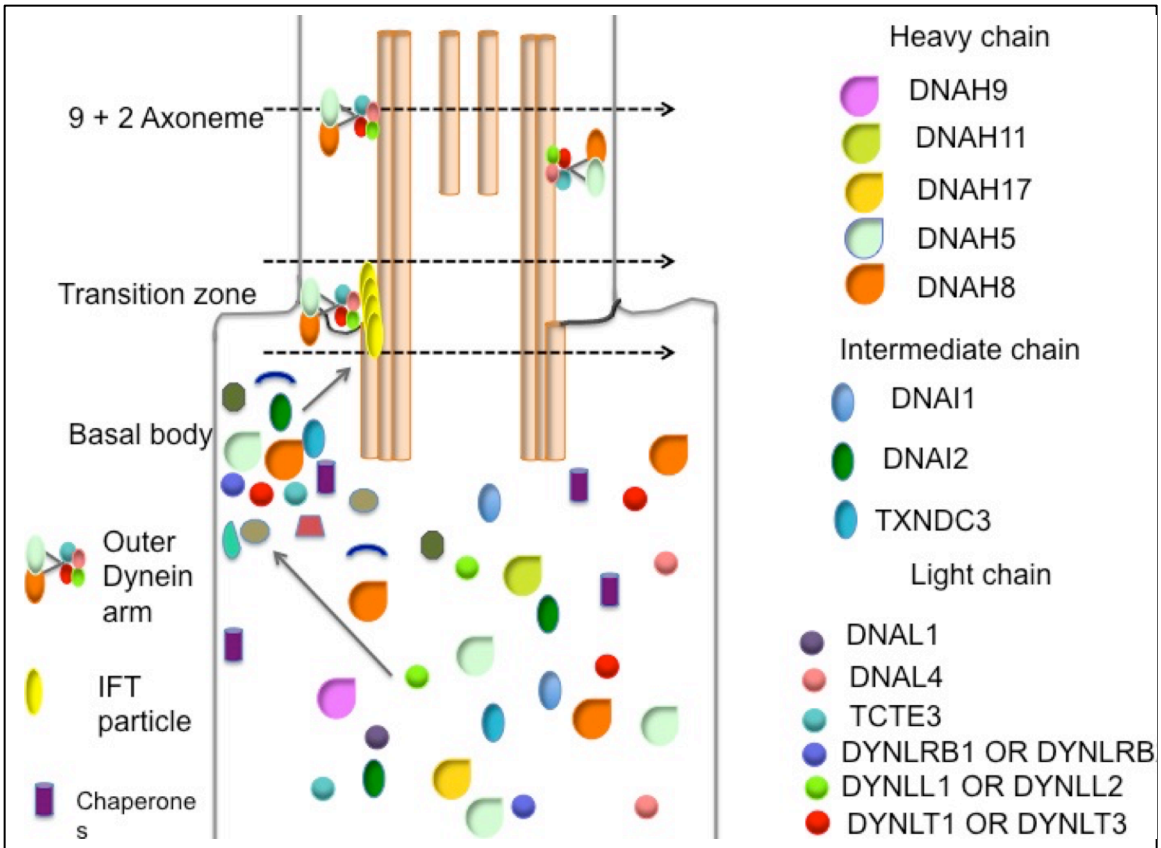

Figure 6-2: Schematic of the cytoplasmic pre-assembly of the outer dynein arm. *The outer dynein arm subunits are synthesized and transported to the base of the cilium at the basal body region. These subunits are then assembled together into a functional outer dynein arm in the presence of the chaperones and assembly factors. The assembled complex is docked onto the IFT particles for their transport into the axoneme and later attached to the microtubules. (Adapted from Fliegauf et al. 2008)*

Most mutations that disrupt this process have been traced to genes encoding subunits of the dynein motor itself, or cytoplasmic assembly factors of axonemal dyneins, or subunits of complexes that form binding sites for motor attachment. Cytoplasmic preassembly of dynein HCs has been found to require at least two steps[61]. The first step involves the folding of the globular dynein head domain, which is required for HC stability. DNAAF1 and DNAAF2 contribute to this step

together with HSP70. The second step involves formation of the HC–IC complex, which requires DNAAF3 (Fig. 6-3). Further experiments are needed to understand the specific role of Dyx1c1 in the assembly process.

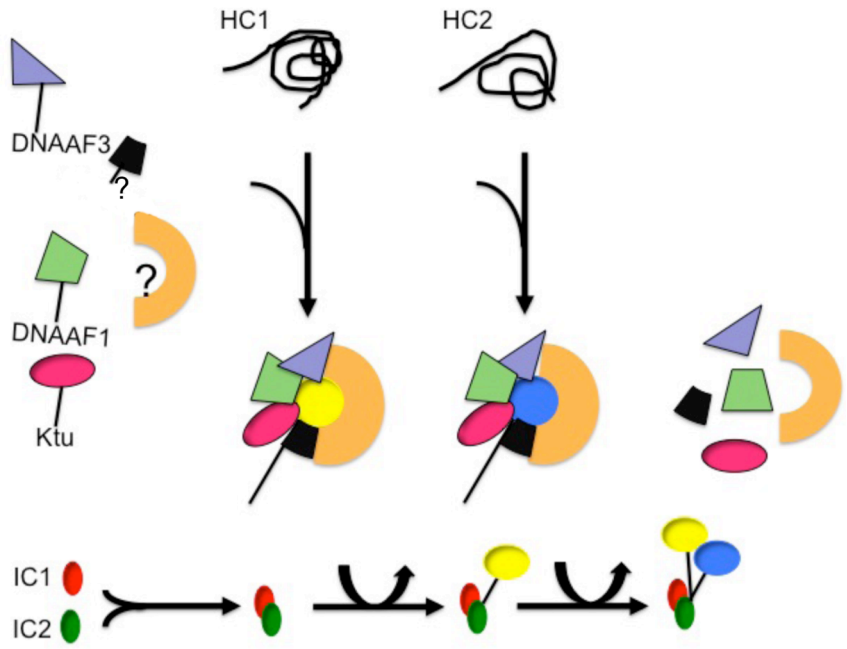

Figure 6-3: Schematic of the proposed outer dynein arm pre-assembly in the presence of the cytoplasmic assembly factors. *The heavy chains require the action of DNAAF1, DNAAF2 and DNAAF3 for the proper folding of their head domains and their stability. These assembly factors may also contribute to later steps in which heavy chains associate with intermediate chains. We hypothesize that these assembly factors work with a chaperone complex (labeled with a question mark). (Adapted from Mitchison et al. 2012)*

Our biochemical analyses provided important insight into the proposed function of Dyx1c1 as a facilitator of dynein pre-assembly, by revealing defects in the interaction of intermediate and light chains in the cytoplasm. Immunoprecipitation experiments demonstrated an interaction between Dyx1c1 and the intermediate

chains, Dnai1 and Dnai2 as well as the light chains Dnal1 and Dnal4 in the cytoplasm of tracheal epithelial cells. Furthermore, the association of Dnai1 to Dnai2 and Dnal1 to Dnal4 was reduced in the mutant tracheal cytoplasm compared to the wildtype. The assembly of the intermediate to light chains was also found to be disrupted in the mutant cytoplasm. Heterologous experiments in transfected HEK cells showed that the light chains interacted with Dyx1c1 via the TPR domains of Dyx1c1. Interestingly these domains are previously identified to be important for Dyx1c1 role in neuronal migration as well as interaction with Hsp70 and CCTs. When the interaction of the light chains Dnal1 and Dnal4 was investigated, we found that Dyx1c1 was necessary to induce the interaction of the light chains. Intriguingly, both the domains of Dyx1c1 were required for the light chain association. Furthermore, the interaction of the light chains could be induced partially in the presence of Ktu/DNAAF2 but with the other assembly factors DNAAF1 or DNAAF3.

6.2 Cytoplasmic preassembly of axonemal dyneins

To understand the cytoplasmic preassembly process and specifically the role of Dyx1c1 in it, the following questions need to be addressed.

6.2.1 Which ultrastructural components does Dyx1c1 localize to?

Cilia are complex organelles requiring the proper functioning of several proteins. Electron microscopy has been useful in providing a detailed knowledge of the ciliary ultra structure. It is necessary to comprehend the specific macromolecules that contribute to the ciliary structures. Hence, to characterize the role of Dyx1c1 in the cytoplasmic preassembly in greater detail, it would be interesting to identify

the subcellular structures that associate with Dyx1c1 to pinpoint the pathway of Dyx1c1. Future studies performed using the immunoEM technique could assist in analyzing the ultrastructural localization of Dyx1c1 in ciliated cells. It could be speculated that since Dyx1c1 plays a role in the cytoplasmic preassembly of the dyneins, it would be localized at the base of the cilia around the basal bodies. Alternately, Dyx1c1 would be arranged almost linearly from the base of the cilia to the transition zone suggesting a function of Dyx1c1 in dynein arm transport. Studies have shown that Dyx1c1 interacts with chaperones and if Dyx1c1 were to function in protein folding or quality control, immunoEM would be able to detect its localization to the ER. The results obtained from these experiments will help us understand the role of Dyx1c1 in cytoplasm.

6.2.2 Is Dyx1c1 necessary for folding/stability of dynein subunits?

Our results show that the axonemal dynein subunits are reduced from the cytoplasm of the Dyx1c1 knockout trachea; thus indicating a role of Dyx1c1 in folding and/or stability of the axonemal dyneins. To determine if Dyx1c1 plays a role in the chaperone dependent assembly of the dynein arms, trypsin sensitivity assays could be performed to examine the folding state of the dynein subunits in the cytoplasm of the mutant. The abnormally folded chains would show an increased sensitivity to tryptic proteolysis in the KO indicating that Dyx1c1 functions in chaperoning steps that aid in the folding of those subunits. Abnormal protein folding leads to rapid degradation of the misfolded proteins, which would lead to reduction in their abundance. If the subunits are misfolded and are getting

depleted from the cytoplasmic pool due to higher rates of degradation, protein turnover rates could be examined by blocking protein synthesis using cycloheximide and probing for dynein subunit-specific antibodies.

6.2.3 Can Dyx1c1 re-expression rescue the ciliary immotility in the KO?

RNAi studies found that knockdown of Dyx1c1 caused abnormal cortical migration in rat neocortex, while overexpression of full-length Dyx1c1 lead to the rescue of the phenotype. Dyx1c1 deficiency leads to loss of ciliary motility and therefore, overexpression of Dyx1c1 in KO ciliated cells will be interesting to assess for the rescue of the immotility phenotype. The rescue experiments would also provide important insights into the assembly state of the dynein arms thus aiding in the understanding of the assembly process.

6.3 Dyx1c1 and ciliogenesis

Study in Chlamydomonas performed by our collaborators, identified an upregulation of Dyx1c1 during flagellar regeneration. This indicates that Dyx1c1 might have a putative function during ciliary regeneration as well as cell stress. It would be interesting to evaluate the differentially expressed genes and changes in localization patterns of Dyx1c1 on wildtype and knockout ciliated epithelial cells at various time points following stress-induced ciliary sloughing (deciliation).

6.4 Primary Ciliary Dyskinesia: Diagnosis and Treatment

Our knowledge of PCD has greatly increased with the genotype-phenotype correlation being better understood and more information about diagnostic and therapeutic options becoming available. In the future, it would be interesting to

identify pharmacological targets that have the potential to assist in protein expression and in turn overcome ciliary dysfunction. Another key issue is the identification and confirmation of more PCD causing genes. Cilia and flagella require many dynein isoforms for their normal function. The dynein assembly factors studied to date do not seem to be responsible for the formation of all of these axonemal dynein complexes. Future studies may identify additional proteins that are involved in these cytoplasmic assembly steps. This knowledge is crucial to allow for the development of suitable and effective screening methods and therapeutic agents.

6.5 Final Remarks

This study emphasizes the importance of the cytoplasmic preassembly steps in the formation of axonemal dynein arms. Based on the results presented here, the cytoplasmic assembly of axonemal dynein motors requires at least three steps: an earlier step required for chaperone-mediated folding of the axonemal dyneins, next step of aggregating the intermediate and light chains of the axonemal dyneins mediated by assembly factors and a later step that incorporates these dynein chains to generate an assembly competent motor complex (Fig. 5-5). In conclusion, we have shown an essential role for Dyx1c1 (DNAAF4), a conserved dynein assembly factor, in the assembly of multiple ciliary axonemal dyneins.

7. REFERENCES

1. *Cilia*. (Cilia).
2. 1214.full. 1–10 (1998).
3. Chih, B. *et al.* A ciliopathy complex at the transition zone protects the cilia as a privileged membrane domain. *Nature Cell Biology* **14,** 61–U97 (2012).
4. Landmarks in cilia research from leuwenhook to us. 1–6 (2012).
5. Carvalho-Santos, Z., Azimzadeh, J., Pereira-Leal, J. B. & Bettencourt-Dias, M. Evolution: Tracing the origins of centrioles, cilia, and flagella. *The Journal of Cell Biology* **194,** 165–175 (2011).
6. SOROKIN, S. Centrioles and the formation of rudimentary cilia by fibroblasts and smooth muscle cells. *The Journal of Cell Biology* **15,** 363–377 (1962).
7. Cilia peter satir. 1–9 (2012).
8. Sorokin, S. P. Reconstructions of centriole formation and ciliogenesis in mammalian lungs. *Journal of Cell Science* **3,** 207–230 (1968).
9. Fisch, C. & Dupuis-Williams, P. Ultrastructure of cilia and flagella - back to the future! *Biology of the Cell* **103,** 249–270 (2012).
10. Leigh, M. W. *et al.* Clinical and genetic aspects of primary ciliary dyskinesia/Kartagener syndrome. *Genet Med* **11,** 473–487 (2009).
11. MD, T. W. F. & MD, M. W. L. Ciliopathies: The Central Role of Cilia in a Spectrum of Pediatric Disorders. *The Journal of Pediatrics* **160,** 366–371 (2012).
12. Lee, L. Mechanisms of mammalian ciliary motility: Insights from primary ciliary dyskinesia genetics. *Gene* **473,** 57–66 (2011).
13. Structure and function of mammalian cilia - Springer.
14. Li, S., Guan, J.-L. & Chien, S. BIOCHEMISTRY AND BIOMECHANICS OF CELL MOTILITY. *Annu. Rev. Biomed. Eng.* **7,** 105–150 (2005).
15. Hirokawa, N., Tanaka, Y. & Okada, Y. Left-Right Determination: Involvement of Molecular Motor KIF3, Cilia, and Nodal Flow. *Cold Spring Harbor Perspectives in Biology* **1,** a000802–a000802 (2009).
16. Schlueter, J. & Brand, T. Left-right axis development: examples of similar and divergent strategies to generate asymmetric morphogenesis in chick and mouse embryos. *Cytogenet Genome Res* **117,** 256–267 (2007).
17. Vandenberg, L. N. & Levin, M. Far from solved: A perspective on what we know about early mechanisms of left-right asymmetry. *Dev. Dyn.* **239,** 3131–3146 (2010).
18. Pan, J., Wang, Q. & Snell, W. J. Cilium-generated signaling and cilia-related disorders. *Lab Invest* **85,** 452–463 (2005).
19. Carvalho-Santos, Z., Azimzadeh, J., Pereira-Leal, J. B. & Bettencourt-Dias, M. Evolution: Tracing the origins of centrioles, cilia, and flagella. *The Journal of Cell Biology* **194,** 165–175 (2011).
20. Marshall, W. F. The cell biological basis of ciliary disease. *Journal of Experimental Medicine* **205,** 4 (2008).
21. Epting, D. *et al.* The Rac1 regulator ELMO controls basal body migration and docking in multiciliated cells through interaction with Ezrin.

Development **142,** 174–184 (2014).
22. Dawe, H. R., Farr, H. & Gull, K. Centriole/basal body morphogenesis and migration during ciliogenesis in animal cells. *Journal of Cell Science* **120,** 7–15 (2007).
23. Debec, A., Sullivan, W. & Bettencourt-Dias, M. Centrioles: active players or passengers during mitosis? - Springer. *Cellular and molecular life …* (2010).
24. BURTEY, S. *et al.* Centrosome overduplication and mitotic instability in PKD2 transgenic lines. *Cell Biology International* **32,** 1193–1198 (2008).
25. Korzeniewski, N., Cuevas, R., Duensing, A. & Duensing, S. Daughter Centriole Elongation Is Controlled by Proteolysis. *Molecular Biology of the Cell* **21,** 3942–3951 (2010).
26. Bornens, M. & Azimzadeh, J. in *Eukaryotic Membranes and Cytoskeleton* **607,** 119–129 (Springer New York, 2007).
27. Scholey, J. M. I NTRAFLAGELLART RANSPORT. *Annu. Rev. Cell Dev. Biol.* **19,** 423–443 (2003).
28. Qin, H., Diener, D. R., Geimer, S., Cole, D. G. & Rosenbaum, J. L. Intraflagellar transport (IFT) cargo: IFT transports flagellar precursors to the tip and turnover products to the cell body. *The Journal of Cell Biology* **164,** 255–266 (2004).
29. Hou, Y. *et al.* Functional analysis of an individual IFT protein: IFT46 is required for transport of outer dynein arms into flagella. *The Journal of Cell Biology* **176,** 653–665 (2007).
30. Dentler, W. Intraflagellar transport (IFT) during assembly and disassembly of Chlamydomonas flagella. *The Journal of Cell Biology* **170,** 649–659 (2005).
31. Engel, B. D. *et al.* The role of retrograde intraflagellar transport in flagellar assembly, maintenance, and function. *The Journal of Cell Biology* **199,** 151–167 (2012).
32. King, S. M. *Dyneins*. (Academic Press, 2011).
33. King, S. M. *Biochemical and Physiological Analysis of Axonemal Dyneins*. *Cilia, Part B* **524,** 123–145 (Elsevier Inc., 2013).
34. Silflow, C. D. & Lefebvre, P. A. Assembly and Motility of Eukaryotic Cilia and Flagella. Lessons from Chlamydomonas reinhardtii. *PLANT PHYSIOLOGY* **127,** 1500–1507 (2001).
35. King, S. M. Axonemal dyneins winch the cilium. *Nat. Struct. Mol. Biol.* **17,** 673–674 (2010).
36. Goodenough, U. W. & Heuser, J. E. Outer and inner dynein arms of cilia and flagella. *Cell* **41,** 341–342 (1985).
37. Kutomi, O. *et al.* Outer Dynein Arm Light Chain 1 Is Essential for Controlling the Ciliary Response to Cyclic AMP in Paramecium tetraurelia. *Eukaryotic Cell* **11,** 645–653 (2012).
38. An outer arm dynein light chain acts in a conformational switch for flagellar motility. 1–13 (2009). doi:10.1083/jcb.200905083
39. An Outer Arm Dynein Conformational Switch Is Required for Metachronal Synchrony of Motile Cilia in Planaria. 1–11 (2010). doi:10.1091/mbc.E10

40. Differential Light Chain Assembly Influences Outer Arm Dynein Motor Function. 1–14 (2005). doi:10.1091/mbc.E05
41. Brokaw, C. J. & Kamiya, R. Bending patterns of Chlamydomonas flagella: IV. Mutants with defects in inner and outer dynein arms indicate differences in dynein arm function. *Cell Motil. Cytoskeleton* **8,** 68–75 (1987).
42. Bui, K. H., Sakakibara, H., Movassagh, T., Oiwa, K. & Ishikawa, T. Asymmetry of inner dynein arms and inter-doublet links in Chlamydomonas flagella. *The Journal of Cell Biology* **186,** 437–446 (2009).
43. DiBella, L. M. A Novel Tctex2-related Light Chain Is Required for Stability of Inner Dynein Arm I1 and Motor Function in the Chlamydomonas Flagellum. *Journal of Biological Chemistry* **279,** 21666–21676 (2004).
44. Zhang, Y. J. Identification of Dynein Heavy Chain 7 as an Inner Arm Component of Human Cilia That Is Synthesized but Not Assembled in a Case of Primary Ciliary Dyskinesia. *Journal of Biological Chemistry* **277,** 17906–17915 (2002).
45. Dyneins: molecular structure and cellular function.
46. Hom, E. F. Y. *et al.* A unified taxonomy for ciliary dyneins. *Cytoskeleton* **68,** 555–565 (2011).
47. Wirschell, M. *et al.* Regulation of ciliary motility: Conserved protein kinases and phosphatases are targeted and anchored in the ciliary axoneme. *Archives of Biochemistry and Biophysics* **510,** 93–100 (2011).
48. Satir, P. Studies on cilia. 3. Further studies on the cilium tip and a 'sliding filament' model of ciliary motility. *The Journal of Cell Biology* **39,** 77–94 (1968).
49. GIBBONS, B. H. & GIBBONS, I. R. The Effect of Partial Extraction of Dynein Arms on the Movement of Reactivated Sea-Urchin Sperm. *Journal of Cell Science* (1973).
50. Bannai, H., Yoshimura, M., Takahashi, K. & Shingyoji, C. Calcium regulation of microtubule sliding in reactivated sea urchin sperm flagella. *Journal of Cell …* (2000).
51. Warner, F. D. & Satir, P. THE STRUCTURAL BASIS OF CILIARY BEND FORMATION: Radial Spoke Positional Changes Accompanying Microtubule Sliding. *The Journal of Cell Biology* **63,** 35–63 (1974).
52. Shingyoji, C. Analysis of the role of nucleotides in axonemal dynein function. *Methods Cell Biol* **92,** 113–131 (2009).
53. Hayashi, S. & Shingyoji, C. Bending-induced switching of dynein activity in elastase-treated axonemes of sea urchin sperm--roles of Ca2+ and ADP. *Cell Motil. Cytoskeleton* **66,** 292–301 (2009).
54. Nakano, I., Kobayashi, T., Yoshimura, M. & Shingyoji, C. Central-pair-linked regulation of microtubule sliding by calcium in flagellar axonemes. *Journal of Cell Science* **116,** 1627–1636 (2003).
55. King, S. M. & Patel-King, R. S. Functional Architecture of the Outer Arm Dynein Conformational Switch. *Journal of Biological Chemistry* **287,** 3108–3122 (2012).

56. Fowkes, M. E. & Mitchell, D. R. The role of preassembled cytoplasmic complexes in assembly of flagellar dynein subunits. *Molecular Biology of the Cell* **9,** 2337–2347 (1998).
57. King, S. M. *Biochemical and Physiological Analysis of Axonemal Dyneins*. *Cilia, Part B* **524,** 123–145 (Elsevier Inc., 2013).
58. Freshour, J., Yokoyama, R. & Mitchell, D. R. Chlamydomonas Flagellar Outer Row Dynein Assembly Protein Oda7 Interacts with Both Outer Row and I1 Inner Row Dyneins. *Journal of Biological Chemistry* **282,** 5404–5412 (2006).
59. Duquesnoy, P. *et al.* Loss-of-Function Mutations in the Human Ortholog of Chlamydomonas reinhardtii ODA7 Disrupt Dynein Arm Assembly and Cause Primary Ciliary Dyskinesia. *The American Journal of Human Genetics* **85,** 890–896 (2009).
60. Omran, H. *et al.* Ktu/PF13 is required for cytoplasmic pre-assembly of axonemal dyneins. *Nature* **456,** 611–616 (2008).
61. Yamamoto, R., Hirono, M. & Kamiya, R. Discrete PIH proteins function in the cytoplasmic preassembly of different subsets of axonemal dyneins. *The Journal of Cell Biology* **190,** 65–71 (2010).
62. Ahmed, N. T., Gao, C., Lucker, B. F., Cole, D. G. & Mitchell, D. R. ODA16 aids axonemal outer row dynein assembly through an interaction with the intraflagellar transport machinery. *The Journal of Cell Biology* **183,** 313–322 (2008).
63. van Reeuwijk, J., Arts, H. H. & Roepman, R. Scrutinizing ciliopathies by unraveling ciliary interaction networks. *Human Molecular Genetics* **20,** R149–57 (2011).
64. Veland, I. R., Awan, A., Pedersen, L. B., Yoder, B. K. & Christensen, S. O. R. T. Primary Cilia and Signaling Pathways in Mammalian Development, Health and Disease. *Nephron Physiol* **111,** p39–p53 (2009).
65. Yokoyama, T. Motor or sensor: a new aspect of primary cilia function. *Anat Sci Int* **79,** 47–54 (2004).
66. Yoder, B. K. Role of Primary Cilia in the Pathogenesis of Polycystic Kidney Disease. *Journal of the American Society of Nephrology* **18,** 1381–1388 (2007).
67. Baker, K. & Beales, P. L. Making sense of cilia in disease: The human ciliopathies. *Am. J. Med. Genet.* **151C,** 281–295 (2009).
68. Gerdes, J. M., Davis, E. E. & Katsanis, N. The Vertebrate Primary Cilium in Development, Homeostasis, and Disease. *Cell* **137,** 32–45 (2009).
69. Schottenfeld, J., Sullivan-Brown, J. & Burdine, R. D. Zebrafish curly up encodes a Pkd2 ortholog that restricts left-side-specific expression of southpaw. *Development* **134,** 1605–1615 (2007).
70. Pazour, G. J. & Witman, G. B. The vertebrate primary cilium is a sensory organelle. *Current Opinion in Cell Biology* **15,** 105–110 (2003).
71. Mykytyn, K. & Sheffield, V. C. Establishing a connection between cilia and Bardet–Biedl Syndrome. *Trends Mol Med* **10,** 106–109 (2004).
72. Bisgrove, B. W. & Yost, H. J. The roles of cilia in developmental disorders and disease. *Development* **133,** 4131–4143 (2006).

73. Tallila, J. Molecular Genetics of Meckel Syndrome. Ciliary Genes are Defective in MKS. 1–95 (2009).
74. Lee, J. E. *et al.* CEP41 is mutated in Joubert syndrome and is required for tubulin glutamylation at the cilium. *Nat Genet* **44,** 193–199 (2012).
75. Afzelius, B. A. A human syndrome caused by immotile cilia. *Science* **193,** 317–319 (1976).
76. Escudier, E., Duquesnoy, P., Papon, J. F. & Amselem, S. Ciliary defects and genetics of primary ciliary dyskinesia. *Paediatric Respiratory Reviews* **10,** 51–54 (2009).
77. Agius, A. M., Smallman, L. A. & Pahor, A. L. Age, smoking and nasal ciliary beat frequency. *Clin Otolaryngol Allied Sci* **23,** 227–230 (1998).
78. Knoll, M. & Talbot, P. Cigarette smoke inhibits oocyte cumulus complex pick-up by the oviduct in vitro independent of ciliary beat frequency. *Reprod Toxicol* **12,** 57–68 (1998).
79. Stanley, P. J., Wilson, R., Greenstone, M. A., MacWilliam, L. & Cole, P. J. Effect of cigarette smoking on nasal mucociliary clearance and ciliary beat frequency. *Thorax* **41,** 519–523 (1986).
80. Brehm, P. & Eckert, R. An electrophysiological study of the regulation of ciliary beating frequency in Paramecium. *J Physiol* **283,** 557–568 (1978).
81. G Di Benedetto, C. J. M. P. T. G. A. M. Calcium regulation of ciliary beat frequency in human respiratory epithelium in vitro. *The Journal of Physiology* **439,** 103 (1991).
82. Garcia-Gonzalo, F. R. & Reiter, J. F. Scoring a backstage pass: Mechanisms of ciliogenesis and ciliary access. *The Journal of Cell Biology* **197,** 697–709 (2012).
83. Schwabe, G. C. *et al.* Primary ciliary dyskinesia associated with normal axoneme ultrastructure is caused by DNAH11 mutations. *Hum. Mutat.* **29,** 289–298 (2008).
84. FLIEGAUF, M. & OMRAN, H. Novel tools to unravel molecular mechanisms in cilia-related disorders. *Trends in Genetics* **22,** 241–245 (2006).
85. Chodhari, R., Mitchison, H. M. & Meeks, M. Cilia, primary ciliary dyskinesia and molecular genetics. *Paediatric Respiratory Reviews* **5,** 69–76 (2004).
86. Guo, X. *et al.* Proteomic analysis of proteins involved in spermiogenesis in mouse. *J. Proteome Res.* **9,** 1246–1256 (2010).
87. Ostrowski, L. E. *et al.* A proteomic analysis of human cilia: identification of novel components. *Mol. Cell Proteomics* **1,** 451–465 (2002).
88. Narita, K. *et al.* Proteomic analysis of multiple primary cilia reveals a novel mode of ciliary development in mammals. *Biol Open* **1,** 815–825 (2012).
89. Inglis, P. N., Boroevich, K. A. & Leroux, M. R. Piecing together a ciliome. *Trends in Genetics* **22,** 491–500 (2006).
90. Escudier, E., Duquesnoy, P., Papon, J. F. & Amselem, S. Ciliary defects and genetics of primary ciliary dyskinesia. *Paediatric Respiratory Reviews* **10,** 51–54 (2009).

91. Hornef, N. *et al.* DNAH5 mutations are a common cause of primary ciliary dyskinesia with outer dynein arm defects. *Am. J. Respir. Crit. Care Med.* **174,** 120–126 (2006).
92. Bartoloni, L. *et al.* Mutations in the DNAH11 (axonemal heavy chain dynein type 11) gene cause one form of situs inversus totalis and most likely primary ciliary dyskinesia. *Proc. Natl. Acad. Sci. U.S.A.* **99,** 10282–10286 (2002).
93. Loges, N. T. *et al.* DNAI2 Mutations Cause Primary Ciliary Dyskinesia with Defects in the Outer Dynein Arm. *The American Journal of Human Genetics* **83,** 547–558 (2008).
94. Guichard, C. *et al.* Axonemal Dynein Intermediate-Chain Gene (DNAI1) Mutations Result in Situs Inversus and Primary Ciliary Dyskinesia (Kartagener Syndrome). *The American Journal of Human Genetics* **68,** 1030–1035 (2001).
95. Duriez, B. *et al.* A common variant in combination with a nonsense mutation in a member of the thioredoxin family causes primary ciliary dyskinesia. *PNAS* **104,** 3336–3341 (2007).
96. Merveille, A.-C. *et al.* CCDC39 is required for assembly of inner dynein arms and the dynein regulatory complex and for normal ciliary motility in humans and dogs. *Nature Publishing Group* **43,** 72–78 (2010).
97. Becker-Heck, A. *et al.* The coiled-coil domain containing protein CCDC40 is essential for motile cilia function and left-right axis formation. *Nat Genet* **43,** 79–84 (2010).
98. Blanchon, S. *et al.* Delineation of CCDC39/CCDC40 mutation spectrum and associated phenotypes in primary ciliary dyskinesia. *J. Med. Genet.* **49,** 410–416 (2012).
99. Moore, D. J. *et al.* Mutations in ZMYND10, a Gene Essential for Proper Axonemal Assembly of Inner and Outer Dynein Arms in Humans and Flies, Cause Primary Ciliary Dyskinesia. *The American Journal of Human Genetics* 1–11 (2013). doi:10.1016/j.ajhg.2013.07.009
100. Guan, J., Ekwurtzel, E., Kvist, U., Hultenby, K. & Yuan, L. DNAJB13 is a radial spoke protein of mouse '9+2' axoneme. *Reprod. Domest. Anim.* **45,** 992–996 (2010).
101. Diggle, C. P. *et al.* HEATR2 Plays a Conserved Role in Assembly of the Ciliary Motile Apparatus. *PLoS Genet* **10,** e1004577 (2014).
102. Mitchison, H. M. *et al.* Mutations in axonemal dynein assembly factor DNAAF3 cause primary ciliary dyskinesia. *Nat Genet* **44,** 381–389 (2012).
103. Horani, A. *et al.* LRRC6 Mutation Causes Primary Ciliary Dyskinesia with Dynein Arm Defects. *PLoS ONE* **8,** e59436 (2013).
104. Loges, N. T. *et al.* Deletions and Point Mutations of LRRC50 Cause Primary Ciliary Dyskinesia Due to Dynein Arm Defects. *The American Journal of Human Genetics* **85,** 883–889 (2009).
105. Panizzi, J. R. *et al.* CCDC103 mutations cause primary ciliary dyskinesia by disrupting assembly of ciliary dynein arms. *Nat Genet* **44,** 714–719 (2012).
106. Onoufriadis, A. *et al.* Splice-Site Mutations in the Axonemal Outer Dynein

Arm Docking Complex Gene CCDC114 Cause Primary Ciliary Dyskinesia. *The American Journal of Human Genetics* **92,** 88–98 (2013).
107. Dong, F. *et al.* Pih1d3 is required for cytoplasmic preassembly of axonemal dynein in mouse sperm. *The Journal of Cell Biology* **204,** 203–213 (2014).
108. Kott, E. *et al.* Loss-of-Function Mutations in LRRC6, a Gene Essential for Proper Axonemal Assembly of Inner and Outer Dynein Arms, Cause Primary Ciliary Dyskinesia. *The American Journal of Human Genetics* **91,** 958–964 (2012).
109. Schulte-Körne, G., Warnke, A. & Remschmidt, H. [Genetics of dyslexia]. *Z Kinder Jugendpsychiatr Psychother* **34,** 435–444 (2006).
110. Benítez-Burraco, A. [Neurobiology and neurogenetics of dyslexia]. *Neurologia* **25,** 563–581 (2010).
111. Bates, T. C. *et al.* Dyslexia and DYX1C1: deficits in reading and spelling associated with a missense mutation. *Mol. Psychiatry* **15,** 1190–1196 (2010).
112. Taipale, M. *et al.* A candidate gene for developmental dyslexia encodes a nuclear tetratricopeptide repeat domain protein dynamically regulated in brain. *Proc. Natl. Acad. Sci. U.S.A.* **100,** 11553–11558 (2003).
113. Paracchini, S., Scerri, T. & Monaco, A. P. The Genetic Lexicon of Dyslexia. *Annu. Rev. Genom. Human Genet.* **8,** 57–79 (2007).
114. Adler, W. T. *et al.* Position of Neocortical Neurons Transfected at Different Gestational Ages with shRNA Targeted against Candidate Dyslexia Susceptibility Genes. *PLoS ONE* **8,** e65179 (2013).
115. Szalkowski, C. E. *et al.* Neocortical disruption and behavioral impairments in rats following in utero RNAi of candidate dyslexia risk gene Kiaa0319. *Int. J. Dev. Neurosci.* **30,** 293–302 (2012).
116. Levecque, C., Velayos-Baeza, A., Holloway, Z. G. & Monaco, A. P. The dyslexia-associated protein KIAA0319 interacts with adaptor protein 2 and follows the classical clathrin-mediated endocytosis pathway. *AJP: Cell Physiology* **297,** C160–C168 (2009).
117. Gabel, L. A., Gibson, C. J., Gruen, J. R. & LoTurco, J. J. Progress towards a cellular neurobiology of reading disability. *Neurobiol. Dis.* **38,** 173–180 (2010).
118. Meng, H. *et al.* TDT-association analysis of EKN1 and dyslexia in a Colorado twin cohort. *Hum. Genet.* **118,** 87–90 (2005).
119. Shastry, B. S. Developmental dyslexia: an update. *J. Hum. Genet.* **52,** 104–109 (2007).
120. Petryshen, T. L. & Pauls, D. L. The genetics of reading disability. *Curr Psychiatry Rep* **11,** 149–155 (2009).
121. Ivliev, A. E., 't Hoen, P. A. C., van Roon-Mom, W. M. C., Peters, D. J. M. & Sergeeva, M. G. Exploring the transcriptome of ciliated cells using in silico dissection of human tissues. *PLoS ONE* **7,** e35618 (2012).
122. Massinen, S. *et al.* Increased expression of the dyslexia candidate gene DCDC2 affects length and signaling of primary cilia in neurons. *PLoS ONE* **6,** e20580 (2011).

123. McGrath, L. M., Smith, S. D. & Pennington, B. F. Breakthroughs in the search for dyslexia candidate genes. *Trends Mol Med* **12,** 333–341 (2006).
124. Wang, Y. *et al.* DYX1C1 functions in neuronal migration in developing neocortex. *Neuroscience* **143,** 515–522 (2006).
125. Rosen, G. D. *et al.* Disruption of neuronal migration by RNAi of Dyx1c1 results in neocortical and hippocampal malformations. *Cereb. Cortex* **17,** 2562–2572 (2007).
126. Currier, T. A., Etchegaray, M. A., Haight, J. L., Galaburda, A. M. & Rosen, G. D. The effects of embryonic knockdown of the candidate dyslexia susceptibility gene homologue Dyx1c1 on the distribution of GABAergic neurons in the cerebral cortex. *Neuroscience* **172,** 535–546 (2011).
127. Chen, Y. *et al.* A novel role for DYX1C1, a chaperone protein for both Hsp70 and Hsp90, in breast cancer. *J. Cancer Res. Clin. Oncol.* **135,** 1265–1276 (2009).
128. Hatakeyama, S., Matsumoto, M., Yada, M. & Nakayama, K. I. Interaction of U-box-type ubiquitin-protein ligases (E3s) with molecular chaperones. *Genes Cells* **9,** 533–548 (2004).
129. Massinen, S. *et al.* Functional interaction of DYX1C1 with estrogen receptors suggests involvement of hormonal pathways in dyslexia. *Human Molecular Genetics* **18,** 2802–2812 (2009).
130. Tapia-Páez, I., Tammimies, K., Massinen, S., Roy, A. L. & Kere, J. The complex of TFII-I, PARP1, and SFPQ proteins regulates the DYX1C1 gene implicated in neuronal migration and dyslexia. *FASEB J.* **22,** 3001–3009 (2008).
131. Tammimies, K. *et al.* Molecular networks of DYX1C1 gene show connection to neuronal migration genes and cytoskeletal proteins. *Biol. Psychiatry* **73,** 583–590 (2013).
132. LoTurco, J. J. & Tarkar, A. DYX1C1 placed in a molecular context. *Biol. Psychiatry* **73,** 497–498 (2013).
133. Chandrasekar, G., Vesterlund, L., Hultenby, K., Tapia-Páez, I. & Kere, J. The Zebrafish Orthologue of the Dyslexia Candidate Gene DYX1C1 Is Essential for Cilia Growth and Function. *PLoS ONE* **8,** e63123 (2013).
134. Fliegauf, M., Benzing, T. & Omran, H. When cilia go bad: cilia defects and ciliopathies. *Nat Rev Mol Cell Biol* **8,** 880–893 (2007).
135. MD, T. W. F. & MD, M. W. L. Ciliopathies: The Central Role of Cilia in a Spectrum of Pediatric Disorders. *The Journal of Pediatrics* **160,** 366–371 (2012).
136. Localization of intraflagellar transport protein IFT52 identifies basal body transitional fibers as the docking site for IFT particles James A. Deane*, Douglas G. Cole. 1–5 (2001).
137. Rosenbaum, J. L. & Witman, G. B. Intraflagellar transport. *Nat Rev Mol Cell Biol* **3,** 813–825 (2002).
138. Omran, H. *et al.* Ktu/PF13 is required for cytoplasmic pre-assembly of axonemal dyneins. *Nature* **456,** 611–616 (2008).
139. Ahmed, N. T., Gao, C., Lucker, B. F., Cole, D. G. & Mitchell, D. R. ODA16

aids axonemal outer row dynein assembly through an interaction with the intraflagellar transport machinery. *The Journal of Cell Biology* **183,** 313–322 (2008).
140. Tarkar, A. *et al.* DYX1C1 is required for axonemal dynein assembly and ciliary motility. *Nat Genet* (2013). doi:10.1038/ng.2707
141. Kobayashi, D. & Takeda, H. Ciliary motility The components and cytoplasmic preassembly mechanisms of the axonemal dyneins. *Differentiation* **83,** S23–S29 (2012).
142. Horani, A. *et al.* LRRC6 Mutation Causes Primary Ciliary Dyskinesia with Dynein Arm Defects. *PLoS ONE* **8,** e59436 (2013).
143. Ghossoub, R. *et al.* Septins 2, 7 and 9 and MAP4 colocalize along the axoneme in the primary cilium and control ciliary length. *Journal of Cell Science* **126,** 2583–2594 (2013).
144. Yam, A. Y. *et al.* Defining the TRiC/CCT interactome links chaperonin function to stabilization of newly made proteins with complex topologies. *Nat. Struct. Mol. Biol.* **15,** 1255–1262 (2008).
145. Knee, K. M., Sergeeva, O. A. & King, J. A. Human TRiC complex purified from HeLa cells contains all eight CCT subunits and is active in vitro. *Cell Stress Chaperones* **18,** 137–144 (2013).
146. Dekker, C. *et al.* The interaction network of the chaperonin CCT. *EMBO J* **27,** 1827–1839 (2008).
147. Cuéllar, J. *et al.* The structure of CCT–Hsc70NBD suggests a mechanism for Hsp70 delivery of substrates to the chaperonin. *Nat. Struct. Mol. Biol.* **15,** 858–864 (2008).
148. Lefebvre, P. A., Nordstrom, S. A., Moulder, J. E. & Rosenbaum, J. L. Flagellar elongation and shortening in Chlamydomonas. IV. Effects of flagellar detachment, regeneration, and resorption on the induction of flagellar protein synthesis. *The Journal of Cell Biology* **78,** 8–27 (1978).
149. Rosenbaum, J. L., Moulder, J. E. & Ringo, D. L. Flagellar elongation and shortening in Chlamydomonas. The use of cycloheximide and colchicine to study the synthesis and assembly of flagellar proteins. *The Journal of Cell Biology* **41,** 600–619 (1969).
150. Kott, E. *et al.* Loss-of-Function Mutations in LRRC6, a Gene Essential for Proper Axonemal Assembly of Inner and Outer Dynein Arms, Cause Primary Ciliary Dyskinesia. *The American Journal of Human Genetics* **91,** 958–964 (2012).
151. Panizzi, J. R. *et al.* CCDC103 mutations cause primary ciliary dyskinesia by disrupting assembly of ciliary dynein arms. *Nature Publishing Group* **44,** 714–719 (2012).
152. Desai, P. B., Freshour, J. R. & Mitchell, D. R. Chlamydomonasaxonemal dynein assembly locus ODA8encodes a conserved flagellar protein needed for cytoplasmic maturation of outer dynein arm complexes. *Cytoskeleton* n/a–n/a (2014). doi:10.1002/cm.21206
153. Pennarun, G. *et al.* Loss-of-function mutations in a human gene related to Chlamydomonas reinhardtii dynein IC78 result in primary ciliary dyskinesia. *Am. J. Hum. Genet.* **65,** 1508–1519 (1999).

154. Omran, H. *et al.* Homozygosity Mapping of a Gene Locus for Primary Ciliary Dyskinesia on Chromosome 5p and Identification of the Heavy Dynein Chain DNAH5as a Candidate Gene. *American Journal of Respiratory Cell and Molecular Biology* **23,** 696–702 (2000).
155. Mazor, M. *et al.* REPOR TPrimary Ciliary Dyskinesia Caused by Homozygous Mutation in DNAL1, Encoding Dynein Light Chain 1. *The American Journal of Human Genetics* **88,** 599–607 (2011).
156. Kobayashi, D. & Takeda, H. Ciliary motility The components and cytoplasmic preassembly mechanisms of the axonemal dyneins. *Differentiation* **83,** S23–S29 (2012).
157. Duquesnoy, P. *et al.* Loss-of-Function Mutations in the Human Ortholog of Chlamydomonas reinhardtii ODA7 Disrupt Dynein Arm Assembly and Cause Primary Ciliary Dyskinesia. *The American Journal of Human Genetics* **85,** 890–896 (2009).
158. Loges, N. T. *et al.* Deletions and Point Mutations of LRRC50 Cause Primary Ciliary Dyskinesia Due to Dynein Arm Defects. *The American Journal of Human Genetics* **85,** 883–889 (2009).

8. SUPPLEMENTARY DATA

Supplemental Table 1a Wildtype MS/MS results. Proteins identified have a minimum of 2 sequenced tryptic peptides each with a minimum E-value of 0.00001.

MSMSPEP_I	PEP_EXP_M	PEP_EXP_M	PEP_EXP_Z	PEP_CALC_N	PEP_DELTA	PEP_START	PEP_END	PEP_SCORE	PEP_HOMOL	PEP_IDENT	PEP_EXPECT	PEP_RES_BE	PEP_SEQ	PEP_RES_AF	PEP_VAR_M	PEP_VAR_M	PROTEIN_ID	PROTEIN_NAME	PEPTIDE_SEQUENCE
1614440883	643.633	1927.8773	3	1927.8842	-0.0069	556	572	73.81	27	32	0.0000037	K	MMEISNEVMSPHGEPIK	M			gi 10442714	soluble guanylyl cyclase alpha 1 subunit [Mu	K.MMEISNEVMSPHGEPIK.M
1614440865	641.8748	1281.7351	2	1281.7405	-0.0054	295	306	74.99	0	28	0.0000012	R	DLAILQLGNGIR	R			gi 10442714	soluble guanylyl cyclase alpha 1 subunit [Mu	R.DLAILQLGNGIR.R
1614440861	550.3075	1098.6005	2	1098.6033	-0.0028	411	420	84.61	0	32	3.80E-07	K	DVVLIGEQAR	A			gi 10442714	soluble guanylyl cyclase alpha 1 subunit [Mu	K.DVVLIGEQAR.A
1614440873	803.8946	1604.7746	2	1604.7794	-0.0048	434	447	87.86	0	33	2.00E-07	K	ATLEHAHQALEEEK	K			gi 10442714	soluble guanylyl cyclase alpha 1 subunit [Mu	K.ATLEHAHQALEEEK.K
1614440876	813.9265	1625.8384	2	1625.8447	-0.0062	541	555	88.16	0	33	1.80E-07	R	ESDTHAVQIALMALK	M			gi 10442714	soluble guanylyl cyclase alpha 1 subunit [Mu	R.ESDTHAVQIALMALK.M
1614440864	570.3729	1138.7313	2	1138.7325	-0.0012	210	220	79.2	0	21	9.00E-08	R	TTALLLPGIIK	A			gi 10442714	soluble guanylyl cyclase alpha 1 subunit [Mu	R.TTALLLPGIIK.A
1614440880	833.4715	1664.9284	2	1664.9348	-0.0064	117	133	91.16	0	30	4.60E-08	K	IAEEAIAAGAPVEALK	D			gi 10442714	soluble guanylyl cyclase alpha 1 subunit [Mu	K.IAEEAIAAGAPVEALK.D
1614440871	791.4381	1580.8617	2	1580.8674	-0.0057	397	410	96.32	23	32	1.90E-08	R	GLYLSDIPIHNALR	D			gi 10442714	soluble guanylyl cyclase alpha 1 subunit [Mu	R.GLYLSDIPIHNALR.D
1614440882	848.4035	1694.7924	2	1694.7981	-0.0057	196	208	103.68	0	32	3.90E-09	K	DQDFLMVYYFFPK	R			gi 10442714	soluble guanylyl cyclase alpha 1 subunit [Mu	K.DQDFLMVYYFFPK.R
1555398866	1065.6233	2129.2301	2	2129.232	-0.002	290	308	86.48	18	26	5.30E-08	R	QIQQQNPSLLPALLQQIGR	E			gi 1044899	MHR23B [Mus musculus]	R.QIQQQNPSLLPALLQQIGR.E
1625584499	917.4999	1832.9852	2	1832.9859	-0.0006	422	438	74.17	18	33	0.0000039	R	TQLVSVSIFGSPWMALK	E			gi 10566953	I-gicerin/MUC18 [Mus musculus]	R.TQLVSVSIFGSPWMALK.E
1625584496	555.3251	1108.6456	2	1108.6453	0.0003	391	400	71.78	26	29	0.000003	K	GPVLQLNNVR	R			gi 10566953	I-gicerin/MUC18 [Mus musculus]	K.GPVLQLNNVR.R
1625584501	573.0514	2288.1765	4	2288.1761	0.0004	94	114	92.69	25	33	6.40E-08	R	LSLQDSVATLALSHVTPHDER	M			gi 10566953	I-gicerin/MUC18 [Mus musculus]	R.LSLQDSVATLALSHVTPHDER.M
1625584497	684.4005	1366.7865	2	1366.786	0.0005	254	265	95.78	0	29	1.20E-08	K	VWVEVEPVGLLK	E			gi 10566953	I-gicerin/MUC18 [Mus musculus]	K.VWVEVEPVGLLK.E
1555382996	584.6056	1750.7949	3	1750.7944	0.0005	22	35	77.11	19	32	0.0000019	K	RPAEDMEEEQAFER	S	Oxidation (M	0.000002000	gi 1083569	kappa-B motif-binding phosphoprotein - mo	K.RPAEDMEEEQAFER.S + Oxidation (M)
1555382998	959.0201	1916.0257	2	1916.0255	0.0002	378	396	85.92	25	33	2.60E-07	R	GSYGDLGGPIITTQVTIPK	D			gi 1083569	kappa-B motif-binding phosphoprotein - mo	R.GSYGDLGGPIITTQVTIPK.D
1555382997	890.9033	1779.79	2	1779.7911	-0.0011	70	86	85.82	28	31	1.80E-07	R	TDYNASVSVPDSSGPER	I			gi 1083569	kappa-B motif-binding phosphoprotein - mo	R.TDYNASVSVPDSSGPER.I
1555382992	630.291	1258.5675	2	1258.5677	-0.0002	423	433	85.61	29	30	1.50E-07	K	IDEPLEGSEDR	I			gi 1083569	kappa-B motif-binding phosphoprotein - mo	K.IDEPLEGSEDR.I
1555382999	1295.1946	2588.3746	2	2588.381	-0.0064	434	456	97.61	29	32	1.40E-08	R	ITITGTQDQIQNAQYLLQNSVK	Q			gi 1083569	kappa-B motif-binding phosphoprotein - mo	R.ITITGTQDQIQNAQYLLQNSVK.Q
1555388441	889.4996	1776.9847	2	1776.9873	-0.0026	195	211	80.75	18	30	5.00E-07	K	TLASISPETSLFRASK	T			gi 109157405	Chain A, Crystal Structure Of Mouse Amf	K.TLASISPETSLFRASK.T
1555388438	838.4763	1674.938	2	1674.9378	0.0001	424	438	105.74	0	30	1.60E-09	K	ELANFLAQTEALMK	G			gi 109157405	Chain A, Crystal Structure Of Mouse Amf	K.ELANFLAQTEALMK.G
1555385294	836.9139	1671.8132	2	1671.8138	-0.0006	367	381	81.38	27	33	8.50E-07	R	LEQGQAIDDLMPAQK	-	Oxidation (M	0.000000000	gi 10946574	creatine kinase B-type [Mus musculus]	R.LEQGQAIDDLMPAQK.- + Oxidation (M)
1555328922	801.9198	1601.825	2	1601.826	-0.001	157	172	88.25	27	34	2.10E-07	K	LAVEALSSLDGDLSGR	Y			gi 10946574	creatine kinase B-type [Mus musculus]	K.LAVEALSSLDGDLSGR.Y
1625850326	879.4587	1756.9049	2	1756.9069	-0.002	170	185	89.2	30	33	1.50E-07	R	LMNETTAVALAYGIYK	Q			gi 1098541	osmotic stress protein 94 [Mus musculus]	R.LMNETTAVALAYGIYK.Q
1614338873	909.478	1816.9414	2	1816.9458	-0.0044	7	23	87.46	24	34	2.50E-07	R	LDGLVDTPTGYIESLPK	V			gi 109866	gene DN38 protein - mouse (fragment)	R.LDGLVDTPTGYIESLPK.V
1614420040	1276.6818	2551.349	2	2551.3533	-0.0043	116	139	74.64	22	32	0.0000029	R	VYQIPGKPEIVDPASELTASVPNK	V			gi 110225341	advanced glycosylation end product-specific	K.VYQIPGKPEIVDPASELTASVPNK.V
1555344625	734.8806	1467.7467	2	1467.747	-0.0004	63	76	79.56	25	34	0.0000015	K	VLSPQGGPWDSVAR	I			gi 110225341	advanced glycosylation end product-specific	K.VLSPQGGPWDSVAR.I
1614338294	723.8198	1445.625	2	1445.627	-0.002	373	383	79.66	0	29	5.30E-07	R	KAPESQEDEEER	A			gi 110225341	advanced glycosylation end product-specific	R.KAPESQEDEEER.A
1555348995	734.88	1467.7454	2	1467.747	-0.0016	63	76	84.31	27	34	5.00E-07	K	VLSPQGGPWDSVAR	I			gi 110225341	advanced glycosylation end product-specific	K.VLSPQGGPWDSVAR.I
1614420037	779.0381	2334.0924	3	2334.0951	-0.0027	140	161	86.44	24	33	2.40E-07	K	VSTCVSEGSYPAGTLSWHLDGK	L	Propionamid	0.000200000	gi 110225341	advanced glycosylation end product-specific	K.VSTCVSEGSYPAGTLSWHLDGK.L + Propionamide (C)
1614429164	723.8189	1445.6232	2	1445.627	-0.0038	373	383	84.84	27	29	1.50E-07	R	KAPESQEDEEER	A			gi 110225341	advanced glycosylation end product-specific	R.KAPESQEDEEER.A
1614429166	734.8786	1467.7426	2	1467.747	-0.0045	63	76	91.14	31	34	1.10E-07	K	VLSPQGGPWDSVAR	I			gi 110225341	advanced glycosylation end product-specific	K.VLSPQGGPWDSVAR.I
1614429171	851.4567	2551.3483	3	2551.3533	-0.005	116	139	89.75	27	32	8.90E-08	R	VYQIPGKPEIVDPASELTASVPNK	V			gi 110225341	advanced glycosylation end product-specific	K.VYQIPGKPEIVDPASELTASVPNK.V
1614420034	734.8789	1467.7433	2	1467.747	-0.0038	63	76	93.88	24	34	5.80E-08	K	VLSPQGGPWDSVAR	I			gi 110225341	advanced glycosylation end product-specific	K.VLSPQGGPWDSVAR.I
1614428053	857.8947	1713.7748	2	1713.7787	-0.0039	415	428	73.69	26	31	0.0000029	R	EYFSWEGTFQHVGK	A			gi 110625979	elongation factor 1-gamma [Mus musculus]	R.EYFSWEGTFQHVGK.A
1614428050	854.4368	1706.859	2	1706.8641	-0.0051	31	45	85.93	25	34	3.60E-07	R	VLSAPPHFHFGQTNR	T			gi 110625979	elongation factor 1-gamma [Mus musculus]	R.VLSAPPHFHFGQTNR.T
1614428058	821.0498	2460.1274	3	2460.1274	0	297	316	86.56	20	32	2.00E-07	K	YSNEDTLSVALPYPWEHFDK	D			gi 110625979	elongation factor 1-gamma [Mus musculus]	K.YSNEDTLSVALPYPWEHFDK.D
1614428037	561.8465	1121.6784	2	1121.6808	-0.0025	138	147	81.27	0	23	8.70E-08	R	ILGLLDTHLK	T			gi 110625979	elongation factor 1-gamma [Mus musculus]	R.ILGLLDTHLK.T
1614428047	786.913	1571.8114	2	1571.8155	-0.0041	401	414	99.98	0	34	1.40E-08	R	KLDPGSEETQTLVR	E			gi 110625979	elongation factor 1-gamma [Mus musculus]	R.KLDPGSEETQTLVR.E
1614428044	674.3711	1346.7277	2	1346.7306	-0.003	18	30	133.68	32	33	9.50E-10	K	ALIAAQYSGAQVR	V			gi 110625979	elongation factor 1-gamma [Mus musculus]	K.ALIAAQYSGAQVR.V
1614441675	972.961	1943.9074	2	1943.9153	-0.0079	138	153	84.57	19	32	3.50E-07	K	DSPVLLDFFEDSELYR	K			gi 11066003	histidine-rich glycoprotein [Mus musculus]	K.DSPVLLDFFEDSELYR.K
1614447080	628.3054	1254.5962	2	1254.5979	-0.0017	441	451	76.07	0	32	0.0000022	R	DYETATLSDIK	A			gi 11230802	alpha-actinin-4 [Mus musculus]	R.DYETATLSDIK.A
1614447090	676.8145	1351.6144	2	1351.619	-0.0046	762	772	76.84	0	31	0.0000016	K	GISQEQMQEFR	A			gi 11230802	alpha-actinin-4 [Mus musculus]	K.GISQEQMQEFR.A
1614447106	754.3516	1506.6886	2	1506.695	-0.0064	68	80	77.49	0	31	0.0000013	K	AGTQIENIDEDFR	D			gi 11230802	alpha-actinin-4 [Mus musculus]	K.AGTQIENIDEDFR.D
1614447089	663.3437	1324.6709	2	1324.6735	-0.0026	634	644	83.18	0	33	5.90E-07	K	RDHALLEEQSK	Q			gi 11230802	alpha-actinin-4 [Mus musculus]	K.RDHALLEEQSK.Q
1614447126	635.3162	1902.9268	3	1902.9323	-0.0055	218	234	85.56	0	34	3.80E-07	R	KDDPVTNLNNAFEVAEK	Y			gi 11230802	alpha-actinin-4 [Mus musculus]	R.KDDPVTNLNNAFEVAEK.Y
1614447076	608.3395	1214.6645	2	1214.6659	-0.0014	302	311	85.76	0	33	3.20E-07	R	LASDLLEWIR	R			gi 11230802	alpha-actinin-4 [Mus musculus]	R.LASDLLEWIR.R
1614445282	693.8885	1385.7624	2	1385.7667	-0.0043	735	746	86.52	31	33	2.80E-07	R	VGWEQLLTTIAR	T			gi 11230802	alpha-actinin-4 [Mus musculus]	R.VGWEQLLTTIAR.T
1614447127	952.4712	1902.9278	2	1902.9323	-0.0045	218	234	93.85	26	34	5.50E-08	R	KDDPVTNLNNAFEVAEK	Y			gi 11230802	alpha-actinin-4 [Mus musculus]	R.KDDPVTNLNNAFEVAEK.Y
1614447129	960.5025	1918.9904	2	1919	-0.0096	606	623	102.06	30	34	7.80E-09	K	LSGSNPYTTVTPQIINSK	W			gi 11230802	alpha-actinin-4 [Mus musculus]	K.LSGSNPYTTVTPQIINSK.W
1614447123	908.9381	1815.8616	2	1815.8672	-0.0056	241	256	101.86	28	33	7.50E-09	K	MLDAEDIVNTARPDEK	A			gi 11230802	alpha-actinin-4 [Mus musculus]	K.MLDAEDIVNTARPDEK.A
1614447122	882.9141	1763.8136	2	1763.8188	-0.0052	884	900	109.79	28	33	1.10E-09	R	MAPYQGPDAAPGALDYK	S			gi 11230802	alpha-actinin-4 [Mus musculus]	R.MAPYQGPDAAPGALDYK.S
1614447118	877.413	1752.8114	2	1752.8179	-0.0065	456	470	110.58	29	33	9.50E-10	R	KHEAFESDLAAHQDR	V			gi 11230802	alpha-actinin-4 [Mus musculus]	R.KHEAFESDLAAHQDR.V
1614447107	757.9046	1513.7947	2	1513.7988	-0.0041	127	141	114.03	26	33	4.40E-10	K	LVSIGAEEIVDGNAK	M			gi 11230802	alpha-actinin-4 [Mus musculus]	K.LVSIGAEEIVDGNAK.M
1614447117	871.4077	1740.8009	2	1740.8054	-0.0045	839	854	113.85	20	32	4.00E-10	R	ETTDTDTADQVIASFK	V			gi 11230802	alpha-actinin-4 [Mus musculus]	R.ETTDTDTADQVIASFK.V
1614447138	969.1338	2904.3797	3	2904.3889	-0.0092	471	495	120.32	32	37	2.40E-10	R	VEQIAAIAQELNELDYYDSHNVNTR	C			gi 11230802	alpha-actinin-4 [Mus musculus]	R.VEQIAAIAQELNELDYYDSHNVNTR.C
1614420247	962.793	2885.3571	3	2885.3607	-0.0036	309	333	87.03	28	33	2.40E-07	K	SDEENLFEITADEVHYYLQAATSK	E			gi 11464971	pleckstrin [Mus musculus]	K.SDEENLFEITADEVHYYLQAATSK.E
1614420249	1005.4905	3013.4497	3	3013.4556	-0.0059	308	333	96.73	26	34	2.90E-08	K	KSDEENLFEITADEVHYYLQAATSK	E			gi 11464971	pleckstrin [Mus musculus]	K.KSDEENLFEITADEVHYYLQAATSK.E
1614420245	832.4516	1662.8886	2	1662.8902	-0.0016	120	134	96.89	31	33	2.40E-08	R	LPETIDLGALYLSMK	D			gi 11464971	pleckstrin [Mus musculus]	R.LPETIDLGALYLSMK.D
1614451630	686.7035	2057.0888	3	2057.0945	-0.0058	1481	1499	74.63	25	33	0.000004	K	IAALQAFADQLIAVDHYAK	G			gi 115496850	spectrin alpha chain, non-erythrocytic 1 isof	K.IAALQAFADQLIAVDHYAK.G
1614451614	622.3546	1242.6946	2	1242.6972	-0.0026	450	459	79.37	0	33	0.0000012	R	TALLEIWELR	R			gi 115496850	spectrin alpha chain, non-erythrocytic 1 isof	R.TALLEIWELR.R
1614451617	655.8693	1309.724	2	1309.7282	-0.0041	2073	2083	80.03	0	31	6.70E-07	R	KVEDLFLTFAK	K			gi 115496850	spectrin alpha chain, non-erythrocytic 1 isof	R.KVEDLFLTFAK.K
1614451633	1105.0712	2208.1278	2	2208.1348	-0.0069	1875	1895	95.9	20	33	3.20E-08	K	MTLVASEDYGDTLAAIQGLLK	K			gi 115496850	spectrin alpha chain, non-erythrocytic 1 isof	K.MTLVASEDYGDTLAAIQGLLK.K
1614451631	1077.5516	2153.0886	2	2153.0964	-0.0077	382	402	97.62	28	34	2.80E-08	K	ALINADELANDVAGAEALLDR	H			gi 115496850	spectrin alpha chain, non-erythrocytic 1 isof	K.ALINADELANDVAGAEALLDR.H
1614451623	815.9487	1629.8828	2	1629.8879	-0.0051	1618	1631	100.69	0	33	1.00E-08	R	LAALADQWQFLVQK	S			gi 115496850	spectrin alpha chain, non-erythrocytic 1 isof	R.LAALADQWQFLVQK.S
1555321244	878.9686	1755.9126	2	1755.9155	-0.0029	20	35	121.58	0	33	8.20E-11	K	LYPIANGNNQSPIDIK	T			gi 116063531	carbonic anhydrase 1 [Mus musculus]	K.LYPIANGNNQSPIDIK.T
1614433978	616.8388	1231.6631	2	1231.666	-0.0028	366	376	78.11	0	34	0.000002	R	ELLTTLQEASK	S			gi 116283802	Ttc38 protein [Mus musculus]	R.ELLTTLQEASK.S
1614433979	649.8533	1297.6901	2	1297.6918	-0.0017	45	55	92.96	0	32	4.70E-08	K	LFDATLTQYVK	W			gi 116283802	Ttc38 protein [Mus musculus]	K.LFDATLTQYVK.W
1614436880	1080.0147	2158.0148	2	2158.0219	-0.007	158	176	75.39	18	33	0.0000035	R	ALYQTEAFTADFQQPTEAK	N			gi 116961	RecName: Full=Serine protease inhibitor A3I	R.ALYQTEAFTADFQQPTEAK.N
1614436864	686.8526	1371.6906	2	1371.6955	-0.005	323	334	75.99	0	33	0.0000031	R	LEEDVLPEMGIK	E			gi 116961	RecName: Full=Serine protease inhibitor A3I	R.LEEDVLPEMGIK.E
1614436859	671.8516	1341.6886	2	1341.6928	-0.0042	145	155	80.54	0	33	9.70E-07	K	DLQILAEFHEK	T			gi 116961	RecName: Full=Serine protease inhibitor A3I	K.DLQILAEFHEK.T
1614436853	498.7941	995.5736	2	995.5764	-0.0028	352	360	78.19	0	29	6.40E-07	K	LSVSQVVHK	A			gi 116961	RecName: Full=Serine protease inhibitor A3I	K.LSVSQVVHK.A
1614436868	814.9466	1627.8786	2	1627.8821	-0.0035	301	314	94.2	27	33	3.90E-08	K	TLFPSQIEELNLPK	F			gi 116961	RecName: Full=Serine protease inhibitor A3I	K.TLFPSQIEELNLPK.F
1614436884	1249.6919	2497.3692	2	2497.3792	-0.0099	67	91	92.74	26	29	2.60E-08	K	NPDTNIVFSPLSISAALALVSLGAK	G			gi 116961	RecName: Full=Serine protease inhibitor A3I	K.NPDTNIVFSPLSISAALALVSLGAK.G
1614436879	714.7167	2141.1282	3	2141.1328	-0.0046	361	383	96.4	29	33	2.40E-08	K	AVLDVAETGTEAAAATGVIGGIR	K			gi 116961	RecName: Full=Serine protease inhibitor A3I	K.AVLDVAETGTEAAAATGVIGGIR.K
1614436873	884.4328	1766.851	2	1766.8574	-0.0065	335	350	102.53	0	33	6.80E-09	K	EVFTEQADLSGITETK	K			gi 116961	RecName: Full=Serine protease inhibitor A3I	K.EVFTEQADLSGITETK.K
1614436882	1105.4911	2208.9676	2	2208.9739	-0.0063	218	235	102.21	19	30	3.60E-09	K	ISFDPQDTFESEFYLDEK	R			gi 116961	RecName: Full=Serine protease inhibitor A3I	K.ISFDPQDTFESEFYLDEK.R
1614436878	1071.5711	2141.1276	2	2141.1328	-0.0052	361	383	105.29	26	33	3.10E-09	K	AVLDVAETGTEAAAATGVIGGIR	K			gi 116961	RecName: Full=Serine protease inhibitor A3I	K.AVLDVAETGTEAAAATGVIGGIR.K

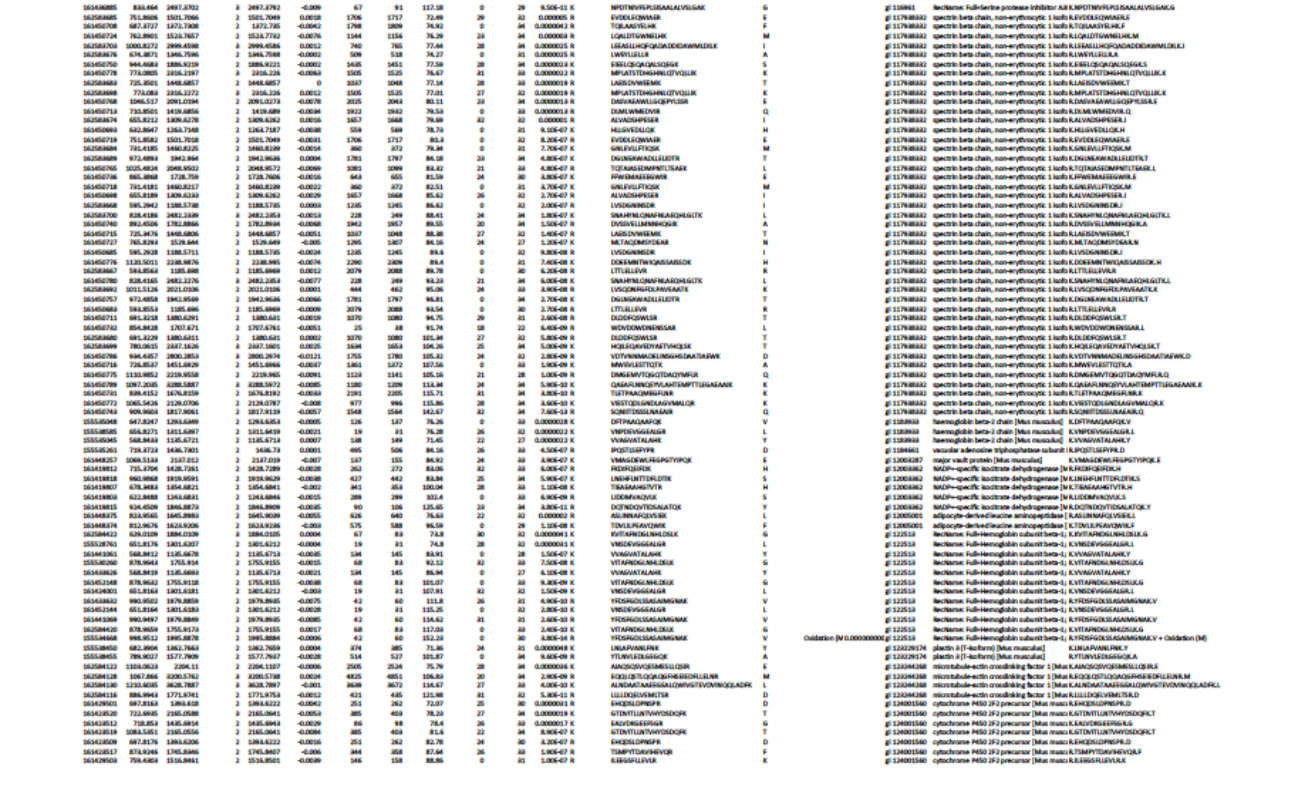

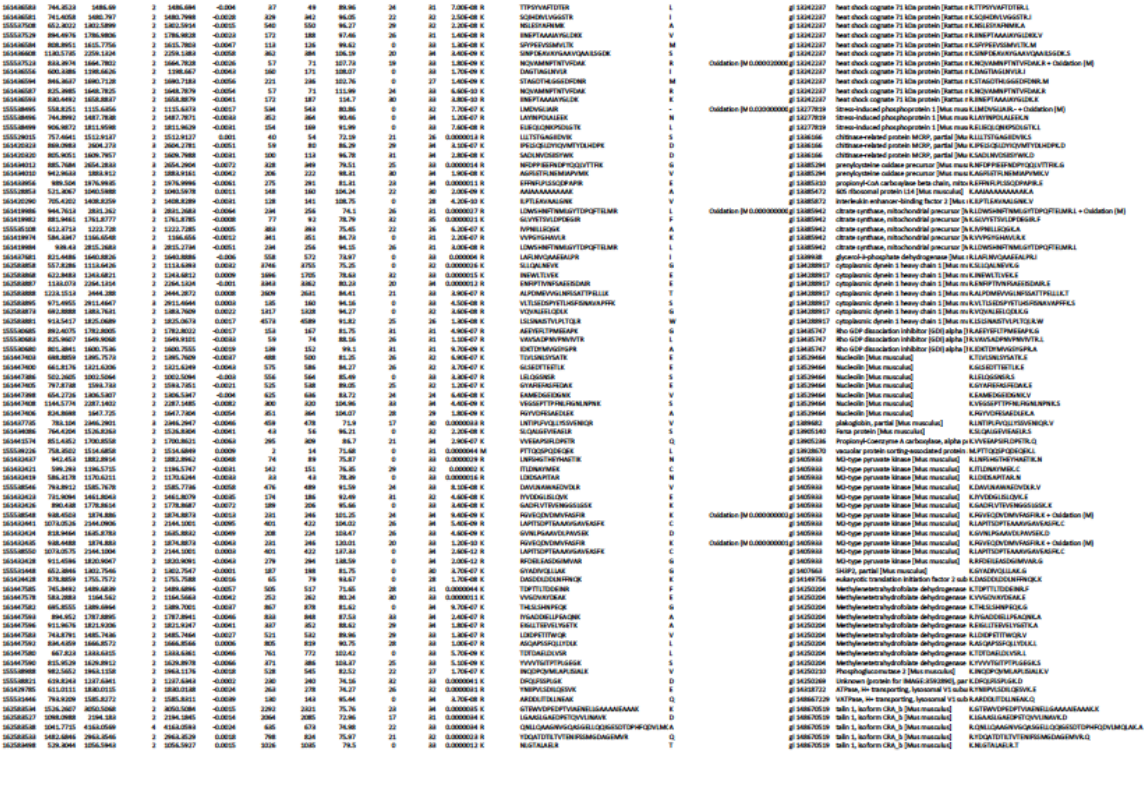

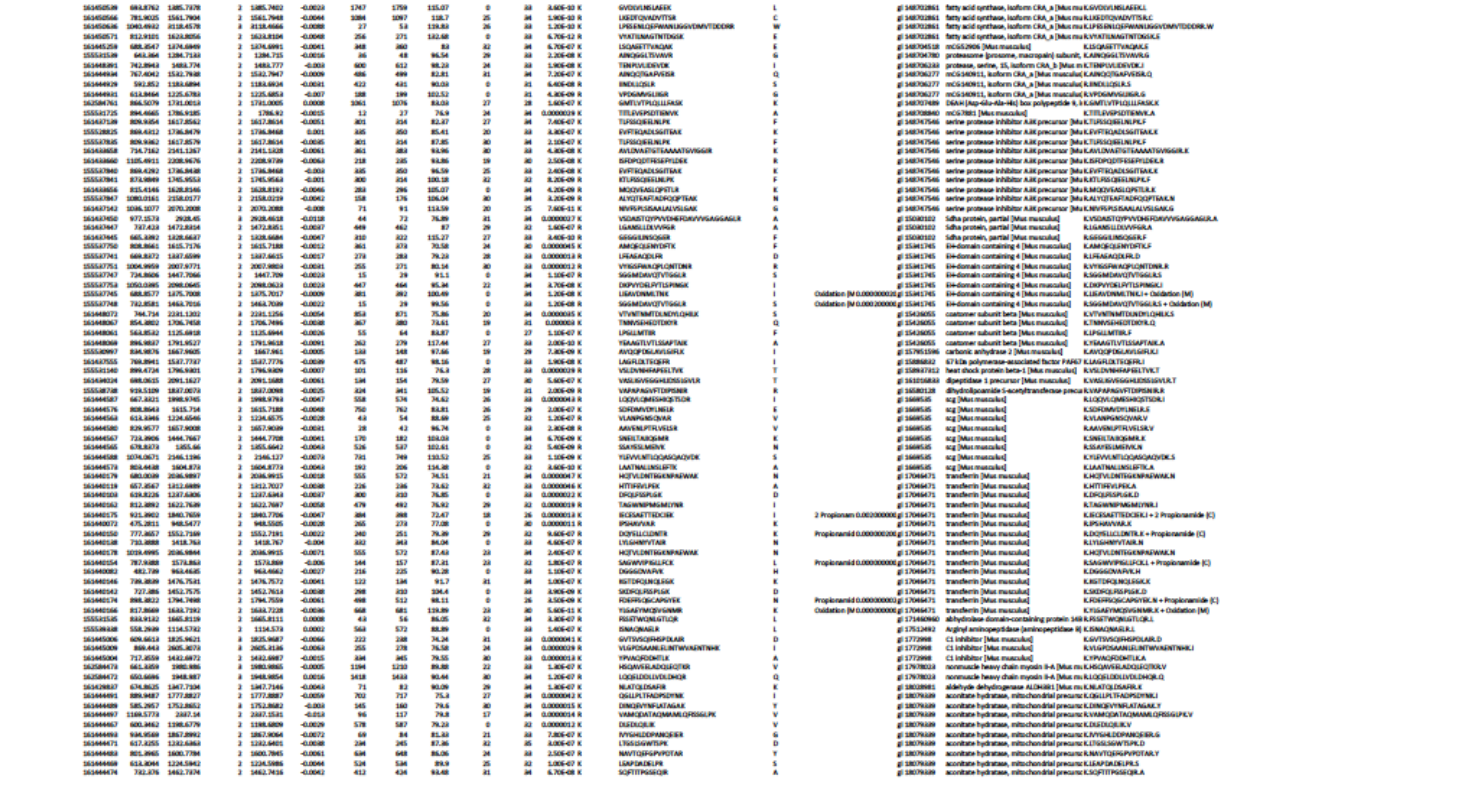

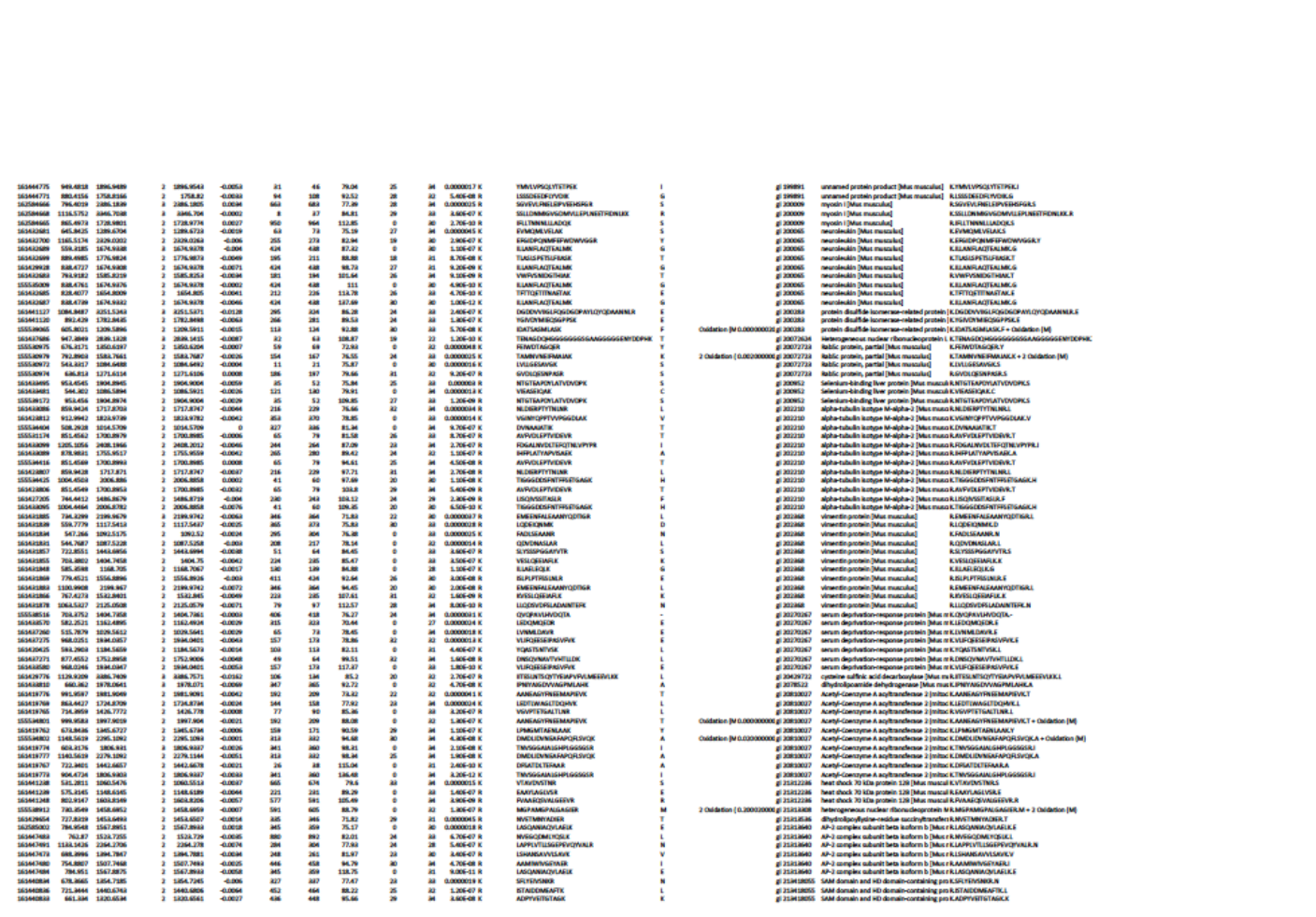

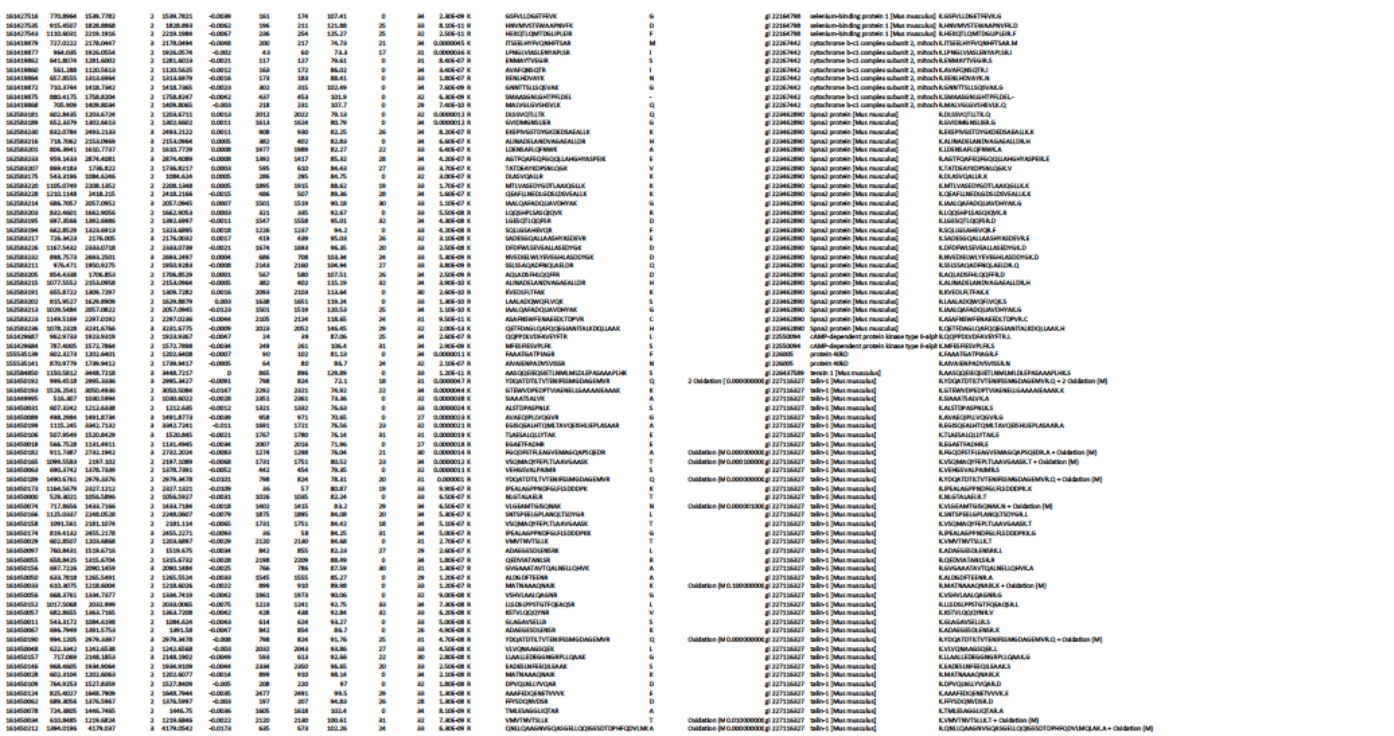

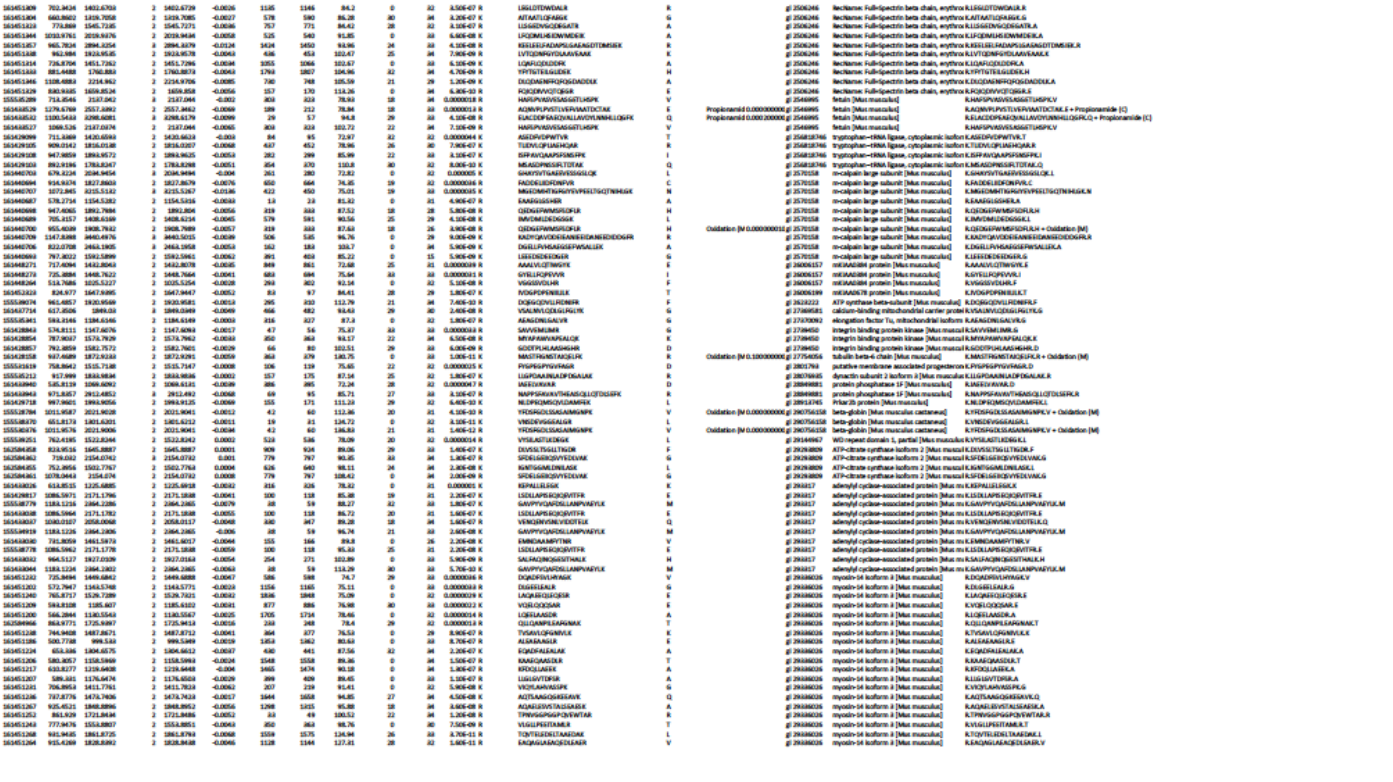

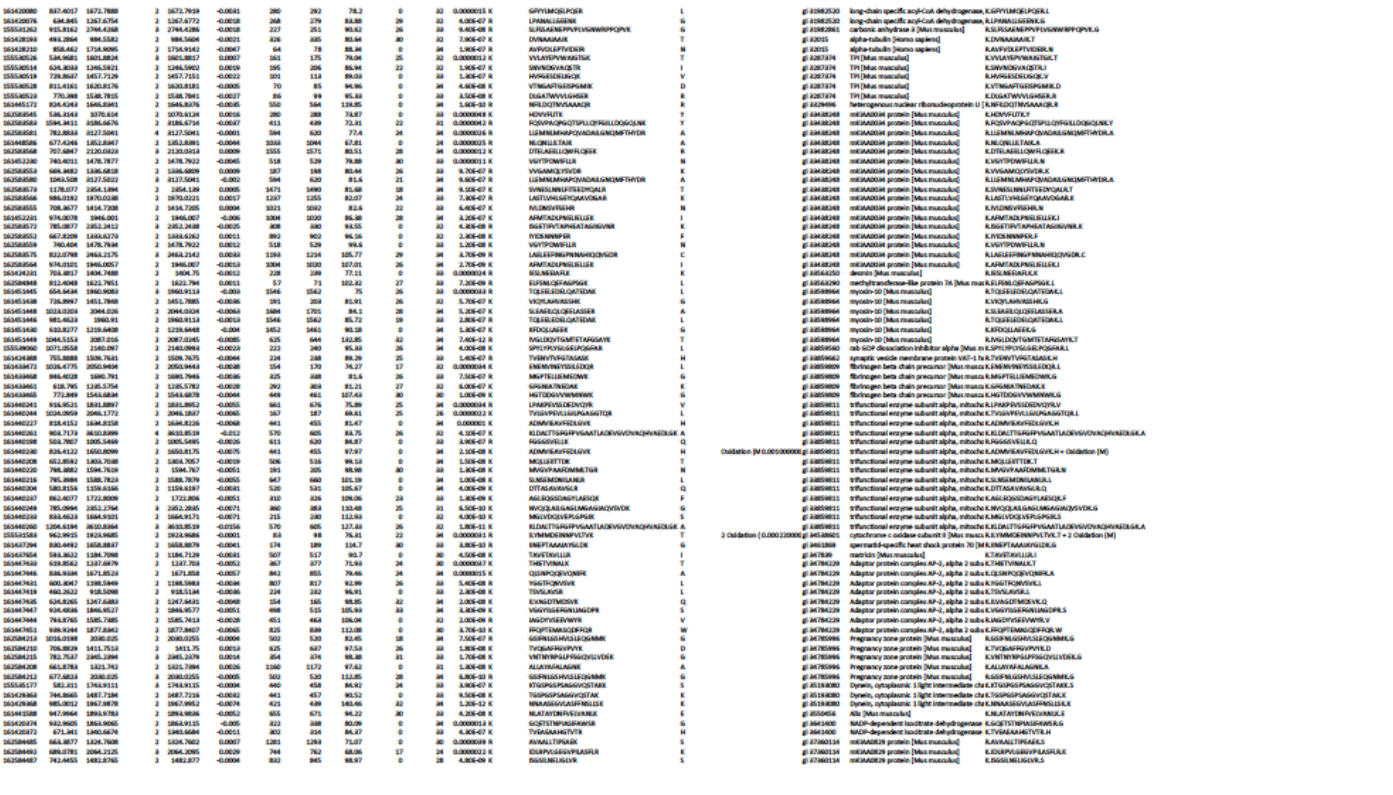

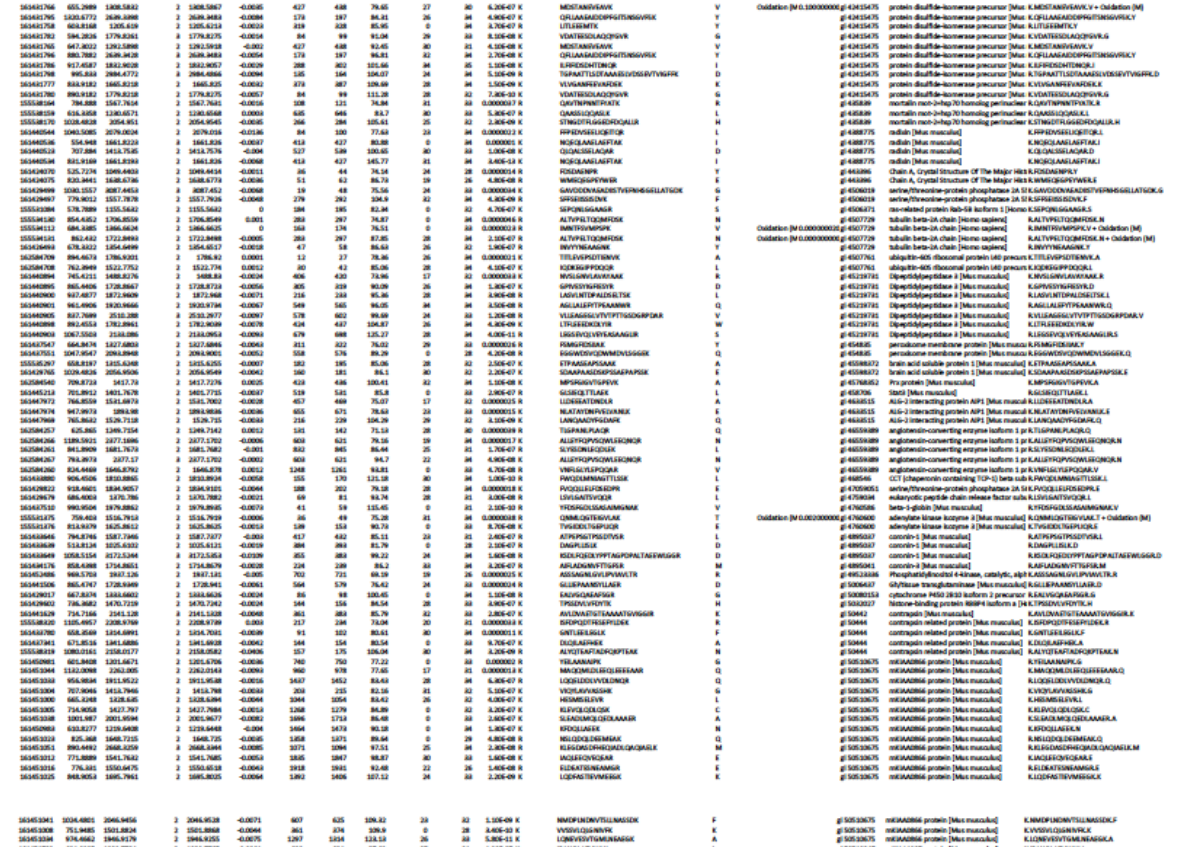

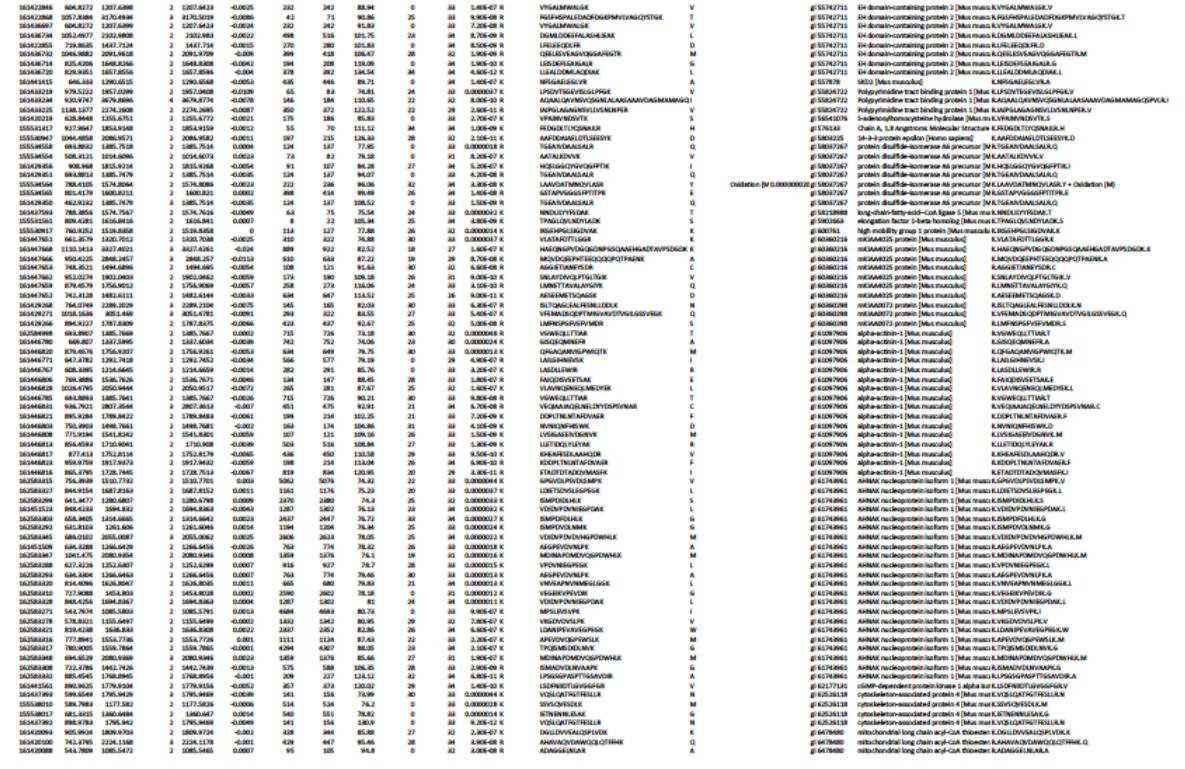

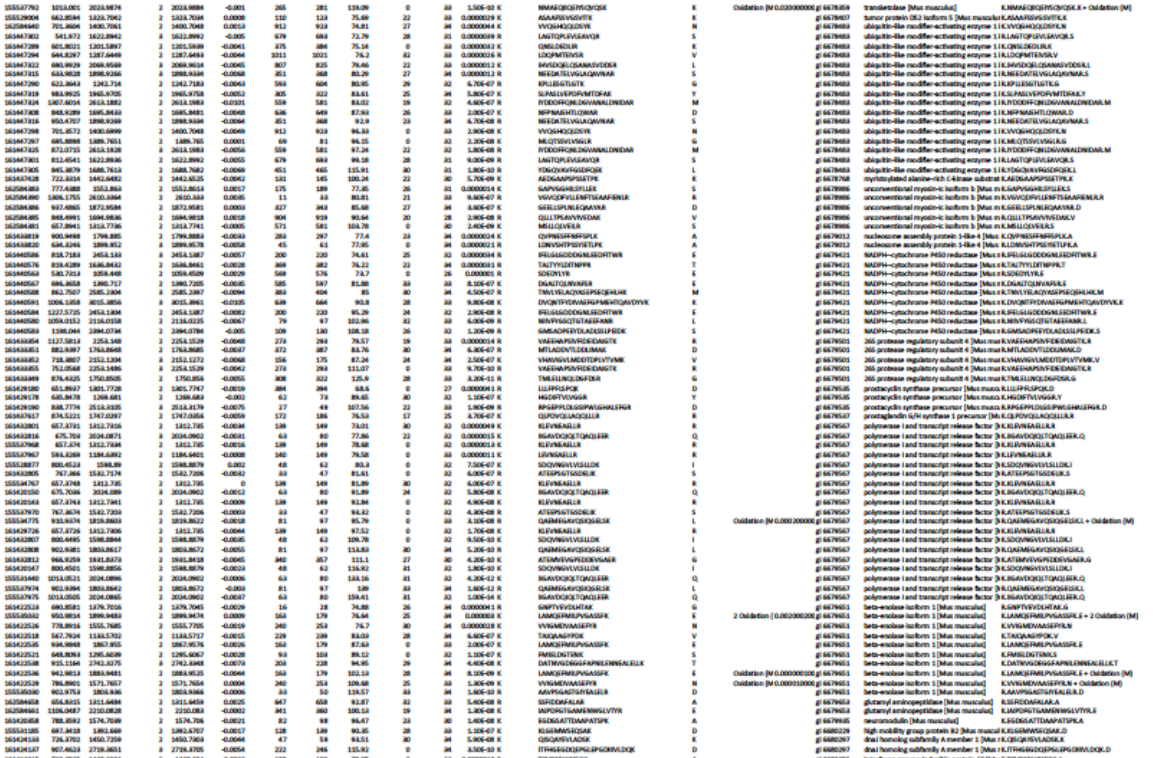

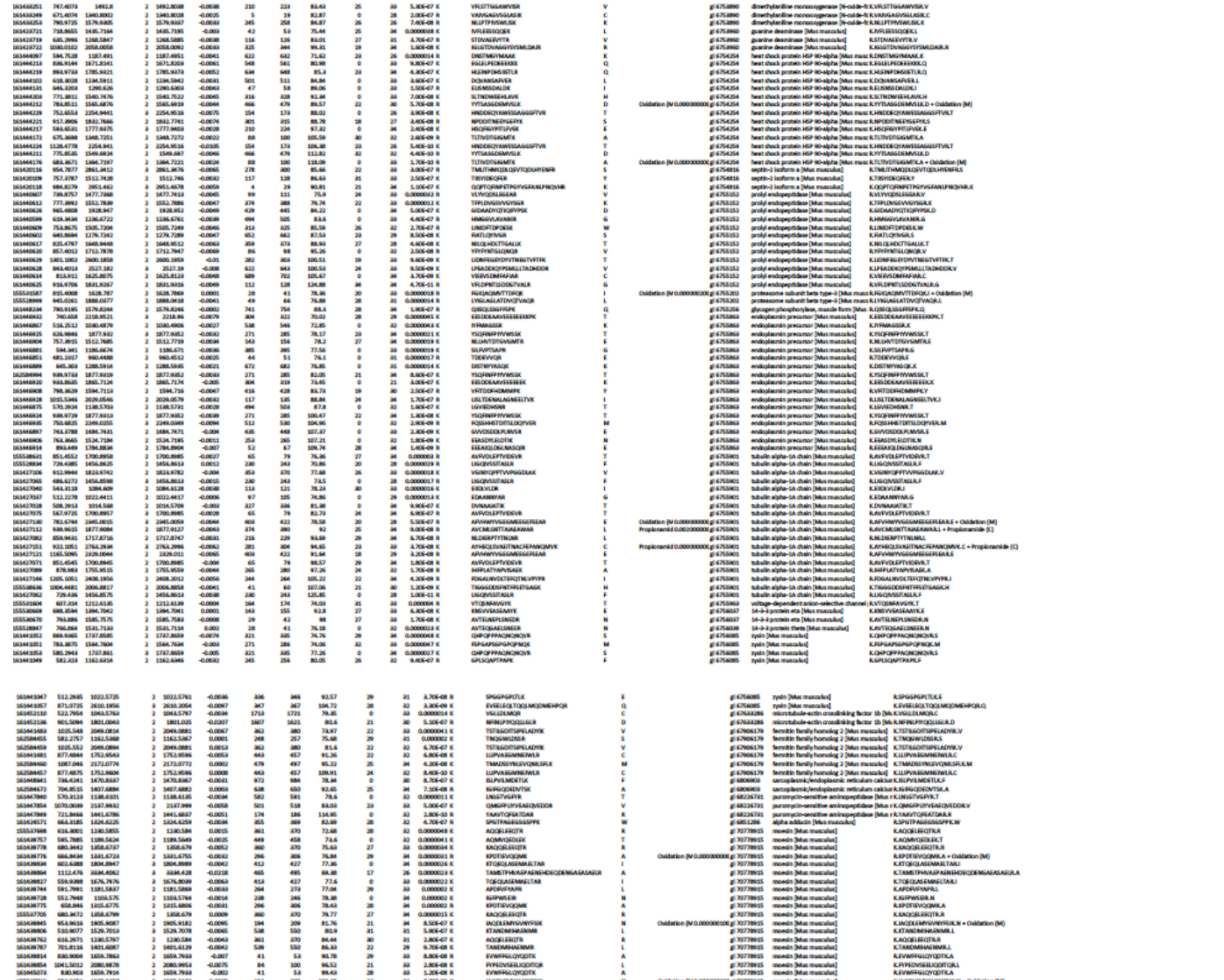

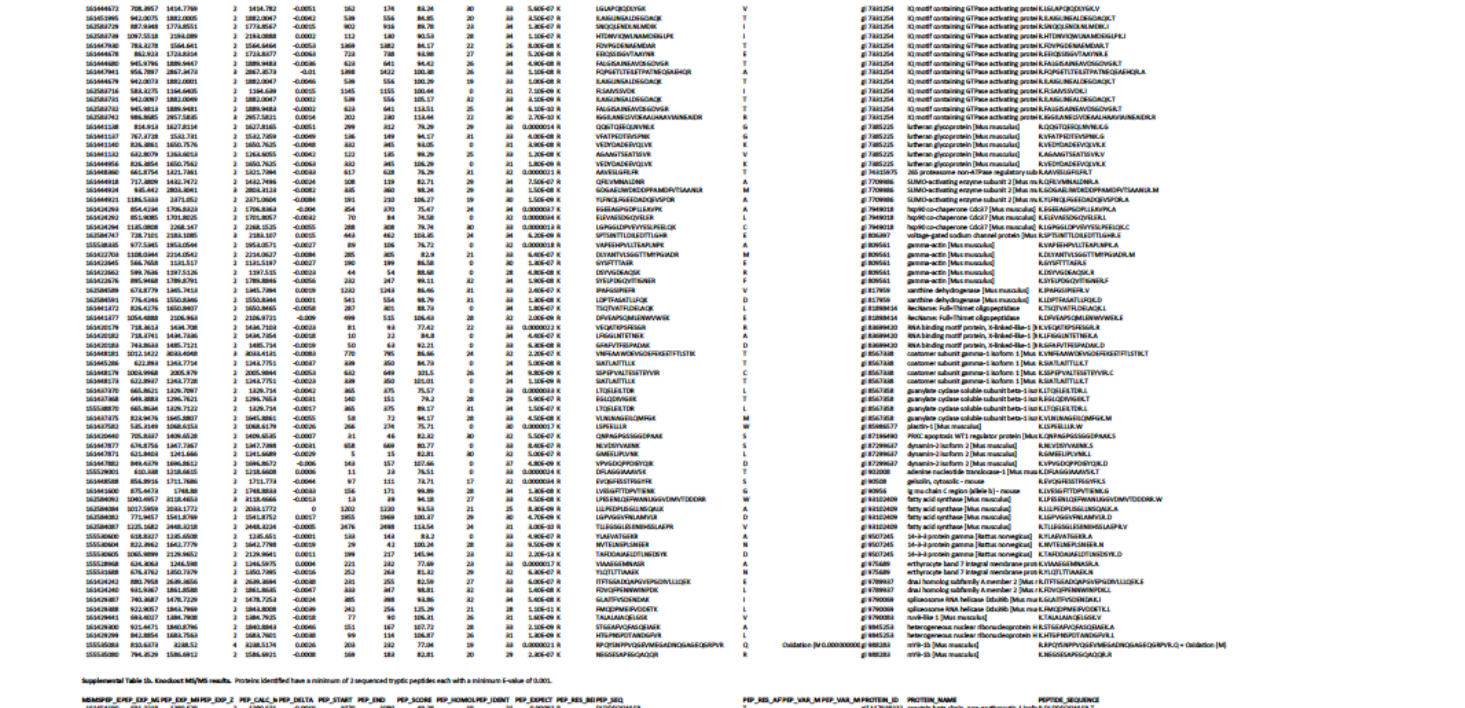

Supplemental Table 1b. Knockout MS/MS results. Proteins identified have a minimum of 2 sequenced tryptic peptides each with a minimum E-value of 0.001.